DOI:10.14753/SE.2022.2638

NEW PERSPECTIVES IN ALVEOLAR RIDGE RECONSTRUCTION AND GUIDED IMPLANT PLACEMENT – NOVEL SURGICAL AND EVALUATION CONCEPTS

PhD thesis

Kristóf Orbán

Doctoral School of Károly Rácz Clinical Medicine

Semmelweis University

Supervisor**:** Bálint Molnár DMD, Ph.D

Official reviewers: Márton Kivovics DMD, Ph.D

Kristóf Boa MD, Ph.D

Head of the Complex Examination Committee: Árpád Joób-Fancsaly DMD, Ph.D

Members of the Complex Examination Committee: Judit Borbély DMD, Ph.D

József Szalma DMD, Ph.D

Budapest

2021

DOI:10.14753/SE.2022.2638

TABLE OF CONTENTS

DOI:10.14753/SE.2022.2638

DOI:10.14753/SE.2022.2638

LIST OF ABBREVIATIONS

3D – Three-dimensional

AB – Autogenous block

ABM – Allogenic bone matrix

AD – Angular deviation

ADM – Acellular dermal matrix

AP - Particulate autogenous bone graft

ARP – Alveolar ridge preservation

ARP – SG - Alveolar ridge preservation via socket grafting

ARP – SS - Alveolar ridge preservation via socket sealing

BDX – Bovine-derived xenograft

CAD - Computer aided design

CBCT – Cone beam computed tomography

C-HD – Clinical horizontal dimension

C-HDG- Clinical horizontal dimension gain

C-VD – Clinical vertical dimension

C-VDG – Clinical vertical dimension gain

DFI – Double flap incision

DO – Distraction osteogenesis

d-PTFE – Dense polytetrafluoroethylene

EDS - Extraction defect sounding

e-PTFE - Expanded polytetrafluoroethylene

FMBS – Full-mouth bleeding score

FMPS – Full-mouth plaque score

GAD – Global apical deviation

GBR – Guided bone regeneration

GCD – Global coronal deviation

HAD – Horizontal apical deviation

HCD – Horizontal coronal deviation

MGJ – Mucogingival junction

MPR – Multiplanar reconstruction

OD – Odds ratio

OV – Orovestibular socket dimension

PRI – Periosteal releasing incision

R-HD – Radiographic horizontal dimension

R-HDG - Radiographic horizontal dimension gain

ROI – Region of interest

R-VD - Radiographic vertical dimension

R-VDG - Radiographic vertical dimension gain

R-VOL – Radiographic volume

SA – Socket area

SCTG - Subepithelial connective tissue graft

SD – Standard deviation

VD – Vertical deviation

VER – Vertical socket dimension

XSD - Extraction-site development

DOI:10.14753/SE.2022.2638

PREAMBLE

At the end of my last undergraduate academic year, in 2013, I had the opportunity to travel to the Osteology Symposium held in Monaco by the generosity of my Students' Science Association mentors, Professor Péter Windisch and Bálint Molnár. I was fascinated by the recent progress of implant dentistry and hard tissue augmentation procedures. In the congress I was completely impressed with the presentation of Istvan Urban, which indicated that excellent clinical practice in Hungary may raise significant interest among clinicians worldwide. After graduation receiving a residency status at the Department of Periodontology my professional interest turned to the possible methods of soft-, and hard tissue reconstructions. During the years of the residency program, I had taken part in several international congresses, and I had slowly incorporated the outstanding clinical knowledge in our Department. The continuous brainstorming in the Department led by Péter and Bálint resulted in various surgical approaches, which were proofs of the success of novel concepts. On the other hand, the large number of patients I had treated gave me the opportunity to improve my surgical skills and to take part in developing new techniques.

At the Department of Periodontology my surgical skills improved step by step. Different flap preparation and suturing techniques from resective periodontal surgeries taught me the solid basis. After numerous successful resective surgeries, the next step was to enter the field of reconstructive surgeries. And as usual, the first complications and failures have arrived since periodontal regeneration is extremely difficult to achieve. Excellent patient compliance and oral hygiene, microsurgical instruments, high magnification in the surgical field and of course skilled hands are needed. And when, despite all this, failures occur, a quick talk with Péter and Bálint would help to make the necessary adjustments. Respecting soft tissue phenotypes, blood circulation in the mucosa, knowledge of defect morphology, minimally invasive flap preparation techniques were all essential to succeed. The cadaver studies on the blood supply of the maxillofacial region conducted by Arvin Shahbazi made it possible to understand the anatomical basis beneath my clinical activities.

DOI:10.14753/SE.2022.2638

Development of split-thickness flap designs by Péter was one of the most interesting novelties in the Department. I remember in the undergraduate lecture he was presenting cases about different surgeries performed by split-thickness flap designs. I did not realize the benefits that time, but its importance has become apparent to me, when I first closed a oroantral fistula with this technique. Thereafter I started using it with surprisingly good results.

I felt privileged to be involved in ridge preservation and vertical augmentation studies, thus I could observe and practice these reconstructive techniques and flap designs. As a result, postoperative complications decreased after my surgeries, and patients' satisfaction was considerably improved. On the other hand, during these studies we tried and developed different digital evaluation methods to collect more precise data from surgeries. As digital dentistry gained ground in the Department, we started to collaborate with Endre Varga Jr. and Gabor Braunitzer representing dicomLAB Kft. to facilitate the application of guided implant surgeries. With their valuable contribution and the guidance of my mentors I was able to be the primary investigator of our third study, where half-guided implant placement accuracy was evaluated digitally.

It has always been a great honour for me to participate in clinical research projects and to publish data, which may raise significant interest in the scientific community thereby improving the techniques applied in daily practice. In my doctoral thesis, the evolution of my doctorate work will be chronologically presented based on three research projects.

DOI:10.14753/SE.2022.2638

1. INTRODUCTION

The era of modern implant dentistry started by the innovative concept of osseointegrating screw-type titanium implants by Per-Ingvar Brånemark. One of the most important key factors for success is the adequate amount of alveolar bone around implants at the time of insertion, as well as long term tissue stability. In the beginning, predominantly edentulous patients with healed extraction sites were rehabilitated with dental implants, fixture placement was limited by the extent of remaining alveolar bone.
With the development of various bone augmentation techniques, the indication field of dental implant placement was expanded. Nowadays implant dentistry has reached a new era, where single-, multiple tooth gaps and total edentulism with severe hard- and soft tissue deficiencies can be restored with adequate surgical methods followed by implant placement.

Dimensional changes of hard tissues following tooth extraction was a well-known phenomenon and it was already observed in the first half of the 20th century by clinicians, compromising dental prosthesis fabrication for edentulous patients. If no advanced atrophy occurred and the height and width of the alveolar ridge was maintained after tooth extraction, a more stable and comfortable prosthesis could be delivered to the patient. Ever since, prevention of ridge resorption reduction after tooth extraction has been in the focus of dental implant related research. In the present, state of the art alveolar hard tissue dimension maintenance and reconstruction approaches allow prosthetically driven implant placement with less extensive bone augmentation methods. To be able to preserve the alveolar ridge (alveolar ridge preservation – ARP) after tooth extraction, the key factors of post-extraction hard tissue resorption must be defined. The amount of bone resorption depends on the patient's local anatomy, trauma related- or inflammatory conditions around teeth to be extracted, wound healing characteristics and iatrogenic factors, or patient related factors, such as systematic diseases, low compliance, smoking habit or bad oral hygiene.

Alveolar resorption after tooth removal is site dependent. Buccal bone resorption has been reported in several human and animal studies since the 60's. Both Lam and Tylman in 1960 described a greater buccal bone plate resorption compared to the palatal plate in the maxilla (Lam 1960, Tylman 1960). Pietrokovski and Massler in 1967 measured the amount of ridge resorption after tooth extraction (Pietrokovski and Massler 1967). They confirmed the observations that buccal hard tissue resorption was more predominant than on the oral aspect. Furthermore, the amount of buccal resorption was significantly increased in the molar region compared to the premolar and incisor region. Nevertheless, these studies did not report about the cause (i.e., periodontal or periapical inflammation) and invasiveness of tooth extraction, neither about the application of temporary prostheses.

In 1963 Atwood found in his cadaver study that the lingual cortical plate is 2 to 3 times thicker than the labial cortical plate and reported that the labial cortical plate may be resorbed after tooth extraction (Atwood 1963). In their research article they admitted, individuals presented in the study had no known medical or dental history, thus the extent of bone resorption could be not identified. Possible etiological factors included mucosally supported dental prostheses, increased mucosal vascularity, muscle action, traumatic surgical technique or constricting mucoperiosteum.

To positively influence the socket-healing process and to reduce alveolar ridge resorption the anatomy of periodontium had to be studied. Anatomical research revealed the correlation between periodontal attachment apparatus morphology and the extent of alveolar bone resorption. Periodontal attachment is formed by periodontal ligaments, root cementum and alveolar bone proper, protected by the gingiva as an outer soft tissue seal. The alveolar process supports natural teeth from the bone crest of socket walls, apically to the bottom of the alveolus. Beyond the alveolar socket it continues as the basal bone of the maxilla or the mandible. The alveolar process develops in close conjunction with natural teeth and has two parts: alveolar bone and alveolar bone proper, also called bundle bone. While bundle is formed by cells from dental follicle and connected to the periodontal ligament, alveolar bone is formed by cells, which are independent from the dental follicle. Bundle bone is a 0.2-0.4 mm wide circumferential lamellar bone without

bone marrow, and it contains thick parallel bundles of collagen fibers. Alveolar bone is also a lamellar type of bone, but it consists of bone marrow, concentric and interstitial lamellae. Frequently, in the buccal bony plate in the anterior region the alveolar bone is missing and only bundle bone is present, thus this thin buccal bone plate is a completely tooth-dependent structure (Araujo et al., 2015, Schroeder 1986). Buccal bone width is the thinnest in the coronal third of the socket wall. Soft tissue architecture is genetically determined, similarly to the underlying bone structure. Patients with thin, scalloped gingival phenotype usually have a thin alveolar bone, frequently associated with dehiscence or fenestration. In contrast, patients with thick, flat gingival phenotype tend to have thick buccal alveolar bone (Sclar 2004).

The blood supply of the teeth (dental arteries) and the surrounding periodontal tissues (intraseptal arteries) originate from the superior and inferior alveolar arteries. The dental artery gives branches to the intraseptal artery, which continues coronally in the septum, while its terminal branches penetrate the alveolar bone proper (rami perforantes). Before the dental artery enters the root canal it ramificates to supply the apical portion of the periodontal ligament and connects by anastomosis with the rami perforantes creating the blood vessels of the periodontal ligaments. Additional blood supply of the alveolar bone derives from the supraperiosteal blood vessels, which anastomose with blood vessels from the alveolar bone (intraseptal artery) and periodontal ligaments supracrestally (Lindhe et al., 2015). In the buccal bony plate, the blood vessels are derived from the periosteum, from periodontal ligaments and from the adjacent interdental septum. The posterior interdental bone blood supply is more pronounced than the vascularity of the anterior interdental tissues. The coronal third of the buccal bone contains the thinnest blood vessels (Al-Hezaimi et al., 2011).

After tooth extraction the blood supply is compromised: blood vessels in the periodontal ligaments are damaged, only intraseptal arteries and supraperiosteal blood vessels are intact. This vasculature disturbance severely affects the stability of the thin buccal bone, thus the extent of bone resorption is increased on the buccal aspect. Cardaropoli et al. in their animal study found a complete bundle bone resorption after 2 weeks following mandibular premolar extraction in dogs (Cardaropoli et al., 2003). Araújo and Lindhe in

2005 in an animal study found missing bundle bone 4-8 weeks after tooth extraction in histology samples (Araújo and Lindhe 2005). Two overlapping phases of buccal socket wall resorption was observed. In the first phase the bundle bone was resorbed and replaced with woven bone due to loss of function. Since the buccal wall of the socket contains mostly bundle bone with a thin cortical layer, this remodelling results in advanced vertical bone loss buccally. During phase two an additional bone resorption is developed, which affects both socket walls. They hypothesized that the reduced blood supply results in osteocyte necrosis and a secondary necrosis of surrounding hard tissues. The necrotised crest may be eliminated by osteoclast activity from the periosteal layer. Since the buccal bone is thinner, than the lingual socket wall, phase two of the resorption will result in extended horizontal buccal bone loss and occasionally slight vertical bone loss. These observations are limited to a non-invasive tooth extraction without removable denture wear.

In the molar region of the maxilla after tooth extraction additional vertical bone loss is observed due to the pneumatization of the maxillary sinus. This resorption begins in the apical area and results a local vertical hard tissue loss, which complicates implant placement thus sinus elevation procedure is frequently required.

The extent of alveolar hard tissue changes after tooth loss depends on socket healing investigated by different authors (Balogh 1932, Boyne 1966, Amler et al., 1960). Amler et al. in 1960 observed different stages of undisturbed healing post extraction in histology samples, which are the following: blood clot formation in the alveolar socket, replacement of blood clot by granulation tissue (Day 7), replacement of granulation tissue by connective tissue (Day 20), appearance of osteoid at the base of the socket (from Day 7) and filling of at least two thirds of socket fundus by trabeculae (until Day 38), and evidence of epithelization (from Day 4). However, despite of the undisturbed wound healing process various degrees of soft- and hard tissue loss could be detected, based on these early observations.

Alveolar ridge resorption after tooth removal is extended if local periodontal or endo-periodontal inflammation is detected. Periodontitis leads to bone loss around teeth, in case of extraction of severely periodontally compromised teeth negative crestal bone level remodelling occurs thus implant placement frequently requires reconstructive surgery.

Furthermore, the regenerative capacity and alveolar bone remodelling is decreased in inflammatory conditions. As a result, during the 3-6 months post extraction healing a more pronounced ridge resorption can be observed (Ahn et al., 2008).
In case of disturbed wound healing, more pronounced alveolar bone resorption occurs compared to undisturbed healing. Claflin in 1936 investigated disturbed wound healing after tooth extractions in dogs and found a delayed healing process compared to undisturbed wound healing (Claflin 1936). In clinical practice a dry socket is one of the most common complications after tooth removal described by Crawford in 1876 (Crawford 1876). Blood clot stability is the key factor of wound healing post-extraction, without blood clot formation or in case of early blood clot loss pathogenic factors compromise the healing process and promote alveolar ridge resorption (Cardoso et al., 2010). Different treatment methods of dry sockets are used in the daily clinical practice but based on literature data, prevention of dry sockets is more effective than treatment. Traumatic extraction is one of the main reasons of post-extraction alveolitis. Atraumatic surgical tooth extractions may result a favourable wound healing, thus minimal invasive extractions are suggested (Taberner-Vallverdú et al., 2015).

Fickl et al. in 2008 compared alveolar ridge alterations after flapless tooth extractions to extractions performed with muco-periosteal flaps in beagle dogs (Fickl et al., 2008). They have found less bucco-oral shrinkage after 4 months of healing in the flapless group. They hypothesized that raising a buccal muco-periosteal flap promotes osteoclast activity in the buccal aspect of the socket thus flapless extraction is recommended, if feasible.
Saldanha et al. in 2006 investigated the possible connection between smoking habits and post-extraction ridge resorption rate (Saldanha et al., 2006). They concluded that smokers presented a significant reduction in alveolar width 6 months after extraction, compared to non-smokers. The vasoconstrictive effect of nicotine may prevent the angioblast response during revascularisation in the early phase of wound healing and it can limit the effect of local factors, such as cytokines.

After tooth extraction ridge resorption of various degree can develop in the edentulous area, which may complicate implant placement (Fig. 1**)**. A mean of 29-63% horizontal

resorption can be observed compared to the vertical resorption 6 months post extraction, which averaged 11-22% resorption (Wah Lay Tan et al., 2012).

In 2003 Schropp et al. performed 46 non-invasive single tooth extractions (Schropp et al., 2003). After tooth extraction and at the follow-up visits impressions were taken and casts were prepared to measure horizontal ridge resorption. Vertical bone changes were also measured based on intraoral radiographs. Patients were not allowed to wear any removable dentures for 12 months post extraction. A more pronounced horizontal resorption was found in the molar region compared to the front and premolar region. Regarding the width of the alveolar ridge, a reduction of approximately 50% was found, two thirds of the resorption occurred during the first 3 months of healing. Mean horizontal bone loss was 6.1 mm, while vertical changes were less than 1 mm. Their results were obtained following non-invasive single tooth extractions without any removable dentures, which would have compressed the underlying tissues, while in other's studies surgical and multiple teeth extractions were performed and/or removable dentures were worn by the patients during healing. Based on the study mentioned above, after minimal invasive tooth extraction mainly horizontal bone resorption develops, while vertical bone loss will be negligible.

DOI:10.14753/SE.2022.2638

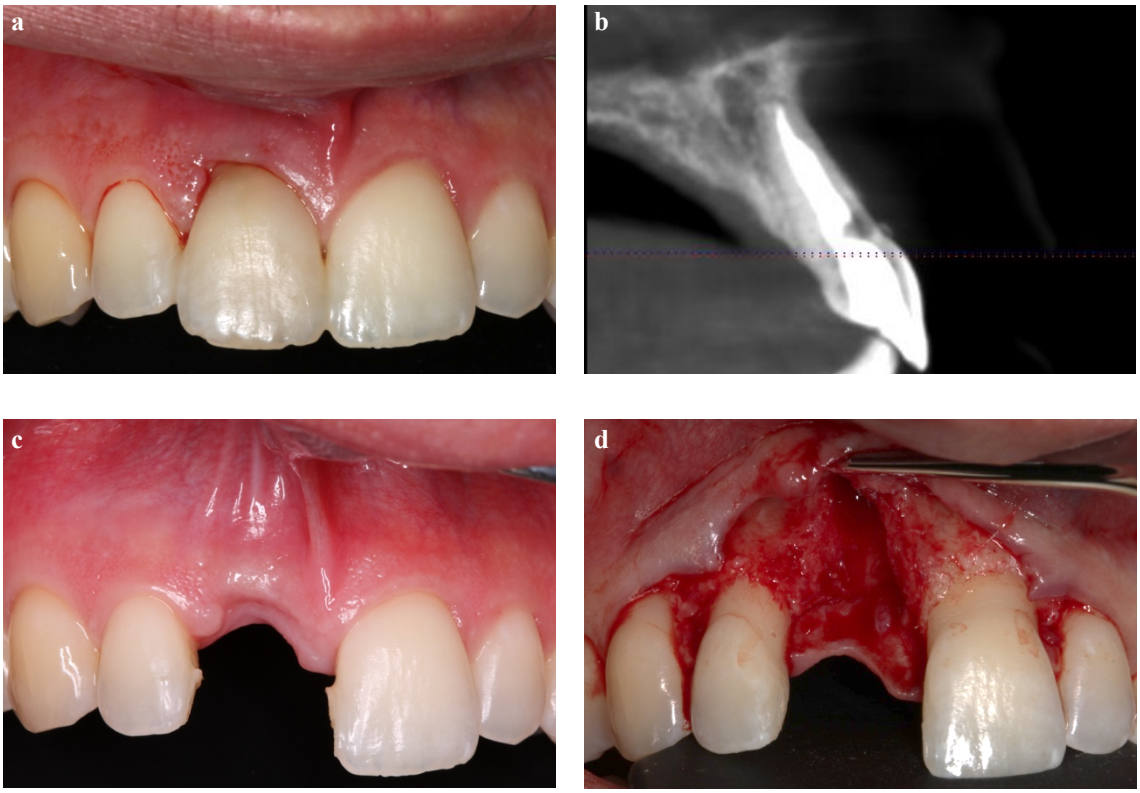

Fig. 1 Alveolar ridge resorption after tooth extraction

a) Baseline clinical situation, untreatable acute infection due to external resorption. b) Baseline CBCT, parasagittal section, thin (non-visible) buccal bony plate. c) Clinical situation 2 months after tooth extraction. Healed soft tissue. d) Severe hard tissue dehiscence after flap elevation. Property of Dr. Kristóf Orbán.

Wound healing of post extraction sockets can be optimized by utilizing current minimally invasive surgical approaches, however, compromised local periodontal anatomy around hopeless teeth is still a challenge for clinicians. Caplanis et al. in 2009 developed the extraction defect sounding classification (EDS), which was based on the hard- and soft tissue conditions at extraction sockets (Caplanis et al., 2009). They recommended to classify alveolar socket morphology immediately after extraction to choose the most adequate treatment modality of reconstructive therapy, aiming at optimal function and aesthetics of implant borne restorations. The EDS classification divides post-extraction sockets into 4 groups after tooth removal and classifies them based on the affected socket walls, the gingival phenotype and the distance between gingival margin and crestal bone.

This classification system recommends a treatment strategy as well. EDS class 1 presents an undamaged socket wall with thick gingival phenotype in a systemically healthy patient. The surrounding bony wall is at least 1 mm thick and the crestal bone is 0-3 mm from the optimal gingival margin. This clinical situation allows for immediate implant placement. EDS class 2 has one damaged socket wall with a maximum of 2 mm bone loss, or the buccal bony wall thickness is less than 1 mm. Any fenestration of the socket wall, which does not compromise the buccal crest, such as apical endodontic damage is also included to this group. Gingival phenotype can be thin or thick. The distance between the optimal gingival margin and the crest is at least 3 mm, but no more than 5 mm. At the extraction an atraumatic ARP technique and late implant placement is recommended. Immediate implant placement with simultaneous regenerative surgery can be performed, but a greater risk for mucosal recession and implant exposure is expected. EDS class 3 has a wider spectrum. A vertical- or horizontal hard- and/or soft- tissue loss of 3 mm to 5 mm can be observed with one or two compromised socket walls, a thick or thin periodontal phenotype, or any combination thereof. The distance between the original gingival margin level and the crestal bone is 6-8 mm. ARP and after healing late implant placement is recommended. At the time of implant placement additional site development can be necessary. EDS class 4 defects have a severely compromised socket wall with greater than 5 mm horizontal-, or vertical soft and/or hard tissue loss. The distance between the ideal gingival contour and the bony crest is more than 8 mm. In this situation a three-stage surgical protocol is recommended: ARP, followed by hard tissue augmentation surgery and finally late implant placement.

This clinical guideline can help the clinician to minimize the extent of hard-and soft tissue resorption after tooth extraction. Nevertheless, in the daily practice clinicians do not always have the opportunity to preserve the alveolar ridge at the time of the extraction due to low patients' compliance, acute infections, systematic diseases etc. Thus, different hard tissue augmentation methods are still necessary and cannot be avoided for optimal periimplant tissue development for long term function and aesthetics.

Following tooth extraction, without any ARP method the most unwanted biological process is the three-dimensional ridge resorption. In patients with periodontal disease due to insufficient hard- and soft tissue conditions the resorption rate may be higher (Trombelli et al., 2008), thus ridge augmentation procedures may be required before or at

the time of implant placement to create optimal hard tissue volume around. Various hard tissue augmentation methods can be applied to increase hard tissue volume. The “gold standard” of augmentation procedures is the transplantation of autogenous bone blocks (AB). Depending on the donor site and the graft size, AB can consist only of cortical bone, or in case of larger graft, AB can be a cortico-cancellous graft. The latter is suitable as an onlay graft for horizonto-vertical augmentation, or as a buccal cortical plate for horizontal ridge augmentation. Bone substitutes can be used as additional grafting material around and between the alveolar ridge and AB (Khoury and Hanser, 2015). The relatively rapid healing time (3-6 months) is an advantage of this technique, but the moderate donor site morbidity and increased resorption rate of AB encouraged clinicians to develop less invasive augmentation methods. Guided bone regeneration (GBR) is based on a secluded space created by a barrier membrane preventing soft tissue migration and stabilizing the blood clot and bone replacement materials (Gottlow et al., 1984, Dahlin et al., 1988, Nyman 1991). During the healing period, graft vascularisation and bone regeneration is undisturbed below the membrane, but a more pronounced healing time of 6-9 months is required for an optimal graft mineralization.

Resorbable, and non-resorbable membranes including titanium-meshes are recommended for different GBR procedures. Resorbable membranes (including native, or cross-linked collagen, pericardium, dura mater, polylactic acid, polyglycolic acid, polyurethane and cortical foil), have an excellent soft tissue compatibility, but their space maintenance function is less effective compared to non-resorbable membranes, thus resorbable membranes are recommended for horizontal ridge augmentations inside the bony envelope without additional fixation, as well as for horizontal ridge augmentation outside of the bony envelope, with pin- or screw fixation. To improve the space maintaining capacity of resorbable membranes, Merli and co-workers in 2013 presented the “Fence Technique” (Merli et al., 2013). They used a resorbable membrane for horizonto-vertical augmentation, which was stabilized with an osteosynthesis plate to create a rigid scaffold for the grafting material and to avoid membrane collapse. Simon et al. in 2010 described a similar technique for ridge augmentation, they used resorbable membranes stabilized with tenting screws (Simon et al., 2010).

Celleti et al. were probably he first in 1994, who performed GBR procedures with pure titanium membranes in dogs (Celleti et al., 1994). They found hard tissue regeneration, when primary soft tissue coverage was maintained above membrane surface. Gluckman and Du Toit in 2014 presented a successful GBR procedure utilized by titanium membrane during immediate implant placement (Gluckman and Du Toit 2014). Windisch et al. in 2017 reached favourable hard tissue gain after GBR procedures in three patients, utilized by titanium membrane and split-thickness flap preparation (Windisch et al., 2017).

Titanium meshes can be also applied during GBR, in the literature various authors observed optimal hard tissue formation after healing. Cucchi and his co-workers in 2019 and in 2021 compared the hard tissue changes after GBR utilized by d-PTFE membranes or titanium-meshes. In the titanium mesh group, the meshes were covered by a resorbable membrane to avoid soft tissue penetration. In both groups approximately 30% newly formed bone was observed after healing (Cucchi et al., 2019, Cucchi et al., 2021).

Expanded polytetrafluoroethylene (e-PTFE) membranes are accepted as the gold standard for vertical GBR. The non-resorbable membranes rigidity is frequently increased by titanium reinforcement to reach a more stable space maintenance, thus risk for graft compression during the healing can be reduced. Assenza et al. in 2001 used titanium meshes above the blood clot for space maintaining during GBR (Assenza et al., 2001). Titanium meshes were covered by e-PTFE membranes to protect the underlying tissues from epithelial migration. They found favourable clinical and histological results after 9 months healing. Main disadvantage of non-resorbable membranes is the bacterial colonization of exposed membrane surfaces in case of flap perforation, which can lead to tissue inflammation and graft disintegration requiring premature membrane removal before the completion of the healing (Simion et al., 1994). In case of exposure of more modern dense polytetrafluoroethylene (d-PTFE) membranes the degree of bacterial colonization is lower and the tissue inflammation with impaired bone formation can be reduced or is easier to manage due to the lower membrane surface porosity (Urban et al., 2014). Tension-free wound closure following GBR, and primary intention wound healing is essential in case of non-resorbable membranes.

Several grafting materials can be used during augmentation procedures. Demineralized freeze-dried bone allografts (DFDBA) can enhance new hard tissue formation, as Nevins and Mellonig in 1992 and Simion et al. in 1998 demonstrated, however the clinical application of DFDBA is limited due to its human origin (Nevins and Mellonig 1992, Simion et al., 1998). Particulate autogenous bone grafts (AP) demonstrate a highly active biological capacity due to their osteoinductive properties, in contrast, early resorption rate is significant when used alone for augmentation (Jensen and Terheyden 2009). Different studies have suggested the combination of AP with xenogeneic grafting materials, such as bovine-derived xenografts (BDX), which can decrease donor site morbidity and graft resorption and prolong graft stability. Recently the 1:1 ratio of AP + BDX was recommended for horizontal or horizonto-vertical GBR procedure by several authors (Merli et al., 2006, Simion et al., 2007, Urban et al., 2014, Meloni et al., 2017).
Recently, in several studies the extracted tooth was used as grafting material during ARP or other regenerative methods (Kim et al., 2013). However, Gharpure and Bhatavadekar in 2018 in their systematic review observed that the tooth borne graft materials have no additional benefits over conventional grafting materials and further long-term investigations are needed to identify their advantages (Gharpure and Bhatavadekar 2018).

Various incision-, flap preparation- and suturing techniques are described in the literature for the GBR approach. To achieve an optimal, undisturbed healing the most important factors during surgery are adequate flap preparation, flap mobilization and wound closure. Without tension-free wound closure, flap perforation and membrane exposure may develop. Tinti and co-workers in 1996, and Tinti and Parma-Benfenati in 1998 described a mucoperiosteal flap preparation technique for vertical GBR approach which is frequently used in regenerative dentistry (Tinti et al., 1996, Tinti and Parma-Benfenati 1998). They recommended vertical releasing incisions at the neighbouring teeth, both mesially and distally. Before wound closure, a horizontal (mesio-distal) periosteal incision is performed on the buccal and if it is necessary on the lingual flap to reach a tension-free wound closure with horizontal mattress and single interrupted sutures. This flap management technique was further developed by Urban and co-workers in 2017 to minimize postoperative swelling, hematoma and pain (Urban et al., 2017). Hur et. al presented the double flap incision technique (DFI) in 2010 which is based on a split-

thickness flap design (Hur et al., 2010). The flap design contains a vertical releasing incision mesially, buccally a full-thickness mucoperiosteal flap is elevated until the mucogingival junction (MGJ), but beyond the MGJ the periosteal layer and mucosa is dissected and flap preparation continues apically supraperiosteally following elevation of periosteum. After graft stabilization and membrane fixation the periosteum is repositioned over the membrane and fixed to the lingual flap with horizontal mattress sutures. The mucosal flap is adapted to the lingual flap and closed using single interrupted sutures. Ogata and his group in 2013 compared the DFI to the conventionally used "Tinti" flap approach in case of horizonto-vertical augmentation procedures, they found an increased flap extensibility, a more favourable postoperative healing and less postoperative complications, such as membrane exposure or nerve injury in the DFI approach group (Ogata et al., 2013). Windisch and co-workers in 2017 introduced a modified split-thickness flap design without vertical incisions to reach a two-layer wound closure and a more predictable healing (Windisch et al., 2017). They found an uneventful healing in all cases due to an intact periosteal vascular circulation by avoiding vertical and horizontal releasing incisions after flap preparation. The two-layer wound closure resulted in improved flap revascularization and primary intention wound healing after surgical approach (Fig. 2).

DOI:10.14753/SE.2022.2638

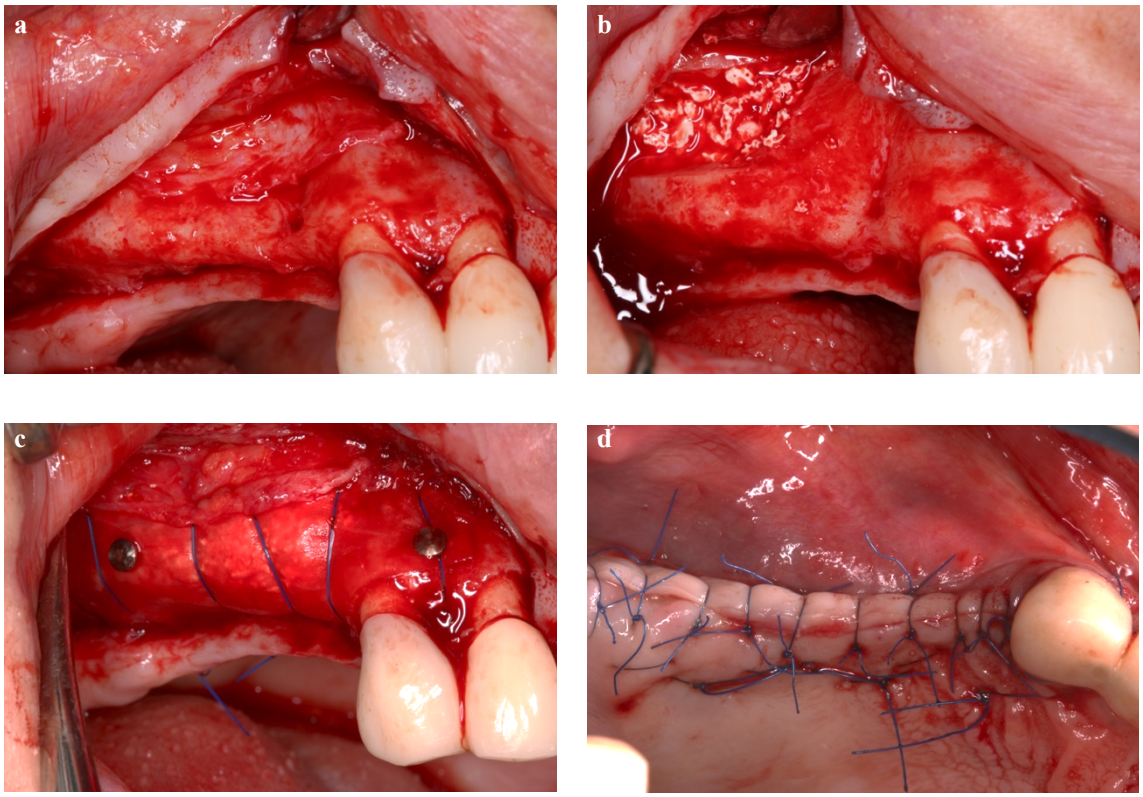

Fig. 2 Split-thickness flap preparation with vertical releasing incision and two-layer wound closure

a) Split-thickness flap preparation: mucosa is reflected, periosteal layer is visible. b) Lateral sinus augmentation with horizontal GBR. c) Periosteal sutures between periosteal layer and palatal mucosa. d) Mucosal sutures between buccal and palatal mucosa. Property of Dr. Kristóf Orbán.

Pneumatization of maxillary sinus can create a special vertical hard tissue loss in upper molar sites after tooth extraction. Horizontal bone loss of the subantral alveolar ridge is usually more compared to the anterior maxilla, usually the remaining bone width still allows for implant placement. Nevertheless, vertical bone dimensions for standard-length implants are insufficient. In case of 2-3 mm vertical bone reconstruction is required, internal sinus lift process, the Summers osteotome technique is recommended (Summers 1994). The surgical process is simultaneously applied with the implant placement.

Osteotomy preparation is performed with surgical drills, not reaching the sinus cavity. The remaining 1-2 mm undisturbed apical bone is gently elevated with a rounded osteotome, the apically increased area can be filled with grafting material before implant insertion. For the reconstruction of the severely pneumatized sinus with less than 5 mm of vertical bone height the lateral sinus elevation technique was first reported by Tatum in 1976 in the Alabama Implant Congress and published by Boyne and James (Boyne and James 1980).

During the lateral sinus-lifting procedure the lateral sinus wall is removed by surgical drills or with piezoelectric devices to reach the Schneiderian membrane. Specially angled sinus elevators are utilized to elevate the sinus membrane to create an adequate space for grafting materials. Implants are inserted if primary stability can be achieved. Usually at least 3 mm remaining vertical hard tissue is necessary to place an implant during external sinus lifting procedure. If the above-mentioned prerequisites for implant placement are not given, the staged approach is indicated, followed by implant placement after 4-6 months.

One of the key elements for long-term success is the maintenance of hard tissues around dental implants. However, crestal bone stability can only be achieved, if the implant borne restauration is in an optimal position, which depends on ideal 3D implant guidance. Implant positioning during conventional free-hand implant placement is based on the quantity of surrounding hard tissue. If an optimal amount of hard tissues is not available or the edentulous area is large without anatomical reference points, implant malpositioning is frequently observed, which makes more complicating the prosthetic procedures. The prosthetically driven surgical approach can improve implant placement precision, which allows for easily retrievable screw retained restorations, eliminating any submucosal cement residues. Several methods are described in literature to improve implant position accuracy. The conventional laboratory-fabricated surgical guide is based on a diagnostic wax-ups allows the surgeon to mark the implant position during surgery, but these types of stents cannot guide the drills for the final osteotomy, thus implant bed preparation and insertion are performed free-hand. An important evolutional step in dentistry was the appearance of various computer aided design (CAD) softwares. Digital

dentistry has become a new standard in implant position planning and navigation for implant placement. Combining a CAD software with CBCT scans to allow for digital implant positioning and fabricating stents for static navigation, called guided implant placement. After planning the implant position digitally, a surgical stent can be 3D printed. Static guided implant placement protocols are classified by the degree of guidance. The pilot drill protocol uses the surgical template only for the initial, usually 2 mm diameter drill. The half- (or partially) guided protocol uses the template for the complete drilling sequence (Fig. 3). During the full-guided protocol the guide is used for all osteotomies and for implant placement. Varga et al. have confirmed the superiority of static guided implant placement over free-hand implant placement, by observing that higher level of guidance results in a more accurate implant position (Varga et al., 2020).

The next evolutional step in guided surgery is the dynamic navigation. The dynamic navigation systems can recognize and track the position of the surgical motor in real time and can lead the implant to the planned position without a surgical template. To recognize the position of the patient's head, dynamic reference frames or invasive markers are required, which can complicate the surgery and increase patient's discomfort (Vercuryssen et al., 2014). Therefore, dynamic navigation is still not routinely applied in implant dentistry.

DOI:10.14753/SE.2022.2638

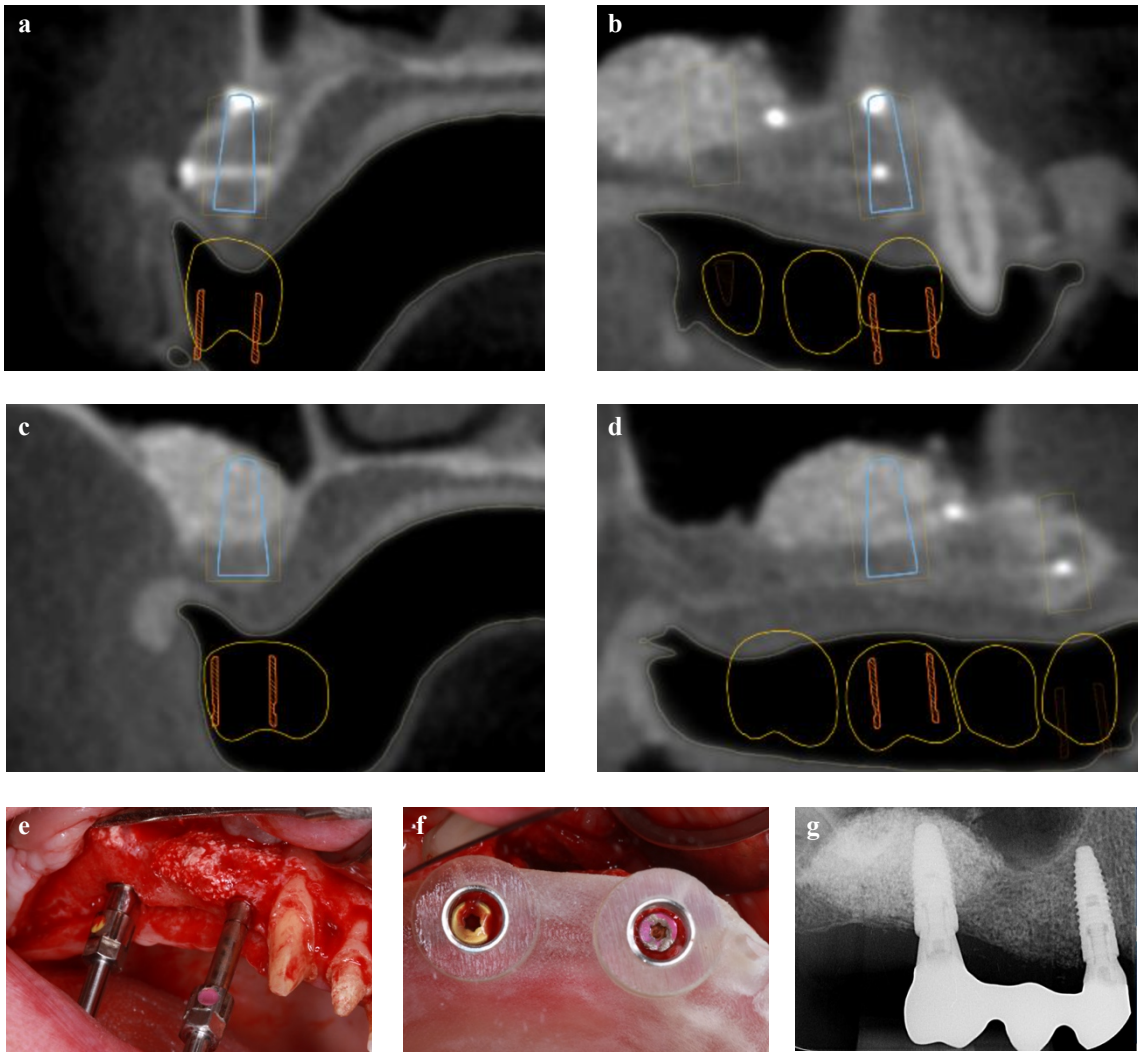

Fig. 3 Prosthetically driven, half-guided implant placement

a) Preoperative digital wax-up and implant position planning. Frontal section at tooth No. 14 position. b) Parasagittal section at tooth No. 14 position. c) Frontal section at tooth No. 16 position. d) Parasagittal section at tooth No. 16 position. e) Guided implant surgery. f) Implant cover screws through the sleeves. g) Postoperative intraoral radiograph after final prosthetic delivery. Ideal implant positions for abutment level screw-retained bridge. Property of Dr. Kristóf Orbán.

DOI:10.14753/SE.2022.2638

2. OBJECTIVES

The goal of my PhD dissertation is to present novel treatment approaches and digital planning- and diagnostic methods in implant dentistry feasible for the complex implant-prosthodontic rehabilitation of periodontal patients. The present thesis reports on three human clinical studies; a retrospective comparative case series and two prospective case series. All surgical interventions were conducted at the Department of Periodontology, Semmelweis University, while the control patients from Study I were collected from the Department of Oro-Maxillofacial Surgery and Stomatology, Semmelweis University. These different, but methodologically related topics may help clinicians in the daily practice to improve their treatment outcomes and to raise patient's satisfaction. For this purpose, following the removal of hopeless teeth ARP is recommended, in healed alveolar ridges horizonto-vertical reconstruction by GBR is proposed, both followed by late guided implant placement for optimal prosthetic outcomes and long-term crestal bone stability. Firstly, the necessity of ARP with a minimally invasive ridge preservation technique with a split-thickness flap design is presented to avoid extensive augmentation after tooth extraction. Secondly, the raison d'etre and the advantages of the split-thickness flap design during GBR procedures is presented to treat severe horizonto-vertical defects. Finally, the implant placement accuracy achieved by a half-guided surgical protocol and evaluation of machine-driven vs. manual implant insertion will be discussed. The data collected in the present research will be assessed by novel digital comparison methods to evaluate hard tissue changes after regenerative surgical approaches as well as the accuracy after guided implant placement.

2.1 Outline of Study I

Demonstration of Radiographic Bone Fill in Postextraction Sockets Using a Novel Implant-Site Development Technique: A Retrospective Comparative Case Series

A novel extraction-site development (XSD) technique was compared with spontaneous healing after tooth extraction. Hopeless teeth with advanced alveolar defects were removed; alveolar sockets of 33 single-rooted teeth were treated by XSD (test group), while 21 extraction sites of single-rooted teeth were left for spontaneous healing (control group). In the test group simultaneously with tooth extraction, two vertical incisions were performed into the alveolar mucosa at the level of neighbouring teeth. After split-thickness flap preparation beyond the MGJ periosteum was elevated and xenogeneic long-term resorbable membrane was fixed by titanium pins. In addition, subepithelial connective tissue graft (SCTG) was inserted into the supraperiosteal tunnel to increase the soft tissue volume. In the control group after extraction no additional therapy was performed. After an average 7.5 months healing control postoperative CBCT scans were performed, pre-, and postoperative CBCT data sets were compared to each other by a digital measurement process. Orovestibular, vertical socket dimensions and socket areas were assessed (Molnar et al., 2019).

2.2 Outline of Study II

Vertical-guided Bone Regeneration with a Titanium-Reinforced D-PTFE Membrane Utilizing a Novel Split-Thickness Flap Design: A Prospective Case Series

Horizonto-vertical GBR procedures were performed with split-thickness flap design to evaluate horizontal and vertical hard tissue changes and demonstrate the efficiency of the split-thickness flap. 19 patients with severe 3D hard tissue volume loss were selected and treated; in 6 surgical sites implants were inserted simultaneously with GBR (simultaneous group), while 18 surgical sites were treated by staged protocol, implants were inserted 9 months after GBR (staged group). After midcrestal incision on the keratinized mucosa at the edentulous area, full-thickness flap preparation was followed by split-thickness flap preparation beyond the MGJ. Periosteal layer was elevated from bone surface, composite graft (1:1 mixture of AP + BDX) was placed laterally and supracrestally to the alveolar

ridge covered by a non-resorbable d-PTFE membrane fixed by titanium pins. In the simultaneous group implants were inserted before the grafting procedure. Double layer wound closure without periosteal incisions was performed. After 9 months healing, membranes and titanium pins were removed and in the simultaneous group implant uncovery, while in the staged group implant placement was performed. During the surgical interventions, horizontal and vertical hard tissue dimensions were measured with UNC-15 probe, in the staged group additional digital measurements of hard tissue changes were performed based on pre-, and postoperative CBCT data sets (Windisch et al., 2021).

2.3 Outline of Study III

Accuracy of Half-Guided Implant Placement with Machine-Driven or Manual Insertion: A Prospective, Randomized Clinical Study

Forty patients received one standardized dental implant each either with surgical motor or torque wrench during half-guided implant placement protocol to evaluate and compare implant placement accuracy. After digital planning and surgical guide fabrication based on preoperative CBCT data sets, full-thickness flap preparation and implant osteotomy was performed as a part of a half-guided surgical protocol. Twenty implant insertions were carried out by a contra-angled surgical handpiece (machine-driven group), while another 20 implants were inserted by a torque-wrench (manual group). Duration of implant insertion and final insertion torque were registered. After the healing, preoperative CBCT data sets were aligned to the postoperative digital intraoral scans to evaluate implant placement accuracy, based on the differences between planned and the actual implant positions (Orban et al., 2021).

DOI:10.14753/SE.2022.2638

3. METHODS

3.1 Study I

Demonstration of Radiographic Bone Fill in Postextraction Sockets Using a Novel Implant-Site Development Technique: A Retrospective Comparative Case Series

The presented retrospective case series was performed in patients with hopeless single-rooted teeth at the Department of Periodontology and at the Department of Oro-Maxillofacial Surgery and Stomatology, Semmelweis University from 2007 to 2014. In the test group, inclusion criteria were at least 1 single-rooted tooth with EDS 3 or 4 defect morphology, while exclusion criteria were the following: any relevant systemic disease (e.g., diabetes, rheumatism, malignant disease), systemic steroid or bisphosphonate use, poor oral hygiene, or smoking more than 10 cigarettes a day. In the control group exclusion criteria were the following: any alveolar ridge preservation or other reconstructive treatment at the extraction site. The study conformed to the tenets of the Declaration of Helsinki (version 2004, updated in 2008) in all respects. The study protocol was approved by the Regional and Institutional Committee of Science and Research Ethics at the Semmelweis University (Approval Number: SE TUKEB 20/2007 and 77/2011). Surgical interventions were undertaken with the understanding and written consent of each subject.

3.1.1 Treatment approach

In the test group, patients presented a severe hard tissue loss around at least one single-rooted tooth. Need for extraction was confirmed by clinical and radiographic examination (CBCT). At the time of the extraction, a novel alveolar ridge preservation method (XSD) was performed (Fig. 4). The surgical approach in the test group was the following:

- Local anaesthesia was given.
- Tooth extraction was performed without flap preparation.
- Extraction socket was debrided.

- Bone sounding was done with UNC-15 probe, confirmation of EDS-3, -4 defect morphology.
- Elevation of the buccal keratinized gingiva was performed in full-thickness full up to the MGJ, extending to the neighbouring papillae with dedicated instruments (Tunnelling knife set, Deppeler, Rolle, Switzerland).
- Two full-thickness vertical incisions were placed parallel to each other at the level of the neighbouring papillae.
- Buccal split-thickness flap preparation was continued apically beyond the MGJ with tunnelling knives.
- Periosteal layer was elevated with blunt instruments.
- A long-term resorbable membrane (Soft Cortical Lamina, OsteoBiol, Tecnoss Dental) was adapted to the bone surface, fixed by titanium pins (Frios membrane tacks, Dentsply Sirona) mesially and distally on the intact bone surface.
- Palatal SCTG was harvested with the single-incision technique (Hürzeler and Weng 1999).
- SCTG was inserted between the periosteum and the gingiva, fixed by 5-0 non-resorbable sutures (Dafilon, Braun, Tutlingen, Germany).
- A resorbable collagen sponge (Lyostypt, Braun, Tutlingen, Germany) was placed into the socket.
- Vertical incisions and alveolar socket were sutured with 5-0 non-resorbable sutures.

In the control group, pre- and postoperative CBCT scans of patients were selected, who underwent tooth extraction without any ridge preservation or other regenerative method, alveolar sockets were left for spontaneous healing.

DOI:10.14753/SE.2022.2638

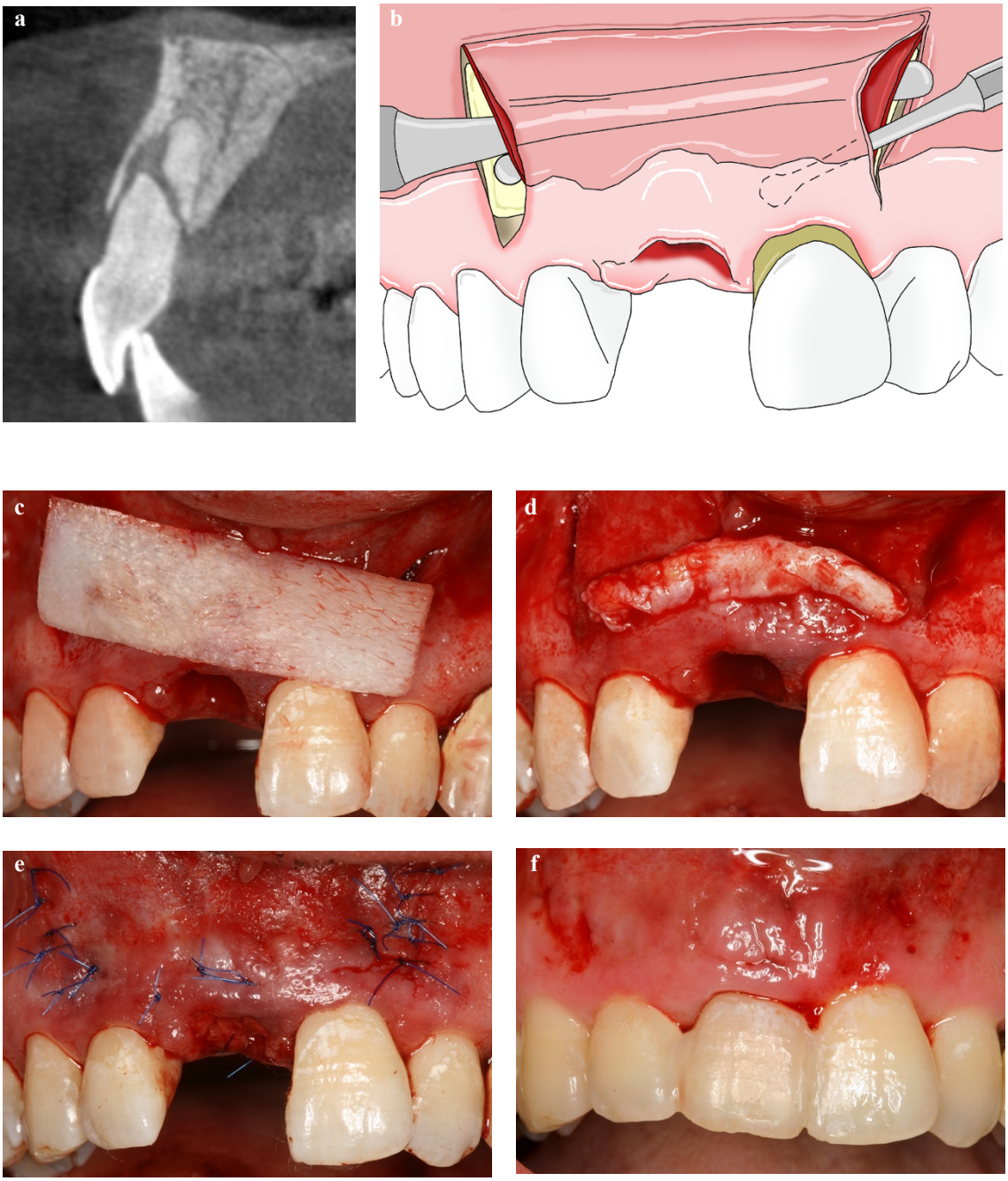

Fig. 4 Surgical steps of XSD approach /Case presentation/

a) Baseline CBCT scan, horizontal fracture in the middle third of tooth 11 (FDI). During tooth removal, buccal bone plate fracture was observed, bone plate was removed. b) Schematic drawing of XSD, presenting the bilaminar flap preparation technique by vertical tunnel access (Courtesy of Dr. Daniel Palkovics). c) Long-term resorbable membrane adaptation to the bone surface by titanium pins d) SCTG insertion between the periosteum and the gingiva. e) Resorbable collagen sponge placement into the socket,

wound closure with 5-0 non-resorbable sutures (Dafilon, Braun, Tutlingen, Germany). f) Early wound healing at suture removal (at 14 days postoperatively). Figure from the publication related to Study I (Molnar et al. 2019), copyrights purchased from Quintessence Publishing Company Inc.

3.1.2 Postoperative care

In the test group, postoperatively, patients received systematic antibiotic treatment (Augmentin Duo, GlaxoSmithKline; 1000 mg twice a day for 7 days) and non-steroid anti-inflammatory drugs (Cataflam, Novartis, 50 mg three times a day for 10 days). In the first 2 weeks, 0,2% chlorhexidine-gluconate mouth rinse (Curasept 220, Curaden Swiss) was prescribed twice a day. Sutures were removed 14 days postoperatively.

3.1.3 Re-entry procedure and implant placement, prosthetic reconstruction

In patients who received dental implants, after an average 7.5 months healing in local anaesthesia, full-thickness flap was elevated, titanium pins and minor remnants of the Lamina membrane were removed. Clinically, every XSD treated surgical site presented newly formed, vital hard tissue. If optimal hard tissue volume was observed, implants were inserted without any additional treatment, while in case of hard tissue dehiscence, simultaneous-, or staged ridge augmentation procedure was performed.

3.1.4 Digital radiographic evaluation

At baseline and after 6-9 months (7.5 months on average) healing, postoperative CBCT scans were taken. Pre-, and postoperative CBCT data sets were compared to each other to evaluate hard tissue changes. At the same time on two separate computer screens the same patient’s preoperative and postoperative CBCT scans were opened with the I-CAT Vision software (Imaging Sciences International, Hatfield, Pennsylvania, USA) at equal magnification level. The mesial tooth next to the tooth to be extracted was chosen as reference. In the multiplanar reconstruction (MPR) view’s frontal section, the image was

rotated until the axis of the reference tooth was superimposed on the sagittal section line. In the sagittal section, the same superimposition was performed, following that, orthoradial cross-sections were created on mid-, mesio- and distobuccal aspects of treatment sites. Images were exported to ImageJ software (National Institutes of Health and the Laboratory for Optical and Computational Instrumentation). A 1 mm^2 grid at the same level was laid over the cross-sections. Oro-vestibular dimension changes were measured in 15 levels (orovestibular socket dimension – OV). To evaluate the vertical hard tissue dimension changes, buccal and oral vertical socket dimension (VER), the distance from a reference point to the crestal bone surface was measured. Additionally, socket areas (SA) were assessed.

3.1.5 Data analysis

The statistical analysis was carried out in SPSS 23.0 (IBM, USA). For descriptive purpose, measured values were presented as means and standard deviations. For the hypothesis tests between baseline and re-entry, data in both groups were analysed by paired t-test. Odds ratio (OD) was evaluated using Fischer exact test. Differences were considered significant at $p<0.05$.

3.2 Study II

Vertical-guided Bone Regeneration with a Titanium-Reinforced D-PTFE Membrane Utilizing a Novel Split-Thickness Flap Design: A Prospective Case Series

The present case series was performed in patients with advanced chronic periodontal disease (grade III, stage B) presenting a partially edentulous area with a localized 3D alveolar defect, which required horizonto-vertical augmentation procedure to allow for implant placement. Exclusion criteria were the following: any relevant systemic disease (e.g., diabetes, rheumatism, cancer), systemic steroid or bisphosphonate use, acute or chronic inflammatory processes, untreated periodontal disease, smoking more than 10 cigarettes a day, inappropriate oral hygiene (full-mouth plaque score (FMPS) <20%, full-mouth bleeding score (FMBS) <15%), tooth-extraction at the surgical area in the last 6 months.

All patients were selected and treated at the Department of Periodontology, Semmelweis University between January 2012 and June 2015.

The study protocol was approved by the Semmelweis University Regional and Institutional Committee of Science and Research Ethics (Approval Number 77/2011). Surgical interventions were undertaken with the understanding and written informed consent of each subject. The patients were treated in full accordance with ethical principles, including the World Medical Association Declaration of Helsinki (version 2008).

3.2.1 Preoperative care

Before surgical intervention, patients underwent supra-and subgingival scaling and individual oral hygiene instructions to maintain a high level of oral hygiene during the whole treatment period. Presurgically, every patient rinsed with a chlorhexidine digluconate 0.2% mouth rinse (Curasept ADS 220, Curaden AG, Kriens, Switzerland) for 2 minutes.

3.2.2 Treatment approach

The GBR procedure was the same in both groups (Fig. 5 and Fig. 6). The surgical steps were the following:

- Local anaesthesia was given (4% articaine-hydrochloride with 0.0001% epinephrine - Ultracain DS Forte, Sanofi-Aventis, Paris, France).
- Midcrestal incision was placed on the keratinized mucosa with No. 15 blades (Aesculap, Braun, Tutlingen, Germany) in the edentulous area, continued intrasulcularly at two neighbouring teeth both mesially and distally with No. 15c blades (Aesculap, Braun, Tutlingen, Germany).
- In case of a free-end gap, midcrestal incision length was two-third of the entire surgical area.
- Vertical releasing incisions were avoided.
- Full-thickness buccal flap was reflected up to the MGJ, beyond the MGJ the periosteal layer was dissected from the mucosal layer (split-thickness flap preparation).
- Periosteal layer was elevated from the underlying bone with elevators.
- On the oral side, full-thickness flap was prepared, mobilized by blunt instruments down to the level of the mylohyoid line.
- In the simultaneous group, 3.3 mm, or 4.1 mm diameter Straumann Bone Level implants (Straumann AG, Basel, Switzerland) were inserted into pre-planned positions using surgical guides.
- Implant shoulders were supracrestal according to the preplanned prosthetic positions.
- In the staged group, no implant placement was performed during the GBR procedure.
- AP was harvested from the alveolar ridge with single use bone collector (Safescraper, Osteogenics Biomedical, Lubbock, TX, USA).
- In the simultaneous group, AP was placed on the implant surface.
- AP was mixed with BDX (Bio-Oss, Geistlich AG, Wolhusen, Switzerland) in a 1:1 ratio (composite graft).

- Composite graft was adapted to the lateral and crestal surface of the alveolar ridge.
- Non-resorbable d-PTFE membrane (Cytoplast, Osteogenics Biomedical, Lubbock, USA) was fixed to the oral and buccal surface of the alveolar ridge with titanium pins (Frios Membrane Tacks, Dentsply, York, USA).
- After membrane fixation, 4-0 horizontal mattress sutures (Supramid, Braun AG, Tuttlingen, Germany) were placed into the oral flap and buccal periosteum to cover the membrane surface with the periosteal layer.
- 5-0 horizontal mattress and non-interrupted sutures (Supramid, Braun AG, Tuttlingen, Germany) were used to close the mucosa above the periosteum.
- Suture removal was performed after 14 days.

In the simultaneous group, 9 months after GBR procedure, if adequate soft tissue thickness and keratinized mucosa width was found, implant uncovery was performed with titanium pin- and membrane removal. If less than 2 mm vertical soft tissue thickness was detected above implant, soft tissue augmentation procedure was performed without implant uncovery. In case of suboptimal keratinized tissue width, additional vestibuloplasty was performed with a free gingival graft from hard palate to create at least 3 mm attached mucosa around the implant neck at the time of implant uncovery process, which was performed 2 months after vestibuloplasty.

In the staged group 9 months after GBR procedure, implant placement was performed. Following split-thickness flap preparation, titanium pins and d-PTFE membranes were removed and Straumann Bone Level Implants (Straumann AG, Basel, Switzerland) were placed utilizing surgical guides. 5-0 horizontal mattress sutures and single interrupted sutures were used to close the flap for submucosal healing. If less than 2 mm vertical soft tissue thickness was detected above implant neck, additional soft tissue augmentation procedure was performed by SCTG. After 2 months of healing, if suboptimal keratinized tissue was present, similar vestibuloplasty procedure was performed as described in the simultaneous group. Implant uncovery was performed 2 months after vestibuloplasty or 3 months after implant insertion if adequate keratinized tissue was presented.

3.2.3 Postoperative care

Systemic antibiotic therapy (Penicillin with Clavulanic acid 2x1000mg/day; Augmentin Duo, GlaxoSmithKline, Brentford, United Kingdom), and non-steroidal anti-inflammatory drugs (Diclofenac-Sodium 4x50mg/day; Cataflam, Novartis International AG, Basel, Switzerland) were prescribed for 1 week after GBR procedure in order to avoid infections and to decrease swelling and pain. Chlorhexidine digluconate mouth wash 0.2% (Curasept ADS 220, Curaden AG, Kriens, Switzerland) was prescribed twice a day for chemical plaque control. Mucosal sutures were removed one week postoperatively, while periosteal mattress sutures were removed two weeks after surgery. Patients were recalled every week in the first month, after the first month patients were scheduled for recall visits every three months. Final fixed partial dentures were delivered 2 weeks after implant uncovery process and patients were enrolled to periodontal supportive therapy after the study.

DOI:10.14753/SE.2022.2638

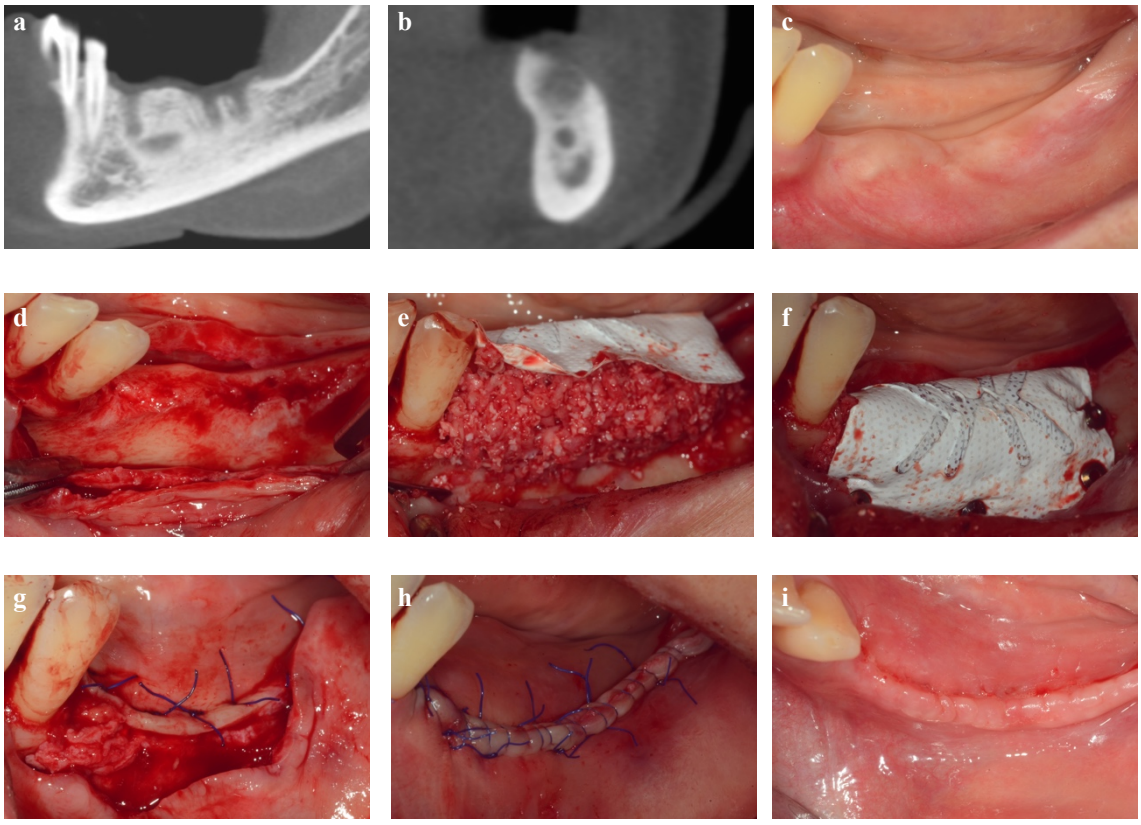

Fig. 5 Staged GBR procedure with split-thickness flap preparation /Case presentation/
a) Baseline CBCT scan, parasagittal section, chronic alveolar defect. b) Baseline CBCT scan, frontal section. c) Clinical view at surgery. d) Buccal split-thickness flap preparation. e) Composite graft on the alveolar ridge. f) Titanium-reinforced non-resorbable membrane fixation over the graft by titanium pins.
g) Double-layer suturing technique: horizontal mattress sutures between lingual flap and buccal periosteal layer. h) Horizontal mattress and single interrupted sutures between buccal and lingual mucosa. i) Early wound healing at 14 days after surgery. Figure from the publication related to Study II (Windisch et al. 2021), open access article.

DOI:10.14753/SE.2022.2638

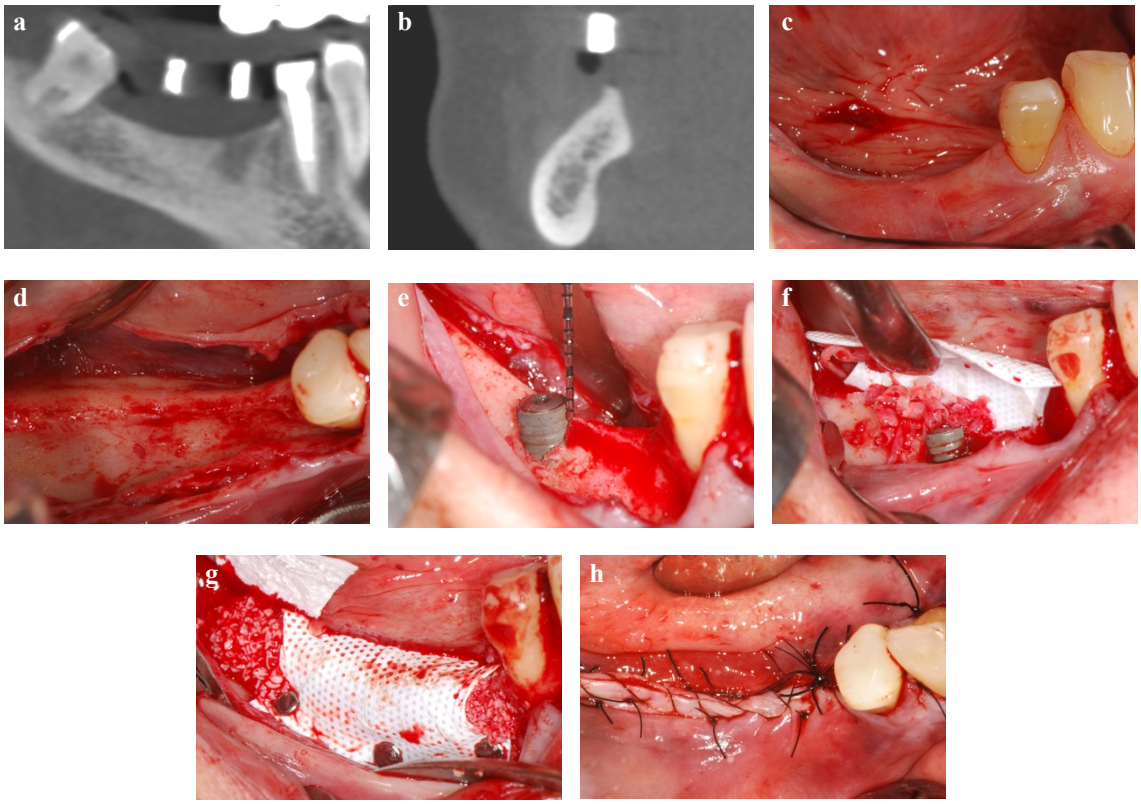

Fig. 6 Simultaneous GBR procedure with split-thickness flap preparation /Case presentation/

a) Baseline CBCT scan, parasagittal section, chronic alveolar defect. b) Baseline CBCT scan, frontal section. c) Clinical view at surgery. d) Buccal split-thickness flap preparation. e) Implant insertion, implant shoulder was supracrestal according to the preplanned prosthetic positions. f) AP around implant, composite graft on the alveolar ridge. g) Titanium-reinforced non-resorbable membrane fixation over the graft by titanium pins. h) Double-layer suturing technique: horizontal mattress sutures between lingual flap and buccal periosteal layer, then horizontal mattress and single interrupted sutures between buccal and lingual mucosa. Figure from the publication related to Study II (Windisch et al. 2021), open access article.

3.2.4 Clinical evaluation

In the simultaneous group, since postoperative CBCT scans were not taken, only direct clinical measurements were performed during GBR and at implant uncovery process. During surgeries, vertical dimension values and horizontal dimension values were measured by UNC-15 probes (HU-Friedy, Chicago, IL, USA). Clinical vertical dimension (c-VD) was the distance between crestal bone level and the most coronal part of the supracrestally positioned implants. During GBR procedure, this distance represented the lack of hard tissue, thus it was recorded as a negative value. C-VD was recorded in the vestibular, oral, mesial and distal aspects of the dental implant and mean values were calculated. Clinical horizontal dimension (c-HD) was the distance between buccal and oral cortical bone at the level of implant neck. This value was by definition zero in every case at the first surgery. After GBR procedure, at the time of implant uncovery process, c-VD and c-HD were measured again, then vertical and horizontal hard tissue dimension gain (c-VDG and c-HDG, respectively) was calculated.
In the staged group, direct clinical measurements were executed by UNC-13 probes. c-VD was the distance between crestal bone level and the top of the surgical guide's sleeve at the planned implant position. c-HD was measured as described in the simultaneous group. At the time of implant placement, measurements were repeated and c-VDG and c-HDG was calculated.

3.2.5 Digital radiographic evaluation

In the simultaneous group only preoperative CBCT datasets were available, thus radiographic evaluation was not possible. In the staged group, postoperative CBCT scans were taken 9 months after GBR procedure, prior to implant placement to investigate the newly formed hard tissue quantity. To obtain more data on hard tissue changes, radiographic evaluation was performed based on CBCT data sets. Radiographic linear measurements were performed by i-CAT Vision software (Imaging Sciences International, Hatfield, Pennsylvania, USA) after data sets alignment. On two separate computer screens the same patient's preoperative and postoperative CBCT scans were opened with the I-CAT Vision software at equal magnification level. The mesial tooth

next to the surgical area was chosen as a reference. In the multiplanar reconstruction (MPR) view's frontal section, the image was rotated until the axis of the tooth was superimposed on the sagittal section line. In the sagittal section, the same superimposition was performed. Pre- and postoperative radiographic vertical (r-VD) and horizontal dimensions (r-HD) were measured at the planned implant position, and changes were calculated as vertical and horizontal dimension gain (r-VDG and r-HDG, respectively). If more than one implant was placed, similar linear measurements were performed at each implant site, but only the highest value was recorded. In addition, radiographic volumetric measurement (r-VOL) was performed with the Osirix software (Pixmeo Sarl, Geneva, Switzerland) to evaluate 3D hard tissue changes.

3.2.6 Statistical Analysis

Patients in the two groups underwent similar surgical procedures, however different measurement protocols were applied, thus intergroup comparison of hard tissue changes was uninterpretable for statistical reasons. Therefore, only descriptive statistics were performed as mean values and standard deviations (SD).

3.3 Study III

Accuracy of Half-Guided Implant Placement with Machine-Driven or Manual Insertion: A Prospective, Randomized Clinical Study

In this prospective, randomized clinical study half-guided implant placements were performed to evaluate the implant position accuracy. Patients were selected at the Department of Periodontology, Semmelweis University between January 2017 and January 2019.

Inclusion criteria were the following: at least one missing upper premolar or molar tooth, and the edentulous area was treated by maxillary sinus floor elevation procedure with BDX (cerabone, botiss biomaterials, Zossen, Germany). Success of surgical intervention was confirmed by CBCT scans. Full- mouth plaque and bleeding scores (FMPS and FMBS) under 20%, with good patient compliance (including willingness to participate in the follow-up procedures). Surgical interventions were undertaken with the understanding and written informed consent of each subject. Exclusion criteria were the following: any clinically relevant diseases (e.g.: diabetes, rheumatism, malignant diseases), untreated periodontitis, systemic steroid or bisphosphonate use, acute or chronic inflammatory processes at the operation site.

The study conformed to the tenets of the Declaration of Helsinki (as amended in 2013) in all respects. The study protocol was approved by the Regional and Institutional Committee of Science and Research Ethics at the Semmelweis University (Approval Number: SE TUKEB 7/2017). Surgical interventions were undertaken with the understanding and written consent of each subject.

3.3.1 Preoperative imaging and planning

Six months after sinus floor elevation procedure, the SMART Guide workflow (SMART Guide, dicomLAB Dental, Szeged, Hungary) was applied to prepare a surgical guide for half-guided implant placement. During the workflow, C-silicone impressions (Zetaplus, Zhermack, Badia Polesine, Italy) were taken of each patients' upper jaw with the SMART Guide plastic impression tray containing radiographic markers. Two CBCT scans (Planmeca Viso, Planmeca, Helsinki, Finland) were taken to allow digital planning

process: the first CBCT scan was taken of the patient with the impression in situ, while the second CBCT scan was taken of the impression alone. After segmentation process, digital implant position planning was performed based on digital wax-ups. In the digital plan each patient received at least one Straumann RN Standard Plus implant (Straumann, Basel, Switzerland) in the augmented area. If needed, further implants were placed by the same protocol, but only the study implant was included in the data analysis. Finally, tooth-supported surgical guides were printed for half-guided implant placement.

3.3.2 Preoperative care

Four weeks before implant placement, all patients underwent professional oral hygiene treatment, which included supra- and subgingival scaling and individual oral hygiene instructions to keep FMPS and FMBS under 25% during the whole treatment period. At the time of implant surgery, patients rinsed with chlorhexidine digluconate 0.2% mouth rinse (Curasept ADS 220, Curaden AG, Kriens, Switzerland) for 2 minutes.

3.3.3 Implant placement

Patients in both groups received at least one Straumann implant in a half-guided implant placement procedure (Fig. 7 and Fig. 8). The steps were the following:

- Local anaesthesia was given (4% articaine-hydrochloride with 0.0001% epinephrine - Ultracain DS Forte, Sanofi-Aventis, Paris, France).
- A slightly palatal paracrestal incision was placed in the keratinized mucosa with No. 15 blades (Aesculap, Braun, Tutlingen, Germany) in the edentulous area, continued intracrevicularly at the neighbouring teeth.
- Mesial vertical releasing incision was placed, if it deemed necessary.
- Full-thickness mucoperiosteal flap was reflected in the buccal side, while no flap elevation was performed in the palatal side.
- Implant osteotomy was performed in the planned implant position based on the SMART Guide drilling protocol with a surgical motor (NSK Surgic Pro, Nakanishi, Kanuma Tochigi, Japan) using SMART Guide Universal drill kit.

- In the machine-driven group, implant insertion was performed with a 20:1 surgical contra-angled handpiece with 50 RPM and up to 35 Ncm torque.
- In the manual group, implant insertion was performed with a torque wrench.
- In both groups implant insertion torque was measured in Ncm.
- Duration of implant insertion was measured in seconds by a stopwatch from the time when implant touched the bone surface till reaching the final position.
- After implant insertion, implant closure screws were placed for submucosal healing.
- The mucoperiosteal flap was closed with 5-0 non-resorbable single interrupted and continuous interlocking sutures (Supramid, Braun, Tuttlingen, Germany).

3.3.4 Postoperative care

Systemic antibiotic therapy (Penicillin with Clavulanic acid 2x1000mg/day; Augmentin Duo, GlaxoSmithKline, Brentford, United Kingdom), and non-steroidal anti-inflammatory drugs (Diclofenac- Sodium 4x50mg/day; Cataflam, Novartis International AG, Basel, Switzerland) were prescribed for 7 days after implant placement. In case of penicillin allergy, 4x300mg/day clindamycin (Dalacin C, Pfizer, New York, USA) was prescribed for 7 days. A 0.2% chlorhexidine digluconate mouth rinse (Curasept ADS 220, Curaden AG, Kriens, Switzerland) was prescribed 3 times a day for chemical plaque control. Sutures were removed 10 days postoperatively. After the study, patients were enrolled into periodontal supportive therapy.

DOI:10.14753/SE.2022.2638

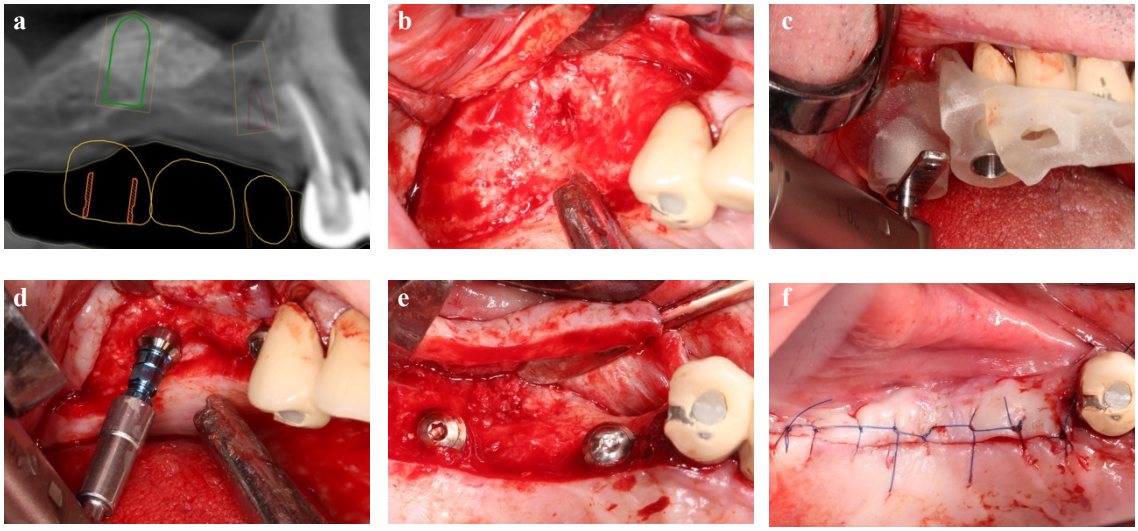

Fig. 7 Half-guided implant placement in the machine-driven group

/Case presentation/

a) Planned implant position on preoperative CBCT scan. b) Clinical view of edentulous maxilla. c) Guided implant osteotomy. d) Motor-driven implant insertion with contra-angled surgical handpiece. e) Inserted implants. f) Wound closure with 5-0 non-resorbable sutures. Figure from the publication related to Study III (Orban et al. 2021), open access article.

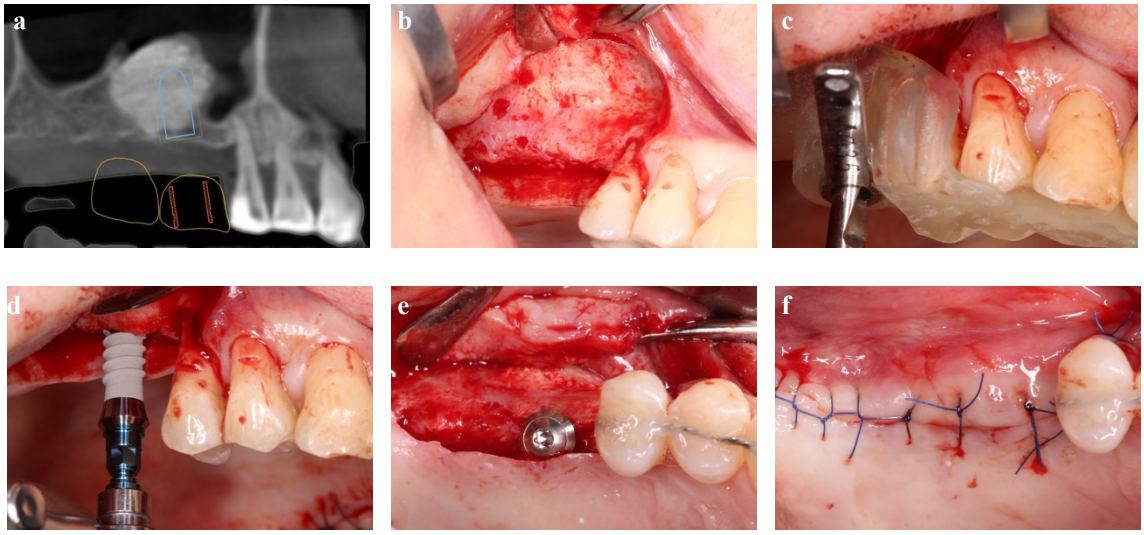

Fig. 8 Half-guided implant placement in the manual group /Case presentation/
a) Planned implant position on preoperative CBCT scan. b) Clinical view of edentulous maxilla. c) Guided implant osteotomy. d) Manual implant insertion with torque wrench. e) Inserted implant. f) Wound closure with 5-0 non-resorbable sutures. Figure from the publication related to Study III (Orban et al. 2021), open access article.

3.3.5 Implant re-entry, intraoral scanning for the positional accuracy analysis

After 3 months of healing, patients were recalled for implant re-entry procedure. After local anaesthesia was given, a mucoperiosteal flap was prepared to visualize the implant cover screw. PMMA implant scanbodies (CARES CI RD Mono Scanbody, Straumann, Basel, Switzerland) were connected to the implants to take a digital impression with an intraoral scanner (Planmeca Planscan; Planmeca, Helsinki, Finland). The scanning process was performed under partial isolation (Optragate, Ivoclar Vivadent, Schaan, Liechtenstein). At least three neighbouring teeth were involved in the region of interest (ROI). After digital scanning, healing abutments were connected and 5-0 sutures (Supramid, Braun AG, Tuttlingen, Germany) were placed. Sutures were removed 7 days postoperatively.

3.3.6 Digital radiographic evaluation

Digital accuracy analysis was conducted in the Amira 5.4.0 software (Thermo Fisher Scientific, USA) with appropriate algorithms (dicomLAB Dental, Hungary). This measurement protocol was published by Varga et al. in 2010, and the workflow was described in detail. Briefly, the preoperative CBCT scans were aligned with postoperative intraoral scans in the coordinate system of the surgical plan. Actual implant position was determined by intraoral scans using the abutment position, thus during the measurement procedure we were able to compare the spatial relation of the planned and actual implant positions with a custom algorithm. Angular deviation (AD) was the angle between the axis of the planned and actual implant positions in degrees. Global coronal deviation (GCD) was the distance between the coronal endpoints of the planned and actual implants in millimetres, while global apical deviation (GAD) was the distance between the apical endpoints of the planned and actual implants in millimetres. To present more precise deviation parameters between planned and actual implant positions, GCD and GAD were broken down to 3 spatial vectors (Cx, Cy, Cz and Ax, Ay, Az, respectively), where x marked the mesio-distal dimension, y the oro-vestibular dimension and z the cranio-caudal dimension in millimetres. Horizontal coronal deviation (HCD) and horizontal apical deviation (HAD) were expressed from spatial coordinates as a vector sum of Cx + Cy and Ax + Ay, respectively in millimetres. Vertical deviation (VD) was measured at the apical endpoints and was equal to Az.

3.3.7 Data analysis

Statistical analysis was conducted using SPSS 23.0 (IBM, USA). The measured values were descriptively characterized as means and standard deviations. For the hypothesis tests (between-groups comparisons), one-way ANOVA was used. The level of statistical significance was set at $p<0.05$.

DOI:10.14753/SE.2022.2638

4. RESULTS

4.1 Study I

Demonstration of Radiographic Bone Fill in Postextraction Sockets Using a Novel Implant-Site Development Technique: A Retrospective Comparative Case Series

29 patients a total of 33 hopeless single-rooted teeth were extracted, and subsequent ARP was performed in the test group at the Department of Periodontology, Semmelweis University. In 14 patients a total of 21 single-rooted teeth were extracted and left for spontaneous healing in the control group at the Department of Oro-Maxillofacial Surgery and Stomatology, Semmelweis University from 2007 to 2014. Patients' demography and tooth distribution is summarized in Table 1.

Table 1 Patient demography and tooth distribution in test and control group

		Test group	*Control group*
Patient number		*29*	*14*
Age (years)			*50.5± 15.9*
Sex	*Male*	*11*	*6*
	Female	*18*	*8*
Tooth type	*Incisor*	*27*	*16*
	Canine	*2*	*2*
	Premolar	*4*	*3*
Dental arch	*Maxilla*	*29*	*11*
	Mandible	*4*	*10*
Total number of teeth		*33*	*21*

4.1.1 Clinical findings

In the test group after XSD approach healing was uneventful. At re-entry, expected amount of hard tissue was observed, which seemed vital during implant osteotomy. Implant placement was performed in 14 cases without any additional hard tissue augmentation method, 5 cases received implants with minor simultaneous GBR procedure, while 6 sites treated first with GBR procedure and after 6 months healing implants were inserted. Four patients from the remaining 8 patients received fixed partial dentures with pontics at the treated site, while 4 patients received their prosthetic rehabilitation elsewhere. In the control group, clinical data were not recorded, only radiographic evaluation was performed.

4.1.2 Radiographic findings

Since postextractional alveolar hard tissue changes were mainly observed close to the crestal level, thus horizontal hard tissue change evaluations were only reported on the coronal third of the socket, further data are not shown. In the test group, baseline hard tissue dimensions were considerably less in the midbuccal section compared to the control group. For example, in the midbuccal section the mean OV ranged from 1.4 - 4.8 mm in the test group compared to 4.7 - 7.5 mm in the control group. A similar baseline situation was observed in terms of VER and SA. In the test group, baseline midbuccal VER averaged 11.6 ± 4.4 mm buccally, compared to 17.5 ± 5.6 mm was in the control group. Mean baseline midbuccal SA was 122.8 ± 50.5 mm^2 in the test group, 163.8 ± 52.7 mm^2 in the control group.

Hard tissue dimension changes were calculated with subtraction: preoperative values were subtracted from postoperative values. Outcomes were presented in absolute value, thus positive outcomes indicate hard tissue gain, while negative results point towards hard tissue loss. In the midbuccal section, OV, VER and SA changes were significantly less in the test group compared to the control group (Fig. 9 and Fig. 10). In the test group OV changes were significantly less in most sections compared to the control group. Vertical hard tissue dimension changes are best seen in the midbuccal section: in the buccal site VER changes were almost the same in both groups, but while in the control group an

average 2.26 ± 2.41 mm hard tissue loss was observed, in the test group an average 2.23 ± 3.35 mm hard tissue gain was detected. In the test group, SA yielded an average 11.34 ± 23.74 mm^2 hard tissue gain, while an average 26.34 ± 20.13 mm^2 hard tissue loss was found in the control group. The complete pre- and postoperative dimensions and dimension changes are presented in Table 2, Table 3, Table 4 and Fig. 11, Fig. 12, and Fig. 13.

DOI:10.14753/SE.2022.2638

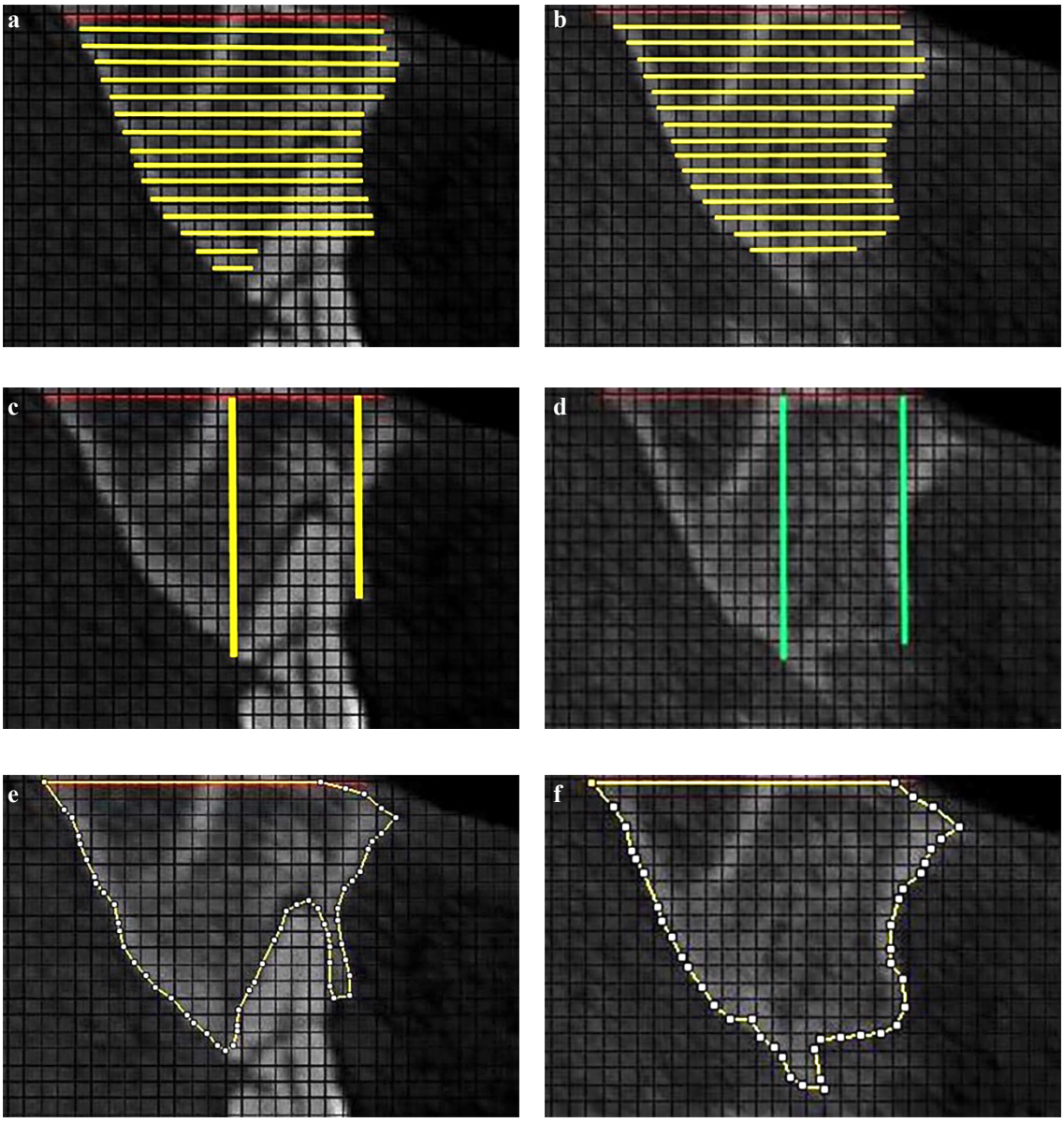

Fig. 9 Radiographic evaluation protocol, hard tissue dimension changes in a test patient a) Baseline OV dimensions. b) Postoperative OV dimensions. c) Baseline VER dimensions. d) Postoperative VER dimensions. e) Baseline SA. f) Postoperative SA. OV = Orovestibular socket dimension, VER = Vertical socket dimension, SA = Socket areas. The presented case is from the Study I (Molnar et al. 2019), copy rights are purchased from Quintessence Publishing Company Inc.

DOI:10.14753/SE.2022.2638

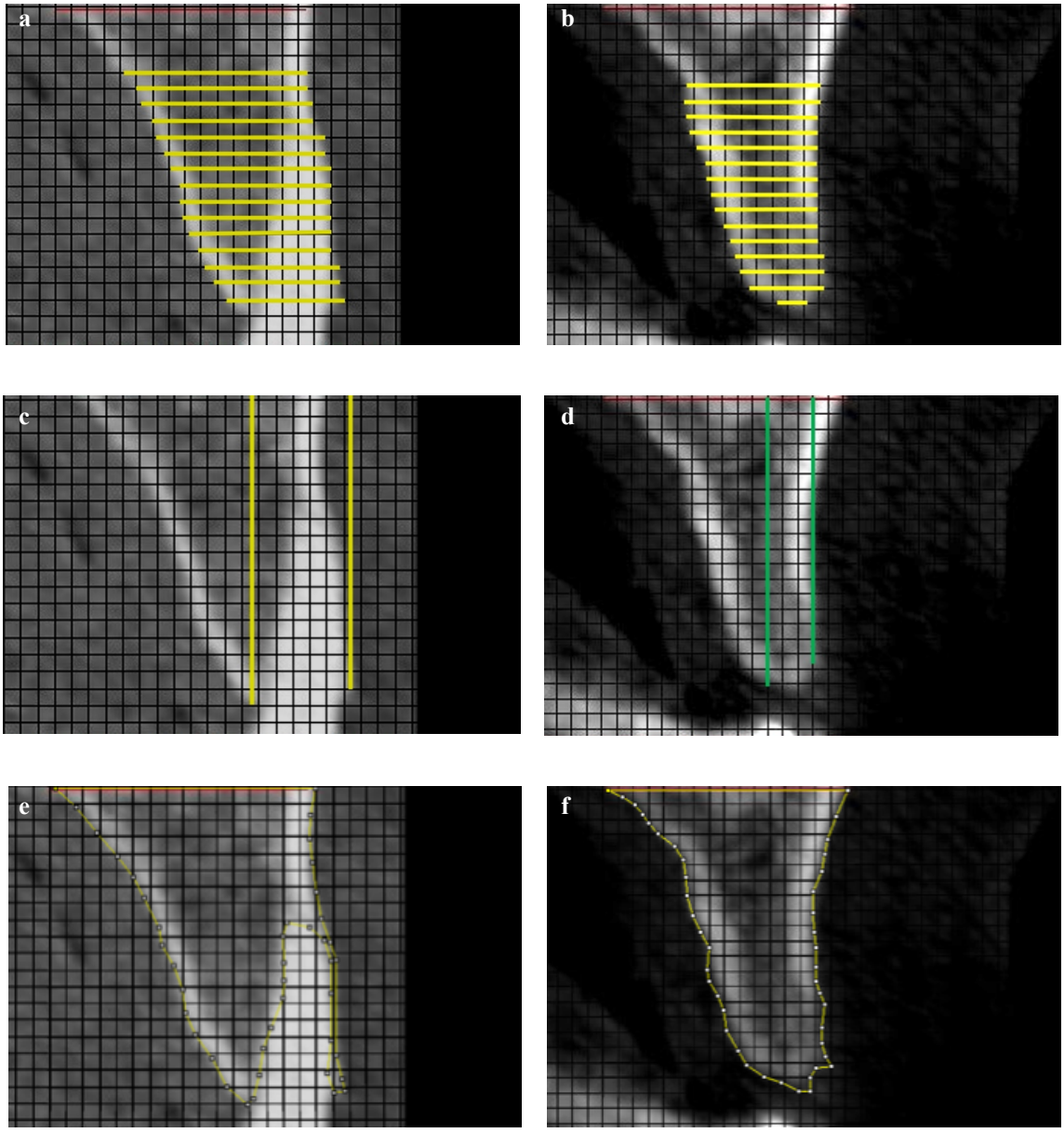

Fig. 10 Radiographic evaluation protocol, hard tissue dimension changes in a control patient

a) Baseline OV dimensions. b) Postoperative OV dimensions. c) Baseline VER dimensions. d) Postoperative VER dimensions. e) Baseline SA. f) Postoperative SA.

OV = Orovestibular socket dimension, VER = Vertical socket dimension, SA = Socket areas. Figure from the publication related to Study I (Molnar et al. 2019), copyrights are purchased from Quintessence Publishing Company Inc.

DOI:10.14753/SE.2022.2638

Table 2 Baseline orovestibular socket dimensions (OV) and postoperative OV changes (ΔOV).
NS = Not significant. Changes measured in the coronal third of the alveoli. Positive differences represent bone gain, negative differences denote bone loss. All numeric P values shown here are statistically significant.

	Mean baseline OV (mm)			*Mean ΔOV (mm)*		
Section	*Test*	*Control*	*P*	*Test*	*Control*	*P*
Mesial						
11	*5.8 ± 2.8*	*6.5 ± 2.3*	*NS*	*-0.19 ± 1.78*	*-0.90 ± 1.55*	*NS*
12	*4.5 ± 3.4*	*6.2 ± 2.6*	*.041**	*0.23 ± 1.76*	*-1.46 ± 2.27*	*.003**
13	*3.8 ± 3.1*	*5.4 ± 3.1*	*NS*	*0.24 ± 1.85*	*-1.33 ± 1.57*	*.002**
14	*2.4 ± 2.5*	*4.8 ± 2.9*	*.002**	*0.39 ± 1.83*	*-1.52 ± 2.30*	*.001**
15	*1.4 ± 1.9*	*3.3 ± 3.2*	*.01**	*0.42 ± 1.51*	*-1.40 ± 3.04*	*.017**
Midbuccal						
11	*4.8 ± 3.4*	*7.5 ± 2.8*	*.004**	*0.73 ± 2.09*	*-2.55 ± 2.52*	*< .001**
12	*3.9 ± 3.4*	*7.0 ± 3.3*	*.002**	*0.86 ± 2.47*	*-2.73 ± 2.90*	*< .001**
13	*3.2 ± 3.5*	*6.3 ± 3.2*	*.002**	*0.73 ± 2.04*	*-2.63 ± 3.09*	*< .001**
14	*2.6 ± 3.4*	*5.8 ± 3.6*	*.003**	*0.16 ± 1.97*	*-2.73 ± 3.12*	*< .001**
15	*1.4 ± 2.3*	*4.7 ± 3.5*	*< .001**	*0.48 ± 1.60*	*-2.71 ± 3.46*	*.001**
Distal						
11	*6.2 ± 3.0*	*6.9 ± 3.0*	*NS*	*0.05 ± 1.30*	*-1.41 ± 2.02*	*.006**
12	*5.5 ± 3.2*	*5.4 ± 2.8*	*NS*	*-0.05 ± 1.76*	*-1.42 ± 1.79*	*.002**
13	*4.2 ± 3.2*	*5.9 ± 2.7*	*NS*	*-0.01 ± 2.13*	*-1.40 ± 2.49*	*.033**
14	*3.8 ± 3.0*	*5.5 ± 2.6*	*.033**	*-0.57 ± 1.98*	*-2.35 ± 3.24*	*.015**
15	*2.4 ± 2.6*	*3.8 ± 2.7*	*NS*	*-0.62 ± 1.70*	*-1.62 ± 3.38*	*NS*

DOI:10.14753/SE.2022.2638

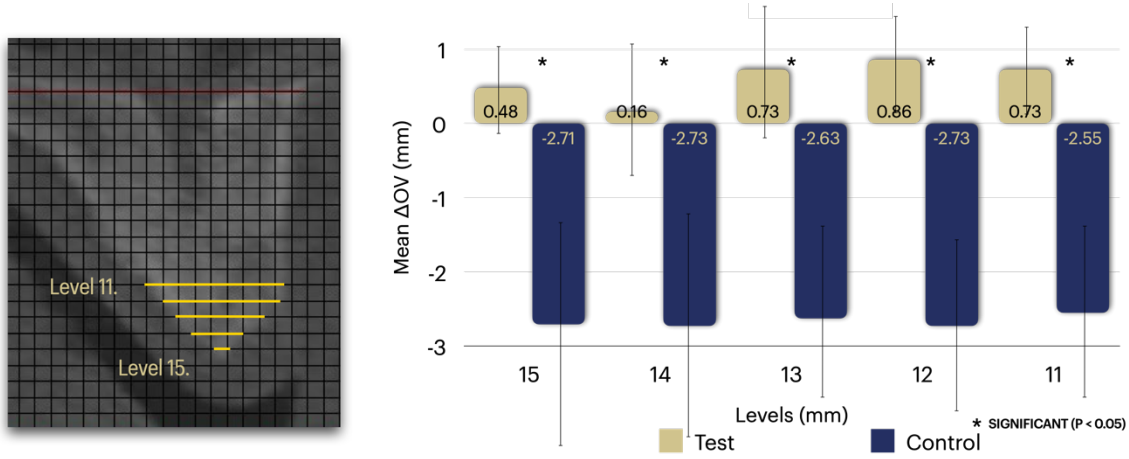

Fig. 11 Orovestibular socket dimensions changes (ΔOV) in the midbuccal sections Positive differences represent bone gain, negative differences denote bone loss.

DOI:10.14753/SE.2022.2638

Table 3 Baseline vertical socket dimensions (VER) and postoperative VER changes (ΔVER)
NS = Not significant. Positive differences represent bone gain, negative differences denote bone loss. All numeric P values shown here are statistically significant.

	Mean baseline VER (mm)			*Mean ΔVER (mm)*		
Section	*Test*	*Control*	*P*	*Test*	*Control*	*P*
Mesial						
Buccal	*13.8 ± 4.7*	*19.1 ± 5.5*	*< .001**	*0.77 ± 2.45*	*-1.31 ± 1.39*	*.001**
Palatal	*15.3 ± 4.4*	*19.0 ± 6.0*	*.001**	*0.01 ± 1.45*	*-1.26 ± 2.21*	*.027**
Midbuccal						
Buccal	*11.6 ± 4.4*	*17.5 ± 5.6*	*.011**	*2.23 ± 3.35*	*-2.26 ± 2.41*	*.001**
Palatal	*15.0 ± 4.0*	*18.5 ± 5.5*	*.010**	*-0.25 ± 2.15*	*-1.64 ± 1.57*	*.013**
Distal						
Buccal	*15.1 ± 5.2*	*18.3 ± 5.3*	*.035**	*-0.36 ± 2.73*	*-0.54 ± 2.17*	*NS*
Palatal	*16.0 ± 4.9*	*18.3 ± 5.2*	*NS*	*-0.97 ± 4.3*	*-1.42 ± 2.24*	*NS*

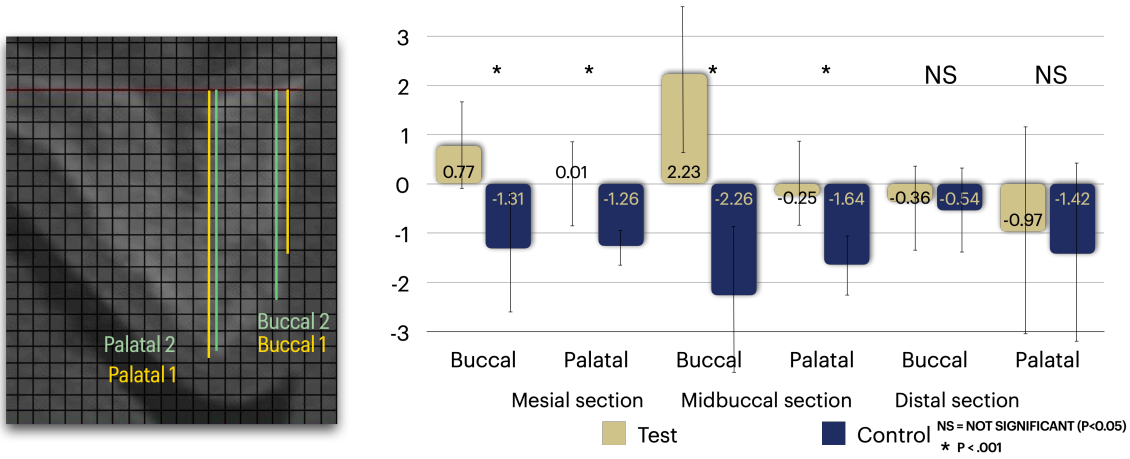

Fig. 12 Vertical socket dimensions changes (ΔVER)
Positive differences represent bone gain, negative differences denote bone loss.

DOI:10.14753/SE.2022.2638

Table 4 Baseline socket areas (SA) and postoperative SA changes (ΔSA)

NS = Not significant. Positive differences represent bone gain, negative differences denote bone loss. All numeric P values shown here are statistically significant.

	Mean baseline SA (mm^2)			*Mean ΔVER (mm^2)*		
Section	*Test*	*Control*	*P*	*Test*	*Control*	*P*
Mesial	*124.3 ± 64.3*	*158 ± 56.4*	*NS*	*5.65 ± 23.34*	*-20.05 ± 13.72*	*.001**
Midbuccal	*122.8 ± 50.5*	*163 ± 52.7*	*.006**	*11.34 ± 23.74*	*-26.34 ± 20.13*	*.001**
Distal	*141.6 ± 49.6*	*159 ± 61.5*	*NS*	*-0.62 ± 21.50*	*-21.76 ± 24.19*	*.001**

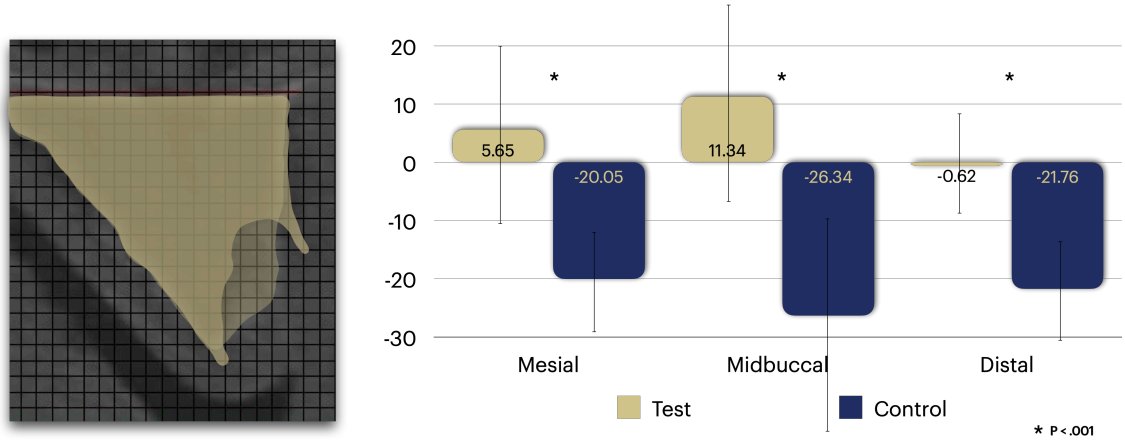

Fig. 13 Socket area changes (ΔSA)

Positive differences represent bone gain, negative differences denote bone loss.

DOI:10.14753/SE.2022.2638

4.2 Study II

Vertical-guided Bone Regeneration with a Titanium-Reinforced D-PTFE Membrane Utilizing a Novel Split-Thickness Flap Design: A Prospective Case Series

Nineteen systemically healthy patients were selected and treated at the Department of Periodontology, Semmelweis University between January 2012 and June 2015. Patients were divided into two groups based on baseline extent of alveolar hard tissue. If at least 6 mm vertical bone was detected at the edentulous area, implant placement was performed simultaneous with GBR procedure (simultaneous group), while if bone extent was less than 6 mm vertically, GBR procedure was performed first, followed by implant insertion 9 months later (staged group). One patient was represented in both groups. All together 24 surgical interventions were performed, patients' demography and surgical site distribution is presented in Table 5.

Table 5 Patients demography and surgical site distribution in the two study groups

		Simultaneous group	*Staged group*
Patient number		*5*	*15*
Age (years)			*50.8 ± 12.2*
Sex	*Male*	*1*	*1*
	Female	*5*	*17*
Surgical area	*Maxilla*	*2*	*6*
	Mandible	*4*	*12*
Inserted implants		*9*	*36*

4.2.1 Clinical findings

The healing of the GBR procedures was uneventful in 23 out of 24 cases, moderate pain and swelling as reported by the patients. Only 1 site from the staged group showed early membrane exposure without bacterial contamination, in this case, 6 weeks after GBR procedure the d-PTFE membrane was replaced by a resorbable collagen membrane (Bio-Gide, Geistlich AG, Wolhusen, Switzerland), after healing the surgical site was suitable for implant placement with additional connective tissue graft augmentation to compensate tissue loss.

In the simultaneous group, 9 implants were placed in 5 patients' 6 surgical sites. Average c-VDG was 3.19 ± 1.88 mm, while average c-HDG was 6.48 ± 0.46 mm. The GBR procedure's success rate was expressed in the simultaneous group, where 100% success rate refers to implant surfaces completely covered with newly formed hard tissue. The success rate of GBR was 92.6% in the simultaneous group. Around 7 of 9 implants were fully covered with hard tissue, around 1 implant a 1 mm buccal bone dehiscence was observed, while around 1 implant a mean 2 mm (Patient 1, implant in position 16) bone dehiscence was recorded. In this case, the success rate was 50%.

In the staged group, after GBR procedure, 36 implants were inserted in 15 patients' 18 surgical sites. Mean c-VDG and c-HDG was 4.50 ± 2.15 mm and 8.72 ± 2.30 mm, respectively. In the staged group percentage-based success rate was not reported, since all implants were placed in a submerged position determined by the newly formed crestal bone level (Fig. 14 and Fig. 15).

4.2.2 Radiographic findings

In the staged group, pre-and postoperative CBCT data sets were available to evaluate hard tissue changes. After data set alignment, linear radiographic measurements were performed at the planned implant positions. Mean r-VDG and r-HDG were 4.22 ± 2.03 mm and 8.53 ± 2.37 mm, respectively.

3D volumetric measurements were performed in 11 of 13 surgical sites, pre-and postoperative volume of the surgical area was calculated and subtracted. The average r-VOL was 1.11 ± 0.42 cm^3.

DOI:10.14753/SE.2022.2638

Clinical hard tissue changes of the simultaneous group are presented in Table 6, clinical hard tissue changes and volumetric measurements of the staged group are presented in Table 7. Clinical hard tissue changes in the staged and simultaneous group, and radiographic volume changes in the staged group are presented in Fig. 16.

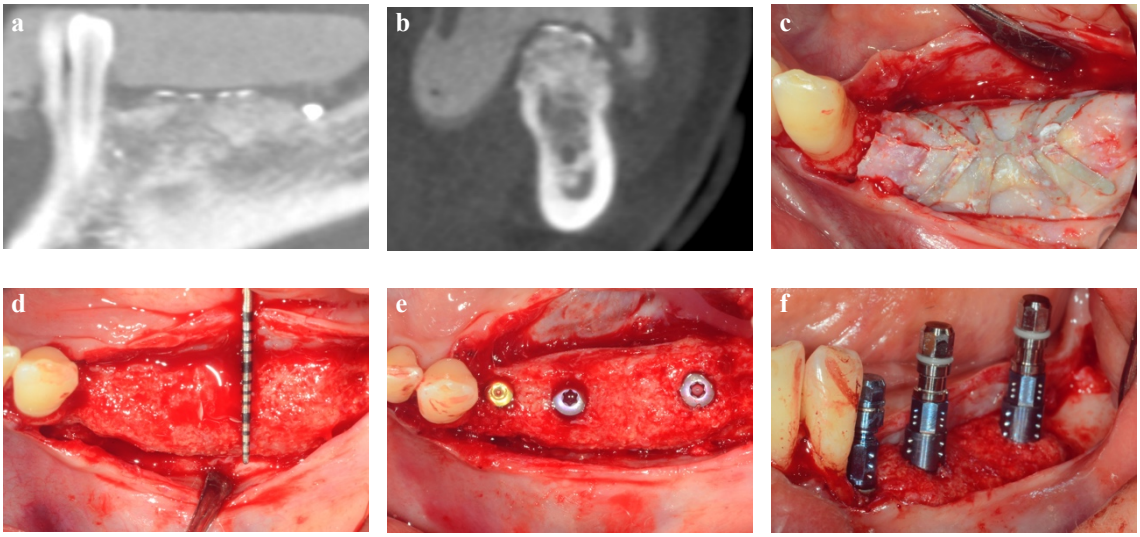

Fig. 14 Postoperative radiographic and clinical findings in the staged group /Case presentation/

a) Postoperative CBCT scan, parasagittal section, vertical hard tissue gain. b) Postoperative CBCT scan, frontal section, horizontal and vertical hard tissue gain. c) Membrane removal at 9 months re-entry. d) Clinical horizontal hard tissue gain. e) Guided implant placement. f) Prosthetically driven implant positioning. Figure from the publication related to Study II (Windisch et al. 2021), open access article.

DOI:10.14753/SE.2022.2638

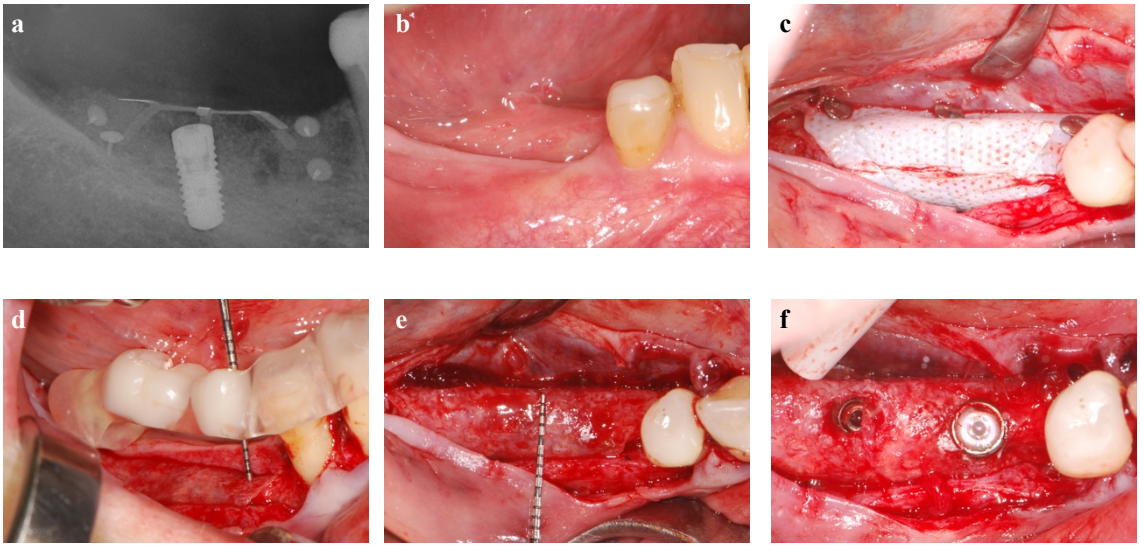

Fig. 15 Postoperative clinical findings in the simultaneous group /Case presentation/ a) Postoperative intraoral radiograph, vertical hard tissue gain. b) Clinical situation 9 months postoperatively. c) Membrane removal at 9 months re-entry. d) Clinical vertical hard tissue gain. e) Clinical horizontal hard tissue gain. f) Implant re-entry and additional prosthetically driven implant positioning. Figure from the publication related to Study II (Windisch et al. 2021), open access article.

DOI:10.14753/SE.2022.2638

Table 6 Clinical hard tissue changes in the simultaneous group

c-VDG = Clinical Vertical Dimension Gain, c-HDG = Clinical Horizontal Dimension Gain, SD = Standard Deviation.

Patient no, (site no.)	*Age (y)*	*Sex*	*Arch*	*Mean c-VDG (mm)*	*Mean c-HDG (mm)*
1 (1)	*38*	*F*	*Maxilla*	*2.00*	*6.60*
2 (2)	*35*	*M*	*Maxilla*	*6.90*	*6.30*
3 (3)	*36*	*F*	*Mandible*	*1.75*	*7.00*
4 (4)	*63*	*F*	*Mandible*	*2.75*	*7.00*
4 (5)	*63*	*F*	*Mandible*	*2.75*	*6.00*
5 (6)	*42*	*F*	*Mandible*	*3.00*	*6.00*
Mean				*3.19*	*6.48*
SD				*1.88*	*0.46*

DOI:10.14753/SE.2022.2638

Table 7 Clinical hard tissue changes and radiographic volumetric measurements in the staged group

c-VDG = Clinical Vertical Dimension Gain, c-HDG = Clinical Horizontal Dimension Gain, r-VOL = Radiographic Volume. SD = Standard Deviation.

Patient no, (site no.)	*Age (y)*	*Sex*	*Arch*	*Mean c-VDG (mm)*	*Mean c-HDG (mm)*	*r-VOL (ccm)*
1 (1)	*69*	*F*	*Mandible*	*1*	*4*	*0.82*
*2 (2) **	*62*	*F*	*Maxilla*	*6*	*11*	
3 (3)	*67*	*F*	*Maxilla*	*2*	*8*	*0.96*
*4 (4) **	*57*	*F*	*Maxilla*	*3*	*15*	
*4 (5) **			*Maxilla*	*3*	*10*	
5 (6)	*57*	*F*	*Mandible*	*5*	*8*	*0.89*
5 (7)			*Mandible*	*9*	*8*	*1.48*
6 (8)	*22*	*F*	*Maxilla*	*4*	*8*	*1.00*
7 (9)	*46*	*F*	*Mandible*	*6*	*8*	*0.87*
8 (10)	*56*	*F*	*Mandible*	*4*	*7*	*1.01*
9 (11)	*42*	*F*	*Mandible*	*6*	*10*	*0.60*
10 (12)	*43*	*M*	*Maxilla*	*8*	*7*	
11 (13)	*49*	*F*	*Mandible*	*6*	*9*	*1.81*
11 (14)			*Mandible*	*4*	*8*	*1.88*
12 (15)	*64*	*F*	*Mandible*	*1*	*7*	
13 (16)	*59*	*F*	*Mandible*	*4*	*10*	*1.49*
14 (17)	*38*	*F*	*Mandible*	*5*	*8*	*0.60*
15 (18)	*60*	*F*	*Mandible*	*4*	*11*	*0.96*
Average				*4.50*	*8.72*	*1.11*
SD				*2.15*	*2.30*	*0.42*

DOI:10.14753/SE.2022.2638

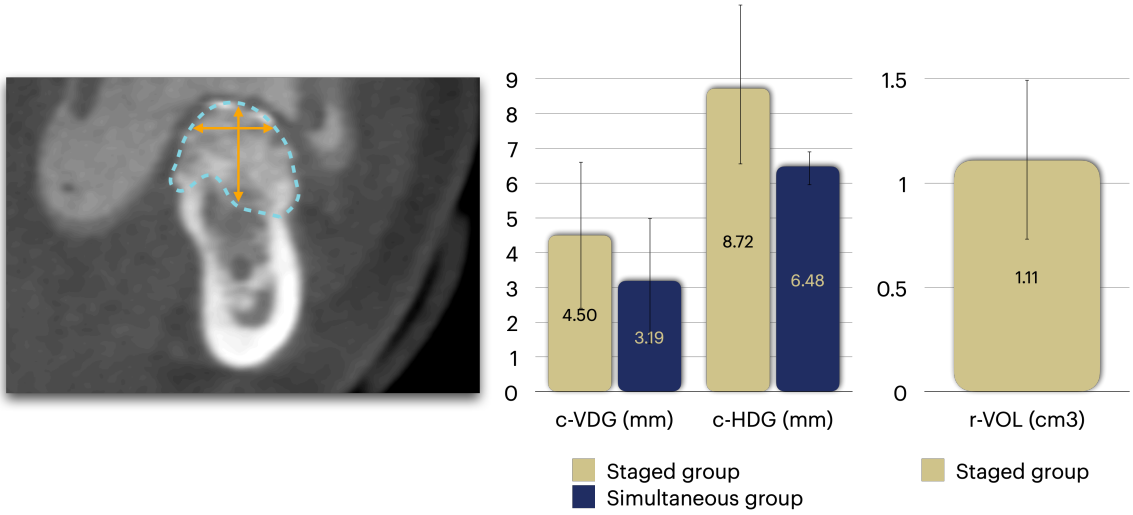

Fig. 16 Clinical hard tissue changes in the staged and simultaneous group. Radiographic volume changes in the staged group

c-VDG = Clinical Vertical Dimension Gain, c-HDG = Clinical Horizontal Dimension Gain, r-VOL = Radiographic Volume.

DOI:10.14753/SE.2022.2638

4.3 Study III

Accuracy of Half-Guided Implant Placement with Machine-Driven or Manual Insertion: A Prospective, Randomized Clinical Study

Forty patients were selected at the Department of Periodontology, Semmelweis University between January 2017 and January 2019. Six months after sinus elevation process, patients were divided into two study groups by a computer-generated randomization protocol (https://www.randomizer.org). In the first group, during half-guided implant placement, 20 implant insertions were performed by a surgical motor (machine-driven group), while in the second group, 20 implant insertions were performed by a torque-wrench (manual group). Table 8 presented the patients' demography and edentulous site distribution.

Table 8 Patient demography and edentulous site distribution

		Machine-driven group	*Manual group*
Patients number		*20*	*20*
Age (years)		*49 ± 10*	
Sex	*Male*	*9*	*10*
	Female	*11*	*10*
Edentulous site distribution	*Single-tooth gap*	*3*	*3*
	Multiple-teeth gap	*2*	*2*
	Free-end tooth gap	*15*	*15*

4.3.1 Clinical findings

Tooth-supported surgical templates created by the SMART Guide workflow were accurate and precisely fitted to the dental arch during half-guided implant placement. After implant osteotomy, in the manual group, implant insertion duration was an average 36.40 ± 8.15 s. In the machine-driven group, duration of implant insertion averaged 9.25 ± 1.86 s, which is significantly faster compared to the manual group.

At the end of implant insertion, insertion torque was measured, in the manual group mean insertion torque was 18.75 ± 7.05 Ncm, compared to 21.75 ± 9.75 Ncm in the machine-driven group. No significant difference was found between the groups.

4.3.2 Radiographic findings

Global deviation parameters were averaged, and results were the following: in the machine-driven group mean GCD was 1.20 ± 0.46 mm, compared to 1.13 ± 0.38 mm in the manual group, while mean GAD in the machine-driven group was 1.45 ± 0.79 mm, compared to 1.18 ± 0.28 mm in the manual group.

Results of horizontal deviation are the following: HCD averaged 1.06 ± 0.52 mm in the machine-driven group and 0.92 ± 0.40 mm in the manual group, while a mean HAD was 1.28± 0.83 mm in the machine-driven group and 0.99 ± 0.28 mm in the manual group.

Vertical dimension deviation was measured in the apical end of the implant, mean VD was 0.55 ± 0.28 mm in the machine-driven group compared to 0.62 ± 0.21 mm in the manual group.

AD was an average 4.82 ± 2.07° in the machine-driven group and 4.11 ± 1.63° in the manual group (Fig. 17, Fig. 18 and Fig. 19).

No significant differences were observed between the groups in any of the examined parameters. Clinical and radiographic results are presented in Table 9 and Table 10.

DOI:10.14753/SE.2022.2638

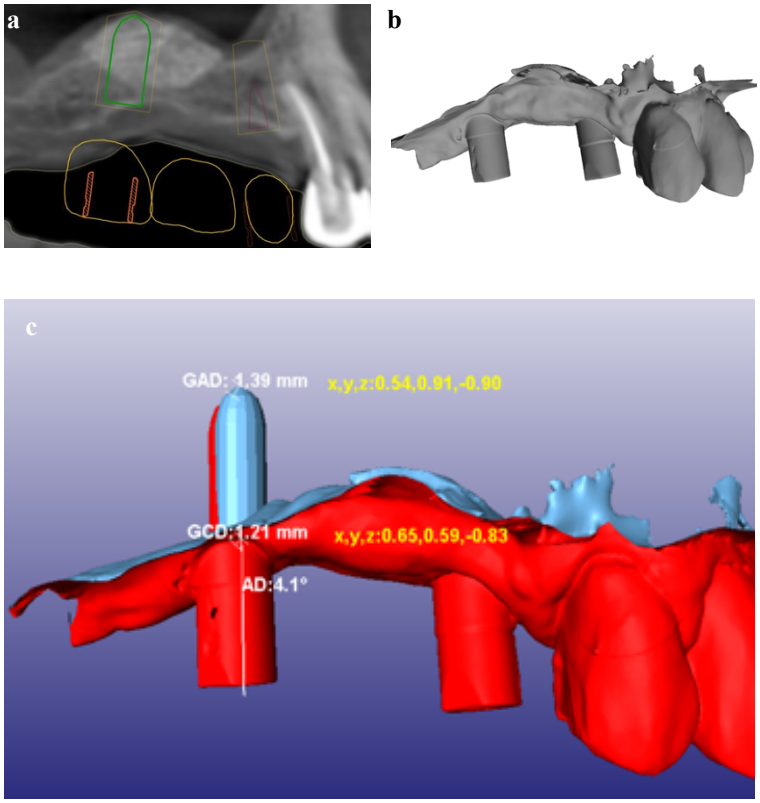

Fig. 17 Postoperative radiographic findings in the motor-driven group /Case presentation/ a) Planned implant position on preoperative CBCT scan. b) Digital model with scan bodies based on intraoral scanning at implant re-entry procedure. c) Comparison method, differences between planned and actual implant position. GCD = Global coronal deviation, GAD = Global apical deviation, AD = Angular deviation. Figure from the publication related to Study III (Orban et al. 2021), open access article.

DOI:10.14753/SE.2022.2638

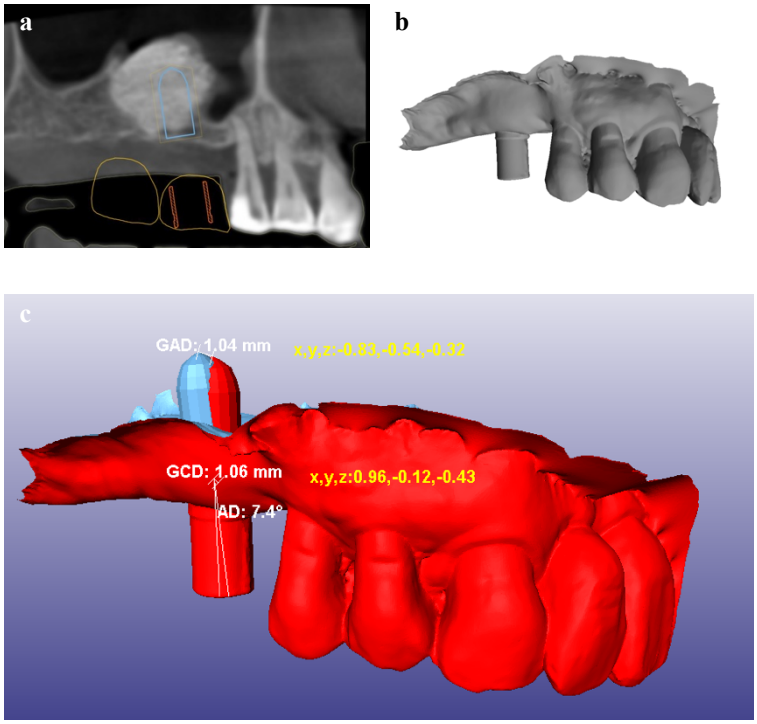

Fig. 18 Postoperative radiographic findings in the manual group /Case presentation/ a) Planned implant position on preoperative CBCT scan. b) Digital model with scan bodies based on intraoral scanning at implant re-entry procedure. c) Comparison method, differences between planned and actual implant position. GCD = Global coronal deviation, GAD = Global apical deviation, AD = Angular deviation. Figure from the publication related to Study III (Orban et al. 2021), open access article.

DOI:10.14753/SE.2022.2638

Table 9 Descriptive statistics of studied parameters in the two study groups and significance levels from the hypothesis tests.

GCD = Global coronal deviation; $C_{x,y,z}$ = Vectoral components of GCD; HCD = Horizontal coronal deviation; GAD = Global apical deviation; $A_{x,y,z}$ = Vectoral components of GAD; HAD = Horizontal apical deviation; AD = Angular deviation; τ = Insertion torque; t = Insertion duration; SD = Standard deviation; P = Significance.
*Az = Vertical deviation.

	Machine-driven group (N=20)		*Manual group (N=20)*		*Intergroup comparison*
	Mean	*SD*	*Mean*	*SD*	P
GCD (mm)	*1.20*	*0.46*	*1.13*	*0.31*	*0.58*
Cx (mm)	*0.81*	*0.31*	*0.75*	*0.32*	*0.31*
Cy (mm)	*1.00*	*0.58*	*0.45*	*0.39*	*0.26*
Cz (mm)	*0.44*	*0.26*	*0.55*	*0.25*	*0.87*
HCD (mm)	*1.06*	*0.52*	*0.92*	*0.4*	*0.37*
GAD (mm)	*1.45*	*0.79*	*1.18*	*0.28*	*0.17*
Ax (mm)	*0.92*	*0.39*	*0.72*	*0.33*	*0.70*
Ay (mm)	*0.76*	*0.88*	*0.58*	*0.31*	*0.72*
*Az (mm)**	*0.55*	*0.28*	*0.62*	*0.21*	*0.52*
HAD (mm)	*1.28*	*0.83*	*0.99*	*0.28*	*0.14*
AD (°)	*4.82*	*2.07*	*4.11*	*1.63*	*0.23*
τ (Ncm)	*21.75*	*9.75*	*18.75*	*7.05*	*0.27*
t (sec)	*9.25*	*1.86*	*36.4*	*8.15*	*<0.001*

DOI:10.14753/SE.2022.2638

Table 10 Descriptive statistics of accuracy parameters used for comparison with the literature, for the entire patient population (N=40).

GCD = Global coronal deviation; GAD = Global apical deviation; HCD = Horizontal coronal deviation; HAD = Horizontal apical deviation; A_z = Vertical deviation; AD = Angular deviation; SD = Standard deviation.

	Mean	*SD*
GCD (mm)	*1.16*	*0.38*
GAD (mm)	*1.32*	*0.54*
HCD (mm)	*0.99*	*0.46*
HAD (mm)	*1.14*	*0.55*
A_z (mm)	*0.59*	*0.24*
AD (°)	*4.46*	*1.85*

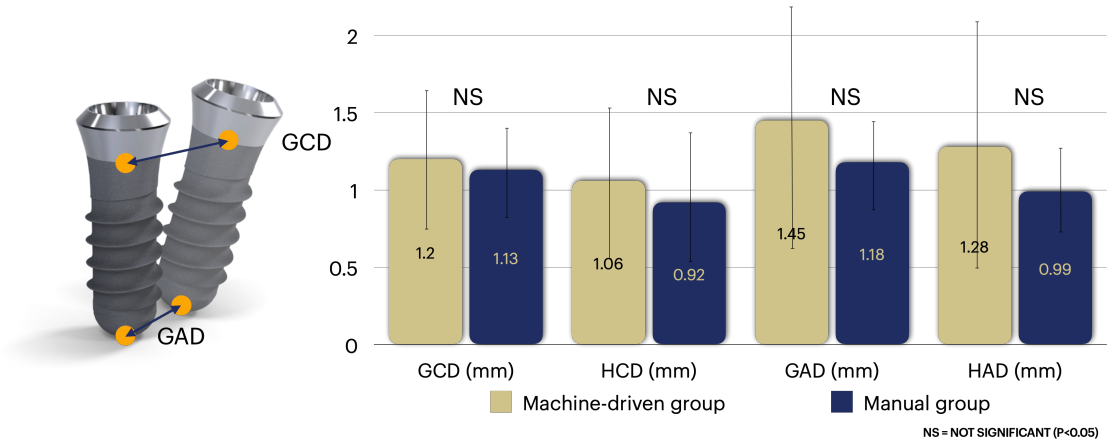

Fig. 19 Implant placement accuracy, global and horizontal deviations

GCD = Global coronal deviation; HCD = Horizontal coronal deviation; GAD = Global apical deviation; HAD = Horizontal apical deviation.

DOI:10.14753/SE.2022.2638

5. DISCUSSION

As a result of evolving treatment modalities in implant dentistry, prosthetic rehabilitation utilized by dental implants is no longer an alternative solution for the patients, but it is the primarily chosen option to treat partial- or full edentulism. In patients presenting hopeless teeth and acute alveolar defects, preservation of soft- and hard tissues at tooth extraction enables clinicians to maintain alveolar process and to avoid increased bone resorption. Without ARP, tooth extraction may lead to extensive alveolar ridge resorption, which can complicate implant placement. For the treatment of chronic alveolar defects, bone augmentation methods in implant dentistry have made significant progression. As a result, nowadays even horizonto-vertical hard tissue defects can be reconstructed by various surgical methods in local anaesthesia during outpatient treatment. Development of digital implant dentistry resulted in more accurate implant positioning by guided implant placement in alveolar sites in native bone or with simultaneous bone augmentation. This allows clinicians to reduce flap elevation and to decrease duration of implant surgery, which positively influence patients' wound healing and satisfaction. Furthermore, prosthetically driven implant placement can improve final aesthetics and function.

Hämmerle and co-workers in 2004 (Hämmerle et al., 2004) classified the time points for implant placement. Based on their consensus statement, 4 different timing approach for implant placement is possible. Type 1 implant requires that the implant is placed at the time of the extraction, also called immediate implantation. In case of type 2 implant placement, the fixture is inserted after complete soft tissue healing of the socket, which usually develops 4-8 weeks after extraction. Type 3 implant placement is applied to place implants 12-16 weeks after extraction, when partial bone fill is detected in the socket. Type 4 implant placement is performed more than 16 weeks post extraction.

Type 1 implant placement was previously highly recommended to maintain the alveolar process, if the gap between the buccal bone and implant body is less than 2 mm (Paolantonio et al., 2001). While overall treatment time and number of surgical procedures can be reduced, recently several disadvantages of immediate implant placement have emerged. The hypothesis of the implant itself capable of socket

preservation has not been confirmed in literature. It is well documented that one of the most frequently occurring unwanted biological sequels after type 1 implant placement is the postoperative midfacial soft tissue recession related to underlying buccal bone resorption.

Botticelli and co-workers in 2004 (Botticelli et al., 2004), Chen et al. in 2007 and in 2009 (Chen et al., 2007, 2009) and Yoshino et al. in 2014 (Yoshino et al., 2014) have demonstrated that immediate implant placement into wide alveolar processes with thick bony walls deliver predictable result, nevertheless alveolar ridge resorption cannot be avoided by implant placement alone. These findings were confirmed by the 2013 International Team for Implantology consensus conference, therefore in the consensus report by Morton et al. from 2014, immediate implant placement is recommended, if:

- Socket walls are intact.
- At least 1 mm facial bone plate width is available.
- Soft tissue is thick.
- Acute infection is not presented in the surgical site.
- There is available apical and palatal bone to reach an adequate primary stability (Morton et al., 2014).

Caplanis and co-workers also found that immediate implant placement is only recommended in case of EDS-1defects, i.e., intact socket walls with thick gingival biotype while in EDS-2 defects first ARP and then implant placement yield more predictable result (Caplanis et al., 2005).

To maintain socket dimensions after tooth extraction, various ARP methods are described in the literature. Based on the consensus report by Tonetti et al. from 2019 (Tonetti et al., 2019), ARP techniques are defined as socket grafting with biomaterials (alveolar ridge preservation via socket grafting – ARP-SG), alveolar ridge preservation via socket sealing with barrier membrane (ARP-SS), or a combination of ARP-SG and ARP-SS.

Tan et al. in 2012 observed in their systematic review based on 20 studies that a mean 29-63% horizontal and a 11-22% vertical resorption can be found after ARP procedures 6 months post extraction (Tan et al., 2012). In the included studies, patients underwent ARP methods at tooth extraction, nonetheless results showed bone loss.

Araújo et al. in 2015 extracted 28 teeth and performed ARP-SG with BDX in the test group, while no regenerative treatment was performed in the control group (Araújo et al., 2015). After 4 months healing, the buccal bone was reduced with 41% in the test group and 36 % in the control group, while the palatal bone wall reduced with 13% in both groups. Kotsakis et al. in 2014 extracted 30 teeth, 12 alveolar socket was filled with BDX, 12 sockets with calcium phosphosilicate putty and 6 sockets were healed without ARP (Kotsakis et al., 2014). At 5 months post extraction, in the BDX and phosphosilicate groups the mean horizontal reduction was 1.39 ± 0.57 mm and 1.26 ± 0.41 mm, respectively. In the control group, where no ARP was performed, the mean horizontal reduction was 2.53 ± 0.59 mm.

In the literature, there is no information about horizontal hard tissue alterations based on CBCT data sets after ARP-SS. Oghli and Steveling in 2010 performed 39 extractions with ARP-SS, mean horizontal ridge shrinkage was 0.8 ± 0.7 mm after 3 months healing (Oghli and Steveling 2010). The measurement process was based pre-, and postoperative silicone impressions, thus only soft tissue alterations were evaluated.

Tomasi et al. in 2018 extracted 28 teeth; in the test group, ARP-SG was combined with ARP-SS utilized by BDX and non-resorbable membrane, in the control group ARP-SS was performed by non-resorbable membrane alone (Tomasi et al., 2018). After 6 months uneventful healing, in the test and control group, the volume reduction amounted 21.3 ± 5.0% and 20.0 ± 9.1%, respectively. The horizontal reduction was 3 mm in both groups at 2 mm subcrestally.

These findings were confirmed by Chappuis et al. in 2017, who declared that neither ridge preservation techniques nor immediate implant placement can maintain alveolar socket dimensions (Chappuis et al., 2017). This statement is applicable for ARP-SS and ARP-SG techniques, nevertheless reinforcement of the buccal plate according to Lekovic et al.

yielded more favourable outcomes, preventing bone loss and resulting in occasional additional bone gain (Lekovic et al., 1997, Lekovic et al., 1998).

Lekovic et al. in 1997 and 1998 presented an ARP method utilizing a membrane, which covers the alveolar socket and the buccal wall (Lekovic et al., 1997, Lekovic et al., 1998). They have removed 2 front or premolar teeth next to each other. In the study from 1997, after tooth extraction and mucogingival flap preparation, the test sockets were covered with an e-PTFE membrane, while in the study from 1998, test sockets were covered with a resorbable membrane. At the control site no ARP or any regenerative procedure was performed. After periosteal releasing incisions, flap was closed tensionless.

In their study from 1997, they observed membrane exposure in 30% of the cases (3 of 10) after 3 months healing (Lekovic et al., 1997). In these cases, ARP procedures were not successful. In the remaining test sites, the average horizontal socket dimension decreased on average by 1.71 ± 0.75 mm 6 months postoperatively, the average vertical socket dimension decreased on average by 0.28 ± 0.18 mm. In contrast, control sites showed a greater horizontal and vertical hard tissue changes between baseline and postoperative situation, socket width and vertical dimension was decreased on average by 4.43 ± 0.72 mm and 1.00 ± 0.00 mm, respectively. However, evaluating the data from the presented tables from the article, 1 patient showed horizontal hard tissue gain in the test group and 1 patient maintained the horizontal socket dimension 6 months postoperative.

In their study from 1998, no resorbable membrane exposure was observed, all sites showed a better, uneventful wound healing (Lekovic et al., 1998). Based on the presented tables from the article, no horizontal hard tissue gain was detected after ARP approach, nevertheless 2 patients showed a maintained horizontal socket dimension after healing. In the test sites, mean horizontal and vertical dimension reduction was 1.31 ± 0.24 mm and 0.38 ± 0.22 mm, respectively. In the control sites, average socket width loss was 4.56 ± 0.33 mm, while vertical hard tissue loss was a mean 1.50 ± 0.26 mm.

The extent of postextractional alveolar ridge resorption depends on many conditions, one of the most important prognostic factors is the width of buccal bone, as Tomasi and co-workers found in 2010 (Tomasi et al., 2010). They placed 93 implants with immediate implant placement protocol and observed that buccal bony wall thickness, distance between buccal bony wall and implant body, and implant positioning are the key factors to reach an aesthetic outcome.

Januário and co-workers in 2011 measured the thickness of buccal bone in the anterior maxilla in 250 subjects. Measurements were based on CBCT scans at 1, 3 and 5 mm from the bone crest around periodontally healthy anterior teeth. They observed that the thickness varied in a narrow range between 0.5 ± 0.4 mm 0.7 ± 0.4 mm (Januário et al., 2011). They found that almost all front teeth have less than 1 mm buccal bone plate and close to 50% of the investigated teeth have less, than 0.5 mm buccal bone. Araujo et al. in 2015 concluded in their study that after tooth extraction the thin buccal bone plate is prone to resorption and alveolar socket fill will be insufficient due to the soft tissue collapse into the alveolar socket (Araújo et al., 2015).

These clinical and histological findings led to us to create a novel ARP procedure. Our XSD method cannot be classified based on the ARP classification system described by Tonetti, since neither socket grafting, nor socket sealing procedure was performed (Tonetti et al., 2019). Practically, our goal was to recreate the buccal wall by a xenogeneic membrane with a long resorption rate, and to thicken the gingival biotype utilizing SCTG without conventional flap preparation. With the novel XSD method a favourable socket environment was created to stabilize the blood clot and to reach a spontaneous hard tissue formation in the socket. Thereby, our results showed in many cases hard tissue gain after healing, which is unique in the literature.

The concept by Lekovic et al. is very similar to our hypothesis, i.e., protecting or recreating the buccal socket wall can increase socket healing and prevent alveolar process resorption. This idea was improved with a bilaminar vestibular tunnel preparation technique and gingiva thickening procedure.

In Study I test group, patients presented EDS-3, or -4 sockets treated by our novel XSD method. After healing, not only less horizontal and vertical resorption was measured, but in some cases horizontal and vertical bone gain was detected compared to the baseline situation. In the midbuccal sections the average horizontal hard tissue gain was between 0.16 ± 1.97 mm and 0.86 ± 2.47 mm, corresponding to 6-34%. Vertically, the midbuccal bone crest yielded an average 2.23 ± 3.35 mm hard tissue gain, while the midpalatal bone crest underwent on average 0.25 ± 2.15 hard tissue loss. Based on the measurement method, it is uninterpretable to convert the vertical hard tissue resorption to percentage (vertical hard tissue changes were measured from an arbitrarily chosen reference point, not from the top of the bone crest).

In the control group, since ARP was not performed, after healing average horizontal bone loss ranged between 2.55 ± 2.52 mm and 2.73 ± 3.12 mm in the midbuccal section. Converted to percentage, we observed a mean of 34-58% horizontal shrinkage. Investigating the vertical hard tissue changes in the midbuccal section, the midbuccal and midpalatal bone crests showed on average 2.26 ± 2.41 mm and 1.64 ± 1.57 mm resorption, respectively, percentage could not be expressed. These results are well in line with the literature.

During the XSD approach the alveolar socket was filled only with resorbable sponge, which can help to stabilize the blood clot. Therefore, newly formed hard tissue inside the socket represented natural bone healing, which was clinically assessed during re-entry and implant placement without histological analysis. In contrast, ARP performed with socket grafting using xenogeneic materials usually results in reparative tissue with newly formed bone and encapsulated xenogeneic materials by connective tissue, which contains “fibroblast like” cells and leukocytes, as Lindhe and co-workers observed in 2014 (Lindhe et al., 2014). It was also reported by Araújo et al. in 2008 that the biomaterial was in direct contact with the newly formed bone but in individually separate areas particles were embedded in a provisional matrix (Araújo et al., 2008). On the other hand, tissue modelling and remodelling process is delayed after socket grafting with biomaterial fillers, as reported by the same authors.

In the literature, measurement processes of most ARP procedures are based on direct clinical measurements and intraoral radiographs (Stimmelmayr et al., 2012, Kotsakis et al., 2014). In a systematic review by Horvath et al. 2013 only 2 from the 14 studies performed 3D radiographic assessment prior and after ARP procedure. Our measurement process was based on the protocol by Nevins et al. 2006 (Nevins et al., 2006) but modifications were performed. Their first CBCT scan was taken after the extraction, and the second CBCT scan was obtained 30 to 90 days postoperative. In contrast, our first CBCT was taken before extraction, while the second one at least 6 months later. In our study the healing was an average 7.5 months after extraction. Based on literature, investigation of hard tissue alteration after an average 8 weeks of healing post extraction can produce different results compare to more prolonged healing (Chappuis et al., 2013). On the other hand, our measurements were not only performed in the midbuccal section, mesial and distal sections were also registered. Most of the studies measured only the vertical dimension of buccal bony wall and the horizontal dimension at an arbitrarily determined level. To collect more data on three-dimensional hard tissue alterations, in our study buccal and palatal bony wall height and in 15 levels the horizontal socket dimension was evaluated, in addition the socket area was also measured in every section. With this modification, our measurement protocol could deliver more detailed data to compare baseline and postoperative hard tissue changes.

The unique horizontal and vertical hard tissue gain after XSD approach from Study I can be explained by the following reasons:

- In the test group sockets showed an EDS-3, or- 4 defect morphology treated by XSD approach; thus, baseline horizontal socket dimension was strongly reduced by the missing buccal bone wall. Therefore, the 6-34% horizontal hard tissue dimension gain means only 0.16 ± 1.97 mm to 0.86 ± 2.47 mm hard tissue changes.
- Membrane placement and fixation was performed without conventional crestal incision and flap elevation. The vestibular incision line did not affect the papilla, thus blood vessels from palatal gingiva are unharmed and blood circulation of the flap is maintained. In addition, no periosteal releasing incision was performed, therefore periosteal blood vessels remained intact. Thereby we could achieve uneventful wound healing and outstanding hard tissue reconstruction with the XSD approach.
- Simultaneously with the buccal cortical wall recreation, the gingiva was thickened with SCTG. Thick gingiva may prevent crestal bone resorption and maintain soft tissue contour, which can improve final aesthetic results and long-term crestal bone stability around dental implants (Grunder et al., 2005, Covani et al., 2007, Esposito et al., 2008).

Jae-Jin and Hong-In in 2008 observed in their histomorphometric study that bone formation is delayed and decreased, if periodontal disease was diagnosed around hopeless and extracted teeth compared to extracted teeth with healthy and maintained sockets (Jae-Jin and Hong-In 2008). They found maximum 60% bone fill in the socket area 42 weeks after extraction in the disease group, while in the healthy socket group they found a 70% bone fill at 20th weeks post extraction. This unpredictable healing pattern can result a severe 3D hard tissue dehiscence in periodontally compromised patients, which can complicate implant placement.

Various reconstructive techniques for vertical augmentation are described in the literature. Elnayef et al. in 2017 found (Elnayef et al., 2017) that GBR procedures entail fewer biologic complications compared to inlay-, and onlay block grafts and distraction osteogenesis (DO). Urban et. al in 2019 observed in their systematic review that with GBR on average 4.18 mm vertical hard tissue gain can be achieved after vertical augmentation with a complication rate of 12.1% (Urban et al., 2019). With DO and AB a mean 8.04 mm and 3.46 mm bone gain with 47.3% and 23.9% complication rate, respectively. Former studies demonstrated successful horizonto-vertical GBR methods utilizing non-resorbable membranes. Since horizonto-vertical hard tissue deficiencies are mostly not self-contained defects, the space-maintenance for blood clot, -and graft stabilisation can only be achieved by a rigid barrier. Therefore, although resorbable membranes demonstrate some advantages over non-resorbable membranes, most horizonto-vertical GBR procedures were performed by e-PTFE membranes with titanium reinforcement or tenting screws. In addition to the space-maintenance effect, e-PTFE membranes have highly biocompatible characteristics with gingival tissues (Simion et al., 1994). As Simion and his co-workers found in 1999, e-PTFE membranes with 5-25 μm pore size have an optimal balance between clinical management and biological capacity, thus e-PTFE membranes with adequate pore size are widely used in the clinical practice for vertical GBR (Simion et al., 1999).

Premature exposure of the e-PTFE membrane after GBR procedure is a well-documented phenomenon, without early intervention and adequate treatment it can result surgical site infection and graft disintegration. Rocchietta et al. in 2008 found in their systematic review a 0.0 – 45.5% complication rate after vertical GBR with e-PTFE membranes, and the most common complication was the barrier membrane exposure (Rocchietta et al., 2018).

In our Study II, due to non-resorbable membrane evolution and discontinuation of e-PTFE membranes from the dental market, a newer type d-PTFE non-resorbable membrane (0.3 μm pore size) with titanium-reinforcement was used during GBR. Partially edentulous patients were selected and treated with GBR procedure to allow implant placement. Patients had chronic periodontal disease and hopeless teeth were extracted before enrolment without ARP by referring dentists. As a result, a localized 3D alveolar ridge defects were diagnosed clinically and by CBCT scans, thus type 4 implant placement was planned either with simultaneous, or staged GBR approach after split-thickness flap preparation, utilizing d-PTFE membranes and composite graft.

Bartee in 2001 presented a combination of ARP-SS and ARP-SG technique using d-PTFE membranes. He filled the alveolar socket with grafting material (not detailed) and covered it with a d-PTFE membrane. After 3-4 weeks of healing, he removed the membrane (Bartee 2001). He postulated that the membrane may resist bacterial incorporation and penetration through the pores in case of membrane exposure, since the d-PTFE membranes have lower porosity compared to e-PTFE membranes. This favourable characteristic may reduce the risk of surgical site infection during exposed healing and subsequent graft disintegration, as Fotek et al. in 2009 also observed at similar ARP approaches. In their investigation, d-PTFE membranes were left exposed after extraction to cover the alveolar socket (Fotek et al., 2009). However, no statistical difference was found in the membrane group compared to the acellular dermal matrix (ADM) group, where sockets were covered with ADM. Barboza et al. in 2010 presented 420 similar ARP cases, no postoperative wound infection was observed (Barboza et al., 2010).

In the literature optimal results were reported after vertical GBR procedure with d-PTFE membranes, however number of articles is scarce. Urban et al. presented a prospective case series in 2014, they performed 20 vertical augmentations with d-PTFE membranes and reached an average 5.45 ± 1.93 mm hard tissue gain (Urban et al., 2014). They presented an uneventful healing period without any complications. Ten single tooth gaps were treated with vertical GBR with d-PTFE membranes by Herzberg in 2017, he found a favourable tissue compatibility of the applied d-PTFE membrane, all treated sites healed successfully without membrane exposure or bacterial graft contamination and disintegration (Herzberg 2017). In our study only one membrane exposure was detected

from 24 surgical sites, 6 weeks after the surgery d-PTFE membrane was replaced with a resorbable membrane. Minor hard tissue loss was observed at re-entry, which was compensated with soft tissue augmentation and the implant was inserted without any additional hard tissue augmentation.

In Study II, composite graft was used as grafting material. The 1:1 mixture of AP and BDX have an optimal biological capacity, since osteoconductive effect of BDX is completed with osteoinductivity by the AP. In addition, during surgery duration and extent of AP harvesting may be reduced, which may lead to decreased donor site morbidity, while graft volume stability during healing is increased by BDX. These benefits of the composite graft were confirmed by Merli et al. 2006, Simion et al. in 2007, Urban et al. in 2011, 2013, 2014 and Meloni et al. in 2017 (Merli et al., 2006, Simion et al., 2007, Urban et al., 2011, Urban et al., 2013, Urban et al., 2014, Meloni et al., 2017). Urban et al. in 2014 collected histologic samples from the area regenerated by a composite graft, histologically BDX particles were connected through a dense network to the newly formed bone, and no inflammatory response was detected around the particles (Urban et al., 2014).

Vertical augmentation with the GBR approach is a highly technique sensitive reconstructive method. In the early 1990s, when e-PTFE membranes were introduced in alveolar bone grafting, Buser et al. treated 12 patients with GBR using e-PTFE membranes, they observed in 2 cases soft tissue dehiscence and in 3 cases abscess formation, which is a 42% complication rate (Buser et al., 1990). However, since the surgical technique and instruments were improved and strict protocols were established with patient selection criteria, the complication rate has decreased.

Various authors also confirmed that one of the main reasons of early membrane exposure might be inadequate flap management, which results in tension between buccal and oral flap sides. Tinti et al. in 1996 presented a surgical description for vertical hard tissue augmentation utilizing an e-PTFE membrane (Tinti et al.,1996). Six patients were treated with a simultaneous GBR approach, one patient had major complication, after membrane removal and healing no newly formed hard tissue was detected around the implants. They observed that uneventful healing can only happen, if the membrane is covered completely

by the flap for 1 year, the membrane is stabilized, and the flap is closed by horizontal sutures.

Tinti and Parma-Benfenati presented in 1998 a detailed surgical protocol for vertical GBR (Tinti and Parma-Benfenati 1998). In this article a novel flap preparation and wound closure technique was established. According to their concept, obtaining and maintaining soft tissue coverage above the membrane is only possible, if the flap is elastic and tension-free. A crestal incision was extended intrasulcularly to the mesial line angle of the adjacent teeth both buccally and lingually. Two vertical releasing incisions were made buccally and lingually, then mucoperiosteal full-thickness flaps were raised on both buccal and lingual sites. To reach a tension-free flap adaptation after graft stabilization with a membrane, periosteal incisions were performed on the buccal and lingual flap. Subsequently, horizontal mattress sutures were used to create two contact surfaces in at least 3 mm width between the flaps. In the mandible both flaps were lengthened with the periosteal incision, but in the maxillary region the palatal flap is not distensible with this technique.

In 1995 Tinti and Parma-Benfenati introduced the coronally positioned palatal sliding flap to decrease the tension of the buccal flap in the maxilla after GBR procedure by reducing the gap between buccal and palatal incision line (Tinti and Parma-Benfenati 1995). Long-term evaluation of GBR with the coronally positioned palatal sliding flap was presented with excellent results by Maiorana et al. in 2018 (Maiorana et al., 2018).

Several flap designs are described in the literature to maintain flap closure after GBR. Fugazzotto in 1999 introduced a palatal split-thickness flap design; the crestal incision was performed 1-2 mm palatal on the crest with a split-thickness preparation, then at the buccal line angle of the crest of the ridge, the flap was continued with full-thickness preparation. Like the Tinti flap, vertical releasing incisions and periosteal incision were made to reach a tension-free buccal flap at closure but if the primary closure could not be achieved, a split-thickness connective tissue pedicle was rotated from beneath the palatal flap (Fugazzotto 1999).

Ronda and Stacchi in 2011 focused on the lingual flap extension in their case series (Ronda and Stacchi 2011). They observed a connective tissue band under the elevated lingual flap in the first molar area, which originated from mylohyoid muscle and attached to the lingual flap's inner part. The connective tissue band was detached from the lingual flap with a blunt instrument. With this development in lingual flap design, they could reach an outstanding result after simultaneous GBR. They observed signs of infection (swelling and purulent exudate) in only 4 cases without flap perforation and membrane exposure from the 69 augmented area. The remaining 65 cases presented uneventful healing with perfectly maintained flaps and complete regeneration 6 months postoperatively.

Urban and co-workers presented in 2017 an improved flap design for vertical GBR (Urban et al., 2017). Both buccal and lingual flap sides were modified to reach a more tension-less wound closure. In the buccal flap the mesial vertical incision is created at least one tooth away from the surgical site, while distally, at the end of the crestal incision, which ends within 2 mm of the retromolar pad, an oblique vertical incision is recommended. In the lingual side a 4 mm vertical incision is placed at the mesiolingual line angle of the most distal tooth. During buccal flap advancement, a superficial periosteal incision is made without reaching the connective tissue, then subperiosteal bundles are released from elastic fibers. The elastic fibers should be separated using blunt instruments to avoid nerve-, or vascular injury. The lingual flap advancement is also crucial; the distal site of the lingual flap is connected to the retromolar pad, which is gently reflected from underlying bone, the middle of the lingual flap is attached to the mylohyoid muscle, which is gently pushed with blunt instruments in a lingual direction, while the mesial site of the lingual flap contains periosteal tissue, which is dissected with semiblunt periosteal incision. This flap design can decrease the risk of anatomic structure injury, as Urban et al. in 2017 in their cadaver study demonstrated (Urban et al., 2017).

The same authors in 2018 described in their split-mouth cadaver study that this novel lingual flap advancement technique results significantly higher vertical flap release compared to the vertical flap release achieved by classic lingual flap preparation described by Ronda and Stacchi in 2011 (Urban flap vs. Ronda flap; Zona I: 9.27 ±2.20

mm vs. 1.00 ± 1.00 mm, Zona II: 16.45 ± 2.88 mm vs. 6.36 ± 2.46 mm, Zona III: 12.64 ± 2.87 mm vs. 2.36 ±2.16 mm) (Urban et al., 2018, Ronda and Stacchi 2011).

The above-described flap preparation techniques are based on full-thickness flap design with vertical releasing incisions and periosteal releasing incisions. If the periosteal releasing incision is too deep, periosteal blood supply may be dissected and blood circulation of the flap may be harmed. The reduced blood circulation can negatively affect the wound healing and increase the risk of flap perforation and membrane exposure. On the other hand, especially in the maxilla, vertical releasing incisions can harm the loop anastomoses between vertical branches and could lead to disturbed wound healing, or scar formation, as Shahbazi et al. in 2021 observed (Shahbazi et al., 2021). They recommended L-shaped flaps with one vertical releasing incision placed in the upper labial frenulum or in the distal site of the canine - first premolar region.

A tension-free flap closure can be achieved by a split-thickness flap design with the respect of blood supply. Novaes in 1997 described a case report performing a split-thickness flap for ARP method to decrease flap tension with promising result (Novaes 1997). Hur et al. in 2010 presented a vertical GBR procedure with a double flap incision design (Hur et al., 2010). They dissected the mucosal layer from the periosteum, which facilitates flap advancement by the tension-free nature of the design, since the tension originates from the periosteal layer. In addition, one mesial vertical releasing incision was placed at the distal papilla of the neighbouring tooth of the defect. After graft insertion and non-resorbable membrane fixation, periosteal layer was sutured to the lingual flap by horizontal mattress sutures, then mucosal layer was sutured to the lingual flap by single interrupted sutures. They observed less postoperative soft tissue complications compared to conventional flaps.

Ogata et al. in 2013 compared the DFI technique to the periosteal releasing incision technique (PRI) during GBR procedures (Ogata et al., 2013). 23 surgical sites were treated by GBR, flap preparation was performed with the PRI technique in 12 cases, while DFI technique was applied in 11 cases by the same operator. The DFI technique resulted in more favourable flap advancement, the average advancement was 9.64 ± 0.92 mm, compared to 7.13 ± 1.45 mm in the PRI group. In the DFI group 1 early membrane

exposure was observed, compared to 2 membrane exposures in the PRI group. In addition, patients' postoperative pain, swelling and bleeding score was less in the DFI group. The authors supposed that the membrane and consequently the graft might be anchored by the periosteum and by the periosteal horizontal sutures during the initial healing period, which resulted an extra membrane stabilization. They also speculated that the DFI flap has an enhanced healing potential compared the PRI flap due to the undisturbed periosteal blood supply, while a deep incision was performed into the mucosa in the PRI flap, which may be the cause of the increased swelling and bleeding.

However, in the article the periosteal releasing incision was performed only with sharp instruments inserted deep into the periosteal layer, while Urban et al. in 2017 recommended a superficial periosteal incision without reaching the connective tissue, then the elastic fibers separation using blunt instruments to avoid nerve-, or vascular injury (Urban et al.,2017). The postoperative patient discomfort might be decreased, if the PRI flap design was properly executed.

Windisch et al. in 2017 presented simultaneous vertical GBR procedures of 3 cases with split-thickness flap design without vertical releasing incisions, utilized by titanium membrane (Windisch et al., 2017). They observed a 3.08 ± 1.25 mm hard tissue gain at implant re-entry, and favourable hard tissue conditions were maintained 5 years postoperatively.

In Study II, 24 GBR approaches were utilized, depending on baseline vertical bone level. If at least 6 mm vertical bone height was detected coronally from the neighbouring anatomic landmarks (floor of maxillary sinus or nasal cavity, mandibular nerve), simultaneous GBR, in the other cases staged GBR was performed. In both groups the same split-thickness flap was created. During healing, a lower complication rate was observed, compared to the literature. One surgical site showed early flap dehiscence with membrane exposure from the 24 treated sites, which corresponds a complication rate of 4.17%. The average vertical dimension gain was in the simultaneous group 3.2 ± 1.9 mm, while 4.5 ± 2.2 mm in the staged group. These results of vertical hard tissue gain are well in line with the literature, however in the study GBR procedures were performed with d-PTFE membrane.

Fontana et al. in 2008 demonstrated 10 vertical augmentations utilizing titanium reinforced e-PTFE membranes with allogenic bone matrix (ABM) or with AP (Fontana et al., 2008). Only 1 membrane exposure was reported in the AP group during healing, which is a lower complication rate compared to other studies. The average vertical bone gain was 4.70 ± 0.48 mm in the ABM, and 4.10 ± 0.88 mm in the AP group, based on clinical measurements. In contrast, Merli and his co-workers presented a randomized controlled clinical trial in 2007, they found complications 5 of 11 vertically augmented sites utilized by e-PTFE membranes, nevertheless only 1 major complication was observed, which determined the complete failure of the GBR process (Merli et al., 2007). On the other hand, they reached an average 2.48 ± 1.13 mm vertical hard tissue gain after healing. The same research group presented a randomized clinical trial in 2014, and they reported complications in 45% of the cases after vertical augmentation with e-PTFE membranes, however the type of complications was not detailed, and the complications were treatable without compromising the outcome (Merli et al., 2014). Rocchietta et al. in 2016 treated 11 horizonto-vertical defects with AP, after 6-10 months healing, they found an average 4.36 mm hard tissue gain, measured by periodontal probe (Rocchietta et al., 2016). Only one surgical site presented minor complication; 4 months after augmentation 2 fistulas were detected, due to antibiotic treatment and surgical membrane removal the inflammation disappeared, and dental implants were inserted after the complete healing.

In the literature, the effectiveness of vertical augmentation procedures is based on postoperative hard tissue gain. In most of the studies direct clinical evaluations with periodontal probe were performed pre-, and postoperatively and hard tissue changes were calculated. In our study, a radiographic measurement protocol was also established to receive more detailed data of hard tissue gain. Measurements were based on pre-, and postoperative CBCT datasets, horizontal, vertical hard tissue dimensional changes and volume changes were evaluated in the staged group. Radiographic vertical hard tissue changes were lower by 0.3 mm on average compared to our direct clinical measurements. One of the benefits of our radiographic measurement protocol is the repeatability, while direct clinical measurements can only be performed at surgery. In addition, during surgery a direct clinical measurement might be more subjective due to the stress and concentration

by the operator, while radiographic measurements can be performed after surgery, in calm conditions with more accurate results.

Our Study II was the first report, which demonstrated favourable results following vertical GBR using a split-thickness flap design utilizing d-PTFE membranes. The favourable postoperative healing may have occurred for the following reasons:

- The d-PTFE membranes have a smaller pore size compared to the e-PTFE membranes. This lower pore size can reduce bacterial incorporation and penetration through the pores, which protects the underlying graft in case of flap perforation and membrane exposure. In addition, the d-PTFE membranes have an excellent biocompatibility. Therefore, in our study the complication rate of 4.17% was observed, which was treated successfully without graft loss and surgical failure.
- The composite graft combines the advantages of the BDX and AP. BDX has an osteoconductive effect and reduces the amount of harvested AP, while AP can increase the regenerative capacity of the graft by its osteoinductive feature.
- The split-thickness flap design allows the clinician to reach an improved buccal flap advancement without periosteal releasing incision, which may compromise blood circulation postoperatively.
- The lack of vertical releasing incisions may be beneficial for early wound healing, since the loop anastomoses between vertical branches are unharmed.

Dental implant placement requires adequate bone quantity for prosthetically driven implant placement. Implant position determines final aesthetics, function and cleansability of implant borne restaurations, which are correlated with long-term success and implant survival. On the other hand, implant malpositioning may damage neighbouring anatomical structures (i.e., mandibular nerve, Schneiderian membrane), and compromise final restauration. Various etiological factors have been identified to be associated with peri-implantitis. Pesce et al. in 2015 observed that cement remnants and incorrect finishing lines can increase the risk of peri-implantitis (Pesce et al., 2015).

Therefore, screw-retained implant borne restorations may be preferred. Canullo et al. in 2016 divided the peri-implantitis into two subgroups: purely plaque-induced and surgically triggered peri-implantitis (Canullo et al., 2016). Based on their observations, optimal implant positioning can enhance long-term success. Implant malpositioning can be avoided with careful planning by the application of digital wax-ups and CBCT scans to allow for navigated implant placement. As Varga et al. in 2020 observed, static guided implant surgeries allow the clinician to improve implant position accuracy compared to free-hand implant placement (Varga et al., 2020).

Implant position accuracy depends on the type of surgical protocol. Based on the study by Varga et al. 2020, GCD, GAD and AD resulted in after free-hand implant placement averaged by 1.82 ± 0.94 mm and 2.43 ± 0.98 mm, 7.03 ± 3.44 degrees, respectively (Varga et al., 2020) By the application of partially- or fully guided surgery, a more accurate implant position can be achieved. Mean GCD, GAD and AD in the half-guided group were: 1.37 ± 0.79 mm, 1.59 ± 0.86 mm, 4.30 ± 3.33 degrees, respectively. Mean GCD, GAD and AD in the full-guided group were: 1.40 ± 0.54 mm, 1.59 ± 059 mm, 3.04 ± 1.51 degrees, respectively. In Study III, all patients received dental implants by partial-guided implant surgery to homogenize the surgical protocol.

Bone quality and surgical location may influence the final position accuracy. Lower bone density can decrease the accuracy, as Ozan et al. in 2011 observed (Ozan et al., 2011). Varga et. al in 2020 found that the global deviation parameters are higher in the maxilla compared to the mandible, which means inferior implant position accuracy in the maxilla during guided surgery (Varga et al., 2020). In contrast, they found preferable AD parameters in the maxilla, compared to the mandible. These controversial results could be eliminated, if implant placement locations were similar in all patients, thus in Study III, patients received dental implants in the maxilla, after sinus elevation procedure.

Support of surgical guides are also related to the position accuracy. Tooth-supported guides are slightly more accurate, compared to bone-, mucosa-, or mucosa and pin-supported guides, as Tahmaseb et al. observed in 2014 in their systematic review (Tahmaseb et al., 2014). Therefore, in Study III only partially edentulous patients were selected and tooth-supported surgical guides were used. Tahmaseb et. al in 2014 also

observed that flapped surgical approaches during navigated implant surgery deliver less accurate result in implant position compared to flapless approaches. However, most of the applied guides were bone-supported during flapped surgery, which controversially resulted in the most inaccurate implant positions. To exclude the differences by flapped-, or flapless approaches, in Study III every surgery was performed with flap preparation.

Derksen et al. in 2019 observed that implant length is also correlated to the final accuracy (Derksen et al., 2019). Longer implants showed less angular deviations, thus in Study III only Straumann RN Standard Plus implants with 4.1 mm diameter and 10 mm length were applied to reduce the differences.

In Study III, intergroup comparison did not result in significant difference between planned and actual implant position, thus accuracy results were averaged in both groups to facilitate data comparison process with similar studies from the literature. On the other hand, the reported measurement parameters are not homogenous in the literature. GCD and GAD were presented in the study among others by di Giacomo et al. in 2005, Ersoy et al. in 2008, Cassetta et al. in 2013, di Giacomo et al. in 2012, Van de Wiele et al. in 2015, Derksen et al. in 2019, Varga et al. in 2020 (di Giacomo et al., 2005, Ersoy et al., 2008, Cassetta et al., 2013, di Giacomo et al., 2012, Van de Wiele et al., in 2015, Derksen et al., in 2019, Varga et al., in 2020). HCD and HAD were reported by Valente et al. in 2009, Cassetta et al. in 2012 (Valente et al., 2009, Cassetta et al., 2012). While implant angulation and vertical deviation parameters are frequently reported, separate linear deviation parameters are rarely presented in the literature to investigate implant position accuracy (Beretta et al., 2014). Therefore, coronal and apical global deviation parameters were broken down to 3 spatial vectors in the three-dimensional space to present more precise deviation parameters between planned and actual implant positions.

In the literature, there is no data of implant position accuracy after flapped half-guided implant placement with tooth-supported guides in the maxilla. Varga et al. in 2020 performed 17 flapless half-guided implant placements with tooth-supported guides in the maxilla, they reached an average 1.51 ± 0.73 mm GCD, 1.83 ± 0.71 mm GAD and 4.14 ± 2.75 degrees AD (Varga et al., 2020). These results are very similar to our results (GCD: 1.16 ± 0.38 mm, GAD: 1.32 ± 0.54 mm, AD: 4.46 ± 1.85 degrees). In 2008, Ersoy et al.

performed full-guided implant placement with tooth-supported surgical stents, they reported a mean GCD and AD of 1.1 ± 0.6 mm and 4.4 ± 1.6 degrees, respectively (Ersoy et al., 2008). Derksen et al. in 2019 reported on an average of 0.75 ± 0.34 mm GCD and a mean of 1.06 mm ± 0.44 mm GAD after full-guided implant placement, which are more accurate compared to our results (Derksen et al., 2019).

Valente and co-workers in 2009 evaluated the horizontal deviations after half-guided implant placement (Valente et al., 2009). Surgical stents were supported by various methods, they found a mean HCD and HAD of 1.4 ± 1.3 mm and 1.6 ± 1.2 mm, respectively. The mean angular deviation was 7.9 ± 4.7 degrees. Tooth-supported guides were used in the clinical study by Cassetta et al. in 2012. After 15 flapless half-guided implant placements, HAD averaged 1.28 ± 0.50 mm, while AD yielded an average of 4.88 ± 3.38 degrees (Cassetta et al., 2012). In our study, average HCD and HAD was 0.99 ± 0.46 mm and 1.14 ± 0.55 mm, respectively, while AD resulted in a mean of 4.46 ± 1.85 degrees. These outcomes point towards slightly more accurate implant positioning.

In Study III, VD was also reported by measuring the vertical distance between the apex of planned and actual implant. We found a mean of 0.59 ± 0.24 mm VD, which indicates superior vertical accuracy compared to the literature. In a systematic review presented by Bover-Ramos in 2018, average VD was based on six selected clinical studies with different clinical settings, they found a mean of 0.74 ± 0.10 mm VD (Bover-Ramos et al., 2018). Cassetta et al. in 2012 found a mean of 1.51 ± 1.06 mm VD after tooth-supported, flapless half-guided implant placement (Cassetta et al., 2012). Valente et al. in 2009 measured an average of 1.1 ± 1.0 mm apical deviation after half-guided implant placement with various stent support (Valente et al., 2009).

The evaluation method of implant position accuracy in Study III was based on preoperative CBCT data sets and postoperative intraoral scan files. Only Derksen et al. in 2019 used this evaluation technique, evaluation protocol of other studies was based on dual CBCT scans (Derksen et al., 2019). This non-invasive method eliminates the need of postoperative CBCT scans to reduce the patient radiation exposure, however further investigation is needed to prove the superiority over the conventional evaluation process. On the other hand, the postoperative scanning image does not give information about

implant position related to the bony environment, it is suitable only for pre-and postoperative implant position comparison. In Study III patients were treated between January 2017 and January 2019. During study planning in 2017, we did not find any article, in which implant placement accuracy was investigated based on CBCT and intraoral scanning. Therefore, we supposed that a new comparison method of implant position accuracy was established, until Derksen et al. presented the same method in 2019.

In the literature, there is no clear recommendation for the method of implant insertion. During manual implant insertion, a torque wrench is connected to the implant driver, while during machine-driven implant insertion, a surgical handpiece is connected to the implant. Buser et al. in 2000 presented the basic surgical principles with ITI implants, they leave the decision to the clinician for implant insertion method (Buser et al., 2000). Therefore, in Study III, we wanted to deliver clinical evidence to find a preferable insertion method in the aspect of implant insertion duration, insertion torque and implant position accuracy. However, no significant difference was found between the two study groups in any insertion torque, while implant insertion duration was significantly faster in the machine-driven group.

After implant placement, all implants were osseointegrated and no implant loss was observed. Statistical analysis did not reveal significant difference between the groups in any of the examined parameters, except for the duration of implant insertion. The implant position accuracy results are well in line with the literature. These results can be explained by the following reasons:

- Heterogeneity was eliminated by using the same half-guided implant placement protocol, the same support method of the surgical stent, the same implant type, same implant diameter and length.
- All implants were placed in the posterior maxillary area into augmented bone; thus, bone quality was similar.
- Surgeries were performed by the same experienced operator.
- Postoperative digital intraoral scanning was performed by the same clinician.

- The same radiographic system was used during preoperative imaging with high quality resolution.
- Insertion speed was 50 RPM in the machine-driven group, which is almost four times faster, than the recommended insertion speed of the Straumann system (15 RPM). Therefore, implant insertion duration was significantly faster in the machine-driven group, compared to the manual group.

6. CONCLUSIONS

Implant dentistry underwent numerous stages of development in the last decades. Previously, implant borne restorations were used to rehabilitate the masticatory function, while nowadays aesthetic aspects have come to the fore, too. To achieve and optimal long-lasting result, sufficient soft-, and hard tissues as well as ideal implant position with precisely fitted restoration is needed. Various surgical techniques are established to reconstruct the damaged alveolar process. However, hard tissue augmentation methods are still stressful for the patients due to the postoperative pain and swelling. Furthermore, there is always a possible risk of surgical site infection, which can jeopardize surgical success. Thereby, if it is possible, hard tissue augmentation should be avoided by optimally timing the tooth extraction and performing an ARP method.

Different factors can influence the postextractional resorption rate of alveolar hard tissues. Damaged, or thin buccal bone plate, invasive tooth extraction, disturbed healing process, local inflammations, such as an acute periodontal condition, or removable denture wear can create extensive horizonto-vertical alveolar defects. Therefore, to avoid a severe alveolar ridge resorption after tooth removal, the clinician should choose carefully the proper treatment before the extraction.

Study I

The presented novel XSD approach is based on the recreation of the buccal bony wall after tooth extraction, which proved to be beneficial in maintaining both horizontal and vertical alveolar socket dimensions. This surgical technique is supremely effective in case of EDS class 3 and 4 socket morphologies, therefore many cases presented not only less ridge reduction, but also horizontal and vertical hard tissue gain. This unique phenomenon was confirmed by pre-, and postoperative CBCT data sets with a digital measurement process.

By applying the XSD approach, the need for extensive hard tissue augmentation procedures may be avoided or reduced. During arbitrary probing and implant osteotomy,

newly formed hard tissues were well vascularized, resembled native bone and allowed for sufficient implant primary stability in all cases. The XSD approach showed an excellent post-operative healing with low complication rate, which can be explained with the maintained blood circulation due to the non-conventional, split-thickness flap preparation technique from a remote vestibular incision.

Study II

In implant dentistry, one of the most challenging surgical procedures is the reconstruction of the horizonto-vertical hard tissue deficiencies. Flap perforation, membrane exposure and graft infection are frequently reported in literature after GBR procedures. The complication rate can be decreased with adequate flap mobilization and tension-free wound closure. Based on our findings, it can be concluded that the GBR procedure in combination with a split-thickness flap design delivered optimal outcomes in the treatment of chronic horizonto-vertical alveolar defects. Excellent wound healing with low patient morbidity and low rate of membrane exposures was observed. The bilaminar flap allows for clinicians to achieve extensive buccal flap advancement and the double-layer suturing technique increases flap closure stability over non-resorbable membranes. The applied d-PTFE membrane and composite graft promoted favourable hard tissue formation. These tissue alterations were not only evaluated clinically, but also by a digital radiographic measurement process presenting quantitative data indicating sufficient amount of newly formed hard tissues, creating optimal periimplant conditions.

Study III

The reported prospective, randomized clinical study demonstrated the proof-of-concept that half-guided implant placement with tooth-supported surgical guides can result in an accurate implant positioning either with a surgical motor, or a torque wrench. No significant difference was found between the study groups in implant placement accuracy and insertion torque, therefore the clinicians should choose the applied method based on their own preference. However, implant insertion duration can be significantly reduced with a surgical motor, which may be beneficial for the patient. To evaluate implant

DOI:10.14753/SE.2022.2638

placement accuracy, deviation of planned and actual position was broken down to vectors in the three-dimensional space, thus detailed deviation parameters were presented, compared to the literature. The evaluation protocol of implant placement accuracy was based on preoperative CBCT data sets and postoperative intraoral scan files to reduce patients' irradiation dose. This imaging process should replace the conventional radiographic imaging protocol during investigation of implant placement accuracy to minimize irradiation dose.

DOI:10.14753/SE.2022.2638

7. SUMMARY

In Study I a novel ARP procedure, the extraction-site development was established to recreate the buccal bone during a minimal invasive surgical approach. With this technique the alveolar resorption can be reversed especially in severely damaged alveolar sockets. Therefore, after 6 months healing, in many cases implants can be inserted without any additional hard tissue augmentation procedure. This observation may enable clinicians to classify the alveolar socket morphology before extraction and perform the XSD method, if it is necessary.

The applied split-thickness flap preparation resulted in an improved wound healing with low complication rate, which lead to the concept of applying a similar bilaminar flap design for GBR procedure. The split-thickness flap design can improve the buccal flap advancement and allow for the clinician to stabilize the membrane over the graft with the double-layer suturing technique. In addition, the maintenance of the buccal flap vascularization can positively influence the wound healing. In Study II, a lower complication rate was observed after horizonto-vertical GBR compared to the literature, which confirms the benefits of the split-thickness flap.

Adequate hard-tissue environment is especially important to achieve optimal implant position. Guided-implant surgery aims at enhancing implant position accuracy after digital planning. However, different implant insertion methods may influence the result. In Study III we proved that implant insertion during half-guided surgical protocol was significantly faster with a surgical motor compared to the manual torque-wrench, however no significant differences were found in terms of implant position accuracy and implant insertion torque. On the other hand, with the applied implant navigation system we were able to achieve a highly accurate implant position compared to the planned position, which can improve functional and aesthetic outcomes.

The evaluation processes of the presented clinical investigations were based on digital radiography. In contrast to the direct clinical measurements, a digital workflow is repeatable and may increase the measurement accuracy, thus strongly recommended during clinical studies.

DOI:10.14753/SE.2022.2638

8. ÖSSZEFOGLALÁS

Az első vizsgálatunkban, egy újszerű alveolus prezervációs technika alkalmazásával helyre lehetett állítani a sérült, vagy hiányzó bukkális csontfalat. Ezzel a technikával az alveoláris reszorpció nem csak megállítható, hanem akár vissza is fordítható, különösen a súlyosan károsodott alveolusok esetén. Ennek köszönhetően sok esetben az implantátumokat további keményszöveti augmentáció nélkül be lehetett helyezni. Ez a megállapításunk arra szeretné biztatni a klinikusokat, hogy fogeltávolítás előtt az eltávolítandó fog körüli alveoláris csont morfológiája alaposan fel legyen térképezve és szükség esetén alveolus prezervációs műtétre kerüljön sor a fogeltávolítást követően.

Az alkalmazott félvastag lebenytechnika az optimális sebgyógyulás mellett alacsony komplikációs rátát eredményez, mely GBR típusú keményszövet augmentáció során is alkalmazható. A félvastag lebeny dizájn növeli a bukkális lebeny nyújthatóságát, valamint kétrétegű sebzárást teszt lehetővé a klinikus számára. A második vizsgálatunkban szakirodalmi adatokkal összevetve, alacsonyabb komplikációs ráta volt megfigyelhető horizonto-vertikális GBR típusú keményszövet augmentációkat követően.

A megfelelő kemény szöveti környezet megléte különösen fontos ahhoz, hogy implantáció során optimális implantátum pozíciót lehessen elérni. Különböző implantátum behelyezési módszerek befolyásolhatják ennek eredményét. A harmadik vizsgálatunk során megállapítottuk, hogy a sebészi motorral végzett implantátum behelyezés időtartama szignifikánsan gyorsabb a kézi nyomatékkulccsal történő implantátum behelyezéshez képest, részleges navigációs protokoll alkalmazása esetén. A két behelyezési metódus között nem található szignifikáns különbség implantáció pontosság és az implantátum behelyezési nyomaték szempontjából.

A bemutatott klinikai vizsgálatok során alkalmazott vizsgálati módszerek digitális radiológián alapultak. A direkt klinikai vizsgálati módszerekkel szemben, a digitális vizsgálatok megismételhetőek és növelhetik a mérési pontosságot, ezért alkalmazásuk klinikai kutatásokban kifejezetten ajánlott.

9. REFERENCES

Al-Hezaimi K, Levi P, Rudy R, Al-Jandan, B, Al-Rasheed A. (2011) An extraction socket classification developed using analysis of bone type and blood supply to the buccal bone in monkeys. Int J Periodontics Restorative Dent, 31: 420-427.

Amler MH, Johnson PL, Salman I. (1960) Histological and histochemical investigation of human alveolar socket healing in undisturbed extraction wounds. J Am Dent Assoc, 61: 32-44.

Araújo MG, Lindhe J. (2005) Dimensional ridge alterations following tooth extraction. An experimental study in the dog. J Clin Periodontol, 32: 212-218.

Araújo M, Linder E, Wennström J, Lindhe J. (2008) The influence of Bio-Oss Collagen on healing of an extraction ocket: an experimental study in the dog. Int J Periodontics Restorative Dent, 28: 123-135.

Araújo MG, da Silva JCC, de Mendonça AF, Lindhe J. (2015) Ridge alterations following grafting of fresh extraction sockets in man. A randomized clinical trial. Clin Oral Implants Res, 26: 407-412.

Araújo MG, Silva CO, Misawa M, Sukekava F. (2015) Alveolar socket healing: what can we learn? Periodontol 2000, 68: 122-134.

Assenza B, Piattelli M, Scarano A, Lezzi G, Petrone G, Piattelli A. (2001) Localized ridge augmentation using titanium micromesh. J Oral Implantol, 27: 287-292.

Atwood DA. (1963) Postextraction changes in the adult mandible as illustrated by microradiographs of midsagittal sections and serial cephalometric roentgenograms. J Prosthet Dent, 13: 810-824.

Balogh K. (1932) Histologie study of healing of extraction wounds following surgical removal of facial alveolar plate. Ztschr. f. Stomatol, 30: 281

Barboza EP, Stutz B, Ferreira VF, Carvalho W. (2010) Guided bone regeneration using nonexpanded polytetrafluoroethylene membranes in preparation for dental implant placements--a report of 420 cases. Implant Dent, 19: 2-7.

Bartee BK. (2001) Extraction site reconstruction for alveolar ridge preservation. Part 2: membrane-assisted surgical technique. J Oral Implantol, 27: 194-197.

Beretta M, Poli PP, Maiorana C. (2014) Accuracy of computer-aided template-guided oral implant placement: a prospective clinical study. J Periodontal Implant Sci, 44: 184-193.

Botticelli D, Berglundh T, Lindhe J. (2004) Hard-tissue alterations following immediate implant placement in extraction sites. J Clin Periodontol, 31: 820-828.

Bover-Ramos F, Viña-Almunia J, Cervera-Ballester J, Peñarrocha-Diago M, García-Mira B. (2018) Accuracy of implant placement with computer-guided surgery: a systematic review and meta-analysis comparing cadaver, clinical, and in vitro studies. Int J Oral Maxillofac Implants, 33: 101–115.

Boyne PJ. (1966) Osseous repair of the postextraction alveolus in man. Oral Surg Oral Med Oral Pathol, 21: 805-813.

Boyne PJ, James RA. (1980) Grafting of the maxillary sinus floor with autogenous marrow and bone. J Oral Surg, 38: 613-616.

Buser D, Brägger U, Lang NP, Nyman S. (1990) Regeneration and enlargement of jaw bone using guided tissue regeneration. Clin Oral Implants Res, 1: 22-32.

Buser D, von Arx T, ten Bruggenkate C, Weingart D. (2000) Basic surgical principles with ITI implants. Clin Oral Implants Res, 11: 59-68.

Canullo L, Tallarico M, Radovanovic S, Delibasic B, Covani U, Rakic M. (2016) Distinguishing predictive profiles for patient-based risk assessment and diagnostics of plaque induced, surgically and prosthetically triggered peri-implantitis. Clin Oral Implants Res, 27: 1243-1250.

Caplanis N, Lozada JL, Kan JY. (2005) Extraction defect assessment, classification, and management. J Calif Dent Assoc, 33: 853-863.

Cardaropoli G, Araújo M, Lindhe J. (2003) Dynamics of bone tissue formation in tooth extraction sites. An experimental study in dogs. J Clin Periodontol, 30: 809-818.

Cardoso CL, Rodrigues MTV, Júnior OF, Garlet GP, de Carvalho PSP. (2010) Clinical Concepts of Dry Socket. J Oral Maxillofac Surg, 68: 1922-1932.

Cassetta M, Stefanelli LV, Giansanti M, Calasso S. (2012) Accuracy of implant placement with a stereolithographic surgical template. Int J Oral Maxillofac Implants, 27: 655-663.

Cassetta M, Giansanti M, Di Mambro A, Calasso S, Barbato E. (2013) Accuracy of two stereolithographic surgical templates: a retrospective study. Clin Implant Dent Relat Res, 15: 448-459.

Celletti R, Davarpanah M, Etienne D, Pecora G, Tecucianu JF, Djukanovic D, Donath K. (1994) Guided tissue regeneration around dental implants in immediate extraction sockets: comparison of e-PTFE and a new titanium membrane. Int J Periodontics Restorative Dent, 14: 242-253.

Chappuis V, Engel O, Reyes M, Shahim K, Nolte LP, Buser D. (2013) Ridge alterations post-extraction in the esthetic zone: a 3D analysis with CBCT. J Dent Res, 92: 195S-201S.

Chappuis V, Araújo MG, Buser D. (2017) Clinical relevance of dimensional bone and soft tissue alterations post-extraction in esthetic sites. Periodontol 2000, 73: 73-83.

Chen ST, Darby IB, Reynolds EC. (2007) A prospective clinical study of non-submerged immediate implants: clinical outcomes and esthetic results. Clin Oral Implants Res, 18: 552-562.

Chen ST, Darby IB, Reynolds EC, Clement JG. (2009) Immediate implant placement postextraction without flap elevation. J Periodontol, 80: 163-172.

Claflin RS. (1936) Healing of disturbed and undisturbed extraction wounds. J Am Dent Assoc, 23: 945-959.

Covani U, Marconcini S, Galassini G, Cornelini R, Santini S, Barone A. (2007) Connective tissue graft used as a biologic barrier to cover an immediate implant. J Periodontol, 78: 1644-1649.

Crawford JY. (1896) Dry sockets after extraction. Dent Cosmos, 38: 929-931.

Cucchi A, Sartori M, Aldini NN, Vignudelli E, Corinaldesi G. (2019) A proposal of pseudo-periosteum classification after GBR by means of titanium-reinforced d-PTFE membranes or titanium meshes plus cross-linked collagen membranes. Int J Periodontics Restorative Dent, 39: 157-165.

Cucchi A, Vignudelli E, Sartori M, Parrilli A, Aldini NN, Corinaldesi G. (2021) A microcomputed tomography analysis of bone tissue after vertical ridge augmentation with non-resorbable membranes versus resorbable membranes and titanium mesh in humans. Int J Oral Implantol (Berl), 14: 25-38.

Dahlin C, Linde A, Gottlow J, Nyman S. (1988) Healing of bone defects by guided tissue regeneration. Plast Reconstr Surg, 81: 672-676.

Derksen W, Wismeijer D, Flügge T, Hassan B, Tahmaseb A. (2019) The accuracy of computer-guided implant surgery with tooth-supported, digitally designed drill guides based on CBCT and intraoral scanning. A prospective cohort study. Clin Oral Implants Res, 30: 1005-1015.

Di Giacomo GA, Cury PR, de Araujo NS, Sendyk WR, Sendyk CL. (2005) Clinical application of stereolithographic surgical guides for implant placement: preliminary results. J Periodontol, 76: 503-507.

Di Giacomo GA, da Silva JV, da Silva AM, Paschoal GH, Cury PR, Szarf G. (2012) Accuracy and complications of computer-designed selective laser sintering surgical guides for flapless dental implant placement and immediate definitive prosthesis installation. J Periodontol, 83: 410-419.

Ersoy AE, Turkyilmaz I, Ozan O, McGlumphy EA. (2008) Reliability of implant placement with stereolithographic surgical guides generated from computed tomography: clinical data from 94 implants. J Periodontol, 79: 1339-1345.

Esposito M, Maghaireh H, Grusovin MG, Ziounas I, Worthington HV. (2012) Soft tissue management for dental implants: what are the most effective techniques? A Cochrane systematic review. Eur J Oral Implantol, 5: 221-238.

Fickl S, Zuhr O, Wachtel H, Bolz W, Huerzeler M. (2008) Tissue alterations after tooth extraction with and without surgical trauma: a volumetric study in the beagle dog. J Clin Periodontol, 35: 356-363.

Fontana F, Santoro F, Maiorana C, Iezzi G, Piattelli A, Simion M. (2008) Clinical and histologic evaluation of allogeneic bone matrix versus autogenous bone chips associated

with titanium-reinforced e-PTFE membrane for vertical ridge augmentation: a prospective pilot study. Int J Oral Maxillofac Implants, 23: 1003-1012.

Fotek PD, Neiva RF, Hom-Lay W. (2009) Comparison of dermal matrix and polytetrafluoroethylene membrane for socket bone augmentation: a clinical and histologic study. J Periodontol, 80: 776-785.

Fugazzotto PA. (1999) Maintenance of soft tissue closure following guided bone regeneration: technical considerations and report of 723 cases. J Periodontol 70: 1085-1097.

Gharpure AS, Bhatavadekar NB. (2018) Clinical efficacy of tooth-bone graft: a systematic review and risk of bias analysis of randomized control trials and observational studies. Implant Dent, 27: 119-134.

Gluckman H, Du Toit J. (2014) Guided bone regeneration using a titanium membrane at implant placement: a case report and literature discussion. Int Dent S A, 4:13-19.

Gottlow J, Nyman S, Karring T, Lindhe J. (1984) New attachment formation as the result of controlled tissue regeneration. J Clin Periodontol, 11: 494-503.

Grunder U, Gracis S, Capelli M. (2005) Influence of the 3-D bone-to-implant relationship on esthetics. Int J Periodontics Restorative Dent, 25: 113-119.

Herzberg R. (2017) Vertical guided bone regeneration for a single missing tooth span with titanium-reinforced d-PTFE membranes: clinical considerations and observations of 10 consecutive cases with up to 36 months follow-up. Int J Periodontics Restorative Dent, 37: 892-899.

Horvath A, Mardas N, Mezzomo L, Needleman I, Donos N. (2013) Alveolar ridge preservation. A systematic review. Clin Oral Investig, 17: 341-363.

Hur Y, Teppei T, Tae-Ho Y, Griffin T. (2010) Double flap incision design for guided bone regeneration: a novel technique and clinical considerations. J Periodontol, 81: 945-952.

Hämmerle CHF, Chen ST, Wilson JTG. (2004) Consensus statements and recommended clinical procedures regarding the placement of implants in extraction sockets. Int J Oral Maxillofac Implants, 19: 26-28.

Hürzeler MB, Weng D. (1999) A single-incision technique to harvest subepithelial connective tissue grafts from the palate. Int J Periodontics Restorative Dent, 19: 279-287.

Jae-Jin A, Hong-In S. (2008) Bone tissue formation in extraction sockets from sites with advanced periodontal disease: a histomorphometric study in humans. Int J Oral Maxillofac Implants, 23: 1133-1138.

Januário AL, Duarte WR, Barriviera M, Mesti JC, Araújo MG, Lindhe J. (2011) Dimension of the facial bone wall in the anterior maxilla: a cone-beam computed tomography study. Clin Oral Implants Res, 22: 1168-1171.

Jensen SS, Terheyden H. (2009) Bone augmentation procedures in localized defects in the alveolar ridge: clinical results with different bone grafts and bone-substitute materials. Int J Oral Maxillofac Implants, 24: 218-236.

Khoury F, Hanser T. (2015) Mandibular bone block harvesting from the retromolar region: a 10-year prospective clinical study. Int J Oral Maxillofac Implants, 30: 688-697.

Kim YK, Lee J, Um IW, Kim KW, Murata M, Akazawa T, Mitsugi M. (2013) Tooth-derived bone graft material. J Korean Assoc Oral Maxillofac Surg, 39: 103-111.

Kotsakis GA, Salama M, Chrepa V, Hinrichs JE, Gaillard P. (2014) A randomized, blinded, controlled clinical study of particulate anorganic bovine bone mineral and

calcium phosphosilicate putty bone substitutes for socket preservation. Int J Oral Maxillofac Implants, 29: 141-151.

Lam RV. (1960) Contour changes of the alveolar processes following extractions. J Prosthet Dent, 10: 25-32.

Lekovic V, Kenney EB, Weinlaender M, Han T, Klokkevold P, Nedic M, Orsini M. (1997) A bone regenerative approach to alveolar ridge maintenance following tooth extraction. Report of 10 cases. J Periodontol, 68(6), 563-570.

Lekovic V, Camargo PM, Klokkevold PR, Weinlaender M, Keaney EB, Dimitrijevic B, Nedic M. (1998) Preservation of alveolar bone in extraction sockets using bioabsorbable membranes. J Periodontol, 69: 1044-1049.

Lindhe, J, Cecchinato D, Donati M, Tomasi C, Liljenberg B. (2014) Ridge preservation with the use of deproteinized bovine bone mineral. Clin Oral Implants Res, 25: 786-790.

Lindhe J, Karring T, Araújo M. Anatomy of periodontal tissues. In: Lindhe J, Lang NP (Eds.), Clinical Periodontology and Implant Dentistry (6th ed., Vol.1). Wiley Blackwell, Chichester, 2015:3-46.

Maiorana C, Poli PP, Beretta M. (2018) Guided bone regeneration and implant placement in association with a coronally positioned palatal sliding flap: a 17-year follow-up case report. J Oral Implantol, 44: 371-376.

Meloni SM, Jovanovic SA, Urban I, Canullo L, Pisano M, Tallarico M. (2017) Horizontal ridge augmentation using GBR with a native collagen membrane and 1:1 ratio of particulated xenograft and autologous bone: a 1-Year prospective clinical study. Clin Implant Dent Relat Res, 19: 38-45.

Merli M, Migani M, Bernardelli F, Esposito M. (2006) Vertical bone augmentation with dental implant placement: efficacy and complications associated with 2 different techniques. a retrospective cohort study. Int J Oral Maxillofac Implants, 21: 600-606.

Merli M, Migani M, Esposito M. (2007) Vertical ridge augmentation with autogenous bone grafts: resorbable barriers supported by ostheosynthesis plates versus titanium-reinforced barriers. a preliminary report of a blinded, randomized controlled clinical trial. Int J Oral Maxillofac Implants, 22: 373-382.

Merli M, Moscatelli M, Mazzoni A, Mazzoni S, Pagliaro U, Breschi L, Motroni A, Nieri M. (2013) Fence technique: guided bone regeneration for extensive three-dimensional augmentation. Int J Periodontics Restorative Dent, 33: 129-136.

Merli M, Moscatelli M, Mariotti G, Rotundo R, Bernardelli F, Nieri M. (2014) Bone level variation after vertical ridge augmentation: resorbable barriers versus titanium-reinforced barriers. A 6-year double-blind randomized clinical trial. Int J Oral Maxillofac Implants, 29: 905-913.

Molnár B, Deutsch T, Marton R, Orbán K, Martin A, Windisch P. (2019) Demonstration of radiographic bone fill in postextraction sockets using a novel implant-site development technique: a retrospective comparative case series. Int J Periodontics Restorative Dent, 39: 845-852.

Morton D, Chen ST, Martin WC, Levine RA, Buser D. (2014) Consensus statements and recommended clinical procedures regarding optimizing esthetic outcomes in implant dentistry. Int J Oral Maxillofac Implants, 29: 216-220.

Nevins M, Mellonig JT. (1992) Enhancement of the damaged edentulous ridge to receive dental implants: a combination of allogroft and the GORE-TEX membrane. Int J Periodontics Restorative Dent, 12: 96-111.

Nevins M, Camelo M, De Paoli S, Friedland B, Schenk RK, Parma-Benfenati S, Simion M, Tinti C, Wagenberg B. (2006) A study of the fate of the buccal wall of extraction sockets of teeth with prominent roots. Int J Periodontics Restorative Dent, 26: 18-29.

Novaes AB. (1997) Soft tissue management for primary closure in guided bone regeneration: surgical technique and case report. Int J Oral Maxillofac Implants, 12: 84-87.

Nyman S. (1991) Bone regeneration using the principle of guided tissue regeneration. J Clin Periodontol, 18: 494-498.

Ogata Y, Griffin TJ, Ko AC, Hur Y. (2013) Comparison of double-flap incision to periosteal releasing incision for flap advancement: a prospective clinical trial. Int J Oral Maxillofac Implants, 28: 597-604.

Oghli AA, Steveling H. (2010) Ridge preservation following tooth extraction: A comparison between atraumatic extraction and socket seal surgery. Quintessence Int, 41: 605-609.

Orban K, Varga E, Windisch P, Braunitzer G, Molnar B. (2021) Accuracy of half-guided implant placement with machine-driven or manual insertion: a prospective, randomized clinical study. Clin Oral Investig, 10.1007/s00784-021-04087-0. Advance online publication.

Ozan O, Orhan K, Turkyilmaz I. (2011) Correlation between bone density and angular deviation of implants placed using CT-generated surgical guides. J Craniofac Surg, 22: 1755-1761.

Paolantonio M, Dolci M, Scarano A, d'Archivio D, di Placido G, Tumini V, Piattelli A. (2001) Immediate implantation in fresh extraction sockets. A controlled clinical and histological study in man. J Periodontol, 72: 1560-1571.

Pesce P, Canullo L, Grusovin MG, de Bruyn H, Cosyn J, Pera P. (2015) Systematic review of some prosthetic risk factors for periimplantitis. J Prosthet Dent, 114: 346-350.

Pietrokovski J, Massler M. (1967) Alveolar ridge resorption following tooth extraction. J Prosthet Dent, 17: 21-27.

Rocchietta I, Fontana F, Simion M. (2008) Clinical outcomes of vertical bone augmentation to enable dental implant placement: a systematic review. J Clin Periodontol, 35: 203-215.

Rocchietta I, Simion M, Hoffmann M, Trisciuoglio D, Benigni M, Dahlin C. (2016) Vertical bone augmentation with an autogenous block or particles in combination with guided bone regeneration: a clinical and histological preliminary study in humans. Clin Implant Dent Relat Res, 18: 19-29.

Ronda M, Stacchi C. (2011) Management of a coronally advanced lingual flap in regenerative osseous surgery: a case series introducing a novel technique. Int J Periodontics Restorative Dent, 31: 505-513.

Schroeder HE. Development, structure, and function of periodontal tissues. In: Schroeder HE (Ed.) The Periodontium. Handbook of Microscopic Anatomy (5th ed., Vol.5). Springer, Berlin, 1986:47-64.

Schropp L, Wenzel A, Kostopoulos L, Karring T. (2003) Bone healing and soft tissue contour changes following single-tooth extraction: a clinical and radiographic 12-month prospective study. Int J Periodontics Restorative Dent, 23: 313-323.
Sclar AG. (2004) Strategies for management of single-tooth extraction sites in aesthetic implant therapy. J Oral Maxillofac Surg, 62: 90-105.

Shahbazi A, Feigl G, Sculean A, Grimm A, Palkovics D, Molnár B, Windisch P. (2021) Vascular survey of the maxillary vestibule and gingiva—clinical impact on incision and flap design in periodontal and implant surgeries. Clin Oral Investig, 25: 539-546.

Simion M, Baldoni M, Rassi P, Zaffe D. (1994) A comparative study of the effectiveness of e-PTFE membranes with and without early exposure during the healing period. Int J Periodontics Restorative Dent, 14: 166-180.

Simion M, Jovanovic SA, Trisi P, Scarano A, Piattelli A. (1998) Vertical ridge augmentation around dental implants using a membrane technique and autogenous bone or allografts in humans. Int J Periodontics Restorative Dent 18: 8-23.

Simion M, Dahlin C, Blair K, Schenk RK. (1999) Effect of different microstructures of e-PTFE membranes on bone regeneration and soft tissue response: a histologic study in canine mandible. Clin Oral Implants Res, 10: 73-84.

Simion M, Fontana F, Rasperini G, Maiorana C. (2007) Vertical ridge augmentation by expanded-polytetrafluoroethylene membrane and a combination of intraoral autogenous bone graft and deproteinized anorganic bovine bone (Bio Oss). Clin Oral Implants Res, 18: 620-629.

Simon BI, Tat Fai C, Drew HJ. (2010) Alternative to the gold standard for alveolar ridge augmentation: Tenting screw technology. Quintessence Int, 41: 379-386.

Stimmelmayr M, Güth JF, Iglhaut G, Beuer F. (2012) Preservation of the ridge and sealing of the socket with a combination epithelialised and subepithelial connective tissue graft for management of defects in the buccal bone before insertion of implants: a case series. Br J Oral Maxillofac Surg, 50: 550-555.

Summers RB. (1994) A new concept in maxillary implant surgery: the osteotome technique. Compendium, 15: 152-162.

Taberner-Vallverdú M, Nazir M, Sánchez-Garcés MÁ, Gay-Escoda C. (2015) Efficacy of different methods used for dry socket management: A systematic review. Med Oral Pat Oral Cir Bucal, 20: 633-639.

Tahmaseb A, Wismeijer D, Coucke W, Derksen W. (2014) Computer technology applications in surgical implant dentistry: a systematic review. Int J Oral Maxillofac Implants, 29: 25-42.

Tan WL, Wong TLT, Wong MCM, Lang NP. (2012) A systematic review of post-extractional alveolar hard and soft tissue dimensional changes in humans. Clin Oral Implants Res, 23: 1-21.

Tinti C, Parma-Benfenati S. (1995) Coronally positioned palatal sliding flap. Int J Periodontics Restorative Dent, 15: 298-310.

Tinti C, Parma-Benfenati S, Polizzi G. (1996) Vertical ridge augmentation: what is the limit? Int J Periodontics Restorative Dent, 16: 220-229.

Tinti C, Parma-Benfenati S. (1998) Vertical ridge augmentation: surgical protocol and retrospective evaluation of 48 consecutively inserted implants. Int J Periodontics Restorative Dent, 18: 434-443.

Tomasi C, Sanz M, Cecchinato D, Pjetursson B, Ferrus J, Lang NP, Lindhe J. (2010) Bone dimensional variations at implants placed in fresh extraction sockets: a multilevel multivariate analysis. Clin Oral Implants Res, 21: 30-36.

Tomasi C, Donati M, Cecchinato D, Szathvary I, Corrà E, Lindhe J. (2018) Effect of socket grafting with deproteinized bone mineral: An RCT on dimensional alterations after 6 months. Clin Oral Implants Res, 29: 435-442.

Tonetti, MS, Jung RE, Avila-Ortiz G, Blanco J, Cosyn J, Fickl S, Figuero E, Goldstein M, Graziani F, Madianos P, Molina A, Nart J, Salvi GE, Sanz-Martin I, Thoma D, Van Assche N, Vignoletti F. (2019) Management of the extraction socket and timing of implant placement: Consensus report and clinical recommendations of group 3 of the XV European Workshop in Periodontology. J Clin Periodontol, 46: 183-194.

Trombelli L, Farina R, Marzola A, Bozzi L, Liljenberg B, Lindhe J. (2008) Modeling and remodeling of human extraction sockets. J Clin Periodontol, 35: 630-639.

Tylman SD. (1960) Theory and practice of crown and bridge prosthodontics. In S. G. Tylman C. V. Mosby Company, St. Louis: 69-71.

Urban IA, Nagursky H, Lozada JL. (2011) Horizontal ridge augmentation with a resorbable membrane and particulated autogenous bone with or without anorganic bovine bone-derived mineral: a prospective case series in 22 patients. Int J Oral Maxillofac Implants, 26: 404-414.

Urban IA, Nagursky H, Lozada JL, Nagy K. (2013) Horizontal ridge augmentation with a collagen membrane and a combination of particulated autogenous bone and anorganic bovine bone-derived mineral: a prospective case series in 25 patients. Int J Periodontics Restorative Dent, 33: 298-307.

Urban IA, Lozada JL, Jovanovic SA, Nagursky H, Nagy K. (2014) Vertical ridge augmentation with titanium-reinforced, dense-PTFE membranes and a combination of particulated autogenous bone and anorganic bovine bone-derived mineral: A prospective case series in 19 patients. Int J Oral Maxillofac Implants, 29: 185-193.

Urban IA, Monje A, Wang HL, Lozada J, Gerber G, Baksa G. (2017) Mandibular regional anatomical landmarks and clinical implications for ridge augmentation. Int J Periodontics Restorative Dent, 37: 347-353.

Urban IA, Monje A, Lozada J, Hom-Lay W. (2017) Principles for vertical ridge augmentation in the atrophic posterior mandible: a technical review. Int J Periodontics Restorative Dent, 37: 639-645.

Urban I, Traxler H, Romero-Bustillos M, Farkasdi S, Bartee B, Baksa G, Avila-Ortiz G. (2018) Effectiveness of two different lingual flap advancing techniques for vertical bone

augmentation in the posterior mandible: A comparative, split-mouth cadaver study. Int J Periodontics Restorative Dent, 38: 35-40.

Urban IA, Montero E, Monje A, Sanz-Sánchez I. (2019) Effectiveness of vertical ridge augmentation interventions: A systematic review and meta-analysis. J Clin Periodontol, 46: 319-339.

Valente F, Schiroli G, Sbrenna A. (2009) Accuracy of computer-aided oral implant surgery: a clinical and radiographic study. Int J Oral Maxillofac Implants, 24: 234-242.

Van de Wiele G, Teughels W, Vercruyssen M, Coucke W, Temmerman A, Quirynen M. (2015) The accuracy of guided surgery via mucosa-supported stereolithographic surgical templates in the hands of surgeons with little experience. Clin Oral Implants Res, 26: 1489-1494.

Varga E, Antal M, Major L, Kiscsatári R, Braunitzer G, Piffkó J. (2020) Guidance means accuracy: a randomized clinical trial on freehand versus guided dental implantation. Clin Oral Implants Res. 31: 417–430.

Vercruyssen M, Fortin T, Widmann G, Jacobs R, Quirynen M. (2014) Different techniques of static/dynamic guided implant surgery: modalities and indications. Periodontol 2000, 66: 214-227.

Windisch P, Martin A, Shahbazi A, Molnar B. (2017) Reconstruction of horizontovertical alveolar defects. Presentation of a novel split-thickness flap design for guided bone regeneration: a case report with 5-year follow-up. Quintessence Int, 48: 535-547.

Windisch P, Orban K, Salvi GE, Sculean A, Molnar B. (2021) Vertical-guided bone regeneration with a titanium-reinforced d-PTFE membrane utilizing a novel split-thickness flap design: a prospective case series. Clin Oral Investig, 25: 2969-2980.

Yoshino S, Kan JY, Rungcharassaeng K, Roe P, Lozada JL. (2014) Effects of connective tissue grafting on the facial gingival level following single immediate implant placement and provisionalization in the esthetic zone: a 1-year randomized controlled prospective study. Int J Oral Maxillofac Implants, 29: 432-440.

DOI:10.14753/SE.2022.2638

10. BIBLIOGRAPHY OF THE CANDIDATE'S PUBLICATIONS

Related publications

Study I

Molnar B, Deutsch T, Marton R, Orban K, Martin A, Windisch P. (2019) Demonstration of radiographic bone fill in postextraction sockets using a novel implant-site development technique: a retrospective comparative case series. Int J Periodontics Restorative Dent, 39: 845-852. IF: 1.513 (2019)

Study II

Windisch P, Orban K, Salvi GE, Sculean A, Molnar B. (2021) Vertical-guided bone regeneration with a titanium-reinforced d-PTFE membrane utilizing a novel split-thickness flap design: a prospective case series. Clin Oral Investig, 25: 2969-2980. IF: 3.573 (2020)

Study III

Orban K, Varga E, Windisch P, Braunitzer G, Molnar B. (2021) Accuracy of half-guided implant placement with machine-driven or manual insertion: a prospective, randomized clinical study. Clin Oral Investig, 10.1007/s00784-021-04087-0. Advance online publication. IF: 3.573 (2020)

DOI:10.14753/SE.2022.2638

11. ACKNOWLEDGEMENTS

Study I

The study was performed at the Department of Periodontology and the Department of Oro-Maxillofacial Surgery and Stomatology, Semmelweis University, Budapest, Hungary.

Study II

The study was conducted at the Department of Periodontology, Semmelweis University, Budapest, Hungary.

Study III

The study was carried out at the Department of Periodontology, Semmelweis University, Budapest, Hungary, the evaluation process and statistical analysis was made by the dicomLAB Kft.

The present study received material support from NSK Europe GmbH, Eschborn, Germany; Botiss Biomaterials GmbH, Zossen, Germany; Straumann AG, Basel, Switzerland; Dicomlab Kft., Szeged, Hungary; the Hungarian Human Resources Development Operational Program (EFOP-3.6.2-16-2017-00006); the Excellence Program of the Ministry for Innovation and Technology in Hungary, within the framework of the Therapy thematic program of the Semmelweis University.

I would like to thank the co-workers of the Department of Oro-Maxillofacial Surgery and Stomatology at the Semmelweis University, Budapest, who contributed to data collection for the Study I. I would like to express a special thanks to György Göndöcs and Boglárka Hermann for the long hours spent together to perform CBCT scan segmentation, radiographic segments' alignment procedure and measurement process. I would like to thank co-author Professor Anton Sculean and Giovanni E. Salvi for a lot of help and positive comments throughout writing the article from Study II. I would like to thank Endre Varga Jr., Gábor Braunitzer and the team of dicomLAB for the material support

DOI:10.14753/SE.2022.2638

and the essential help in the measurement procedure and statistical analysis in Study III. I would also like to thank the staff of the Department of Periodontology.

This thesis is a result of many years of collaboration with my tutor, Balint Molnar, who has always inspired and supported me since 2012. I do not have enough words to express my gratitude for him.

I would like to thank for the guidance of my mentor and leader Professor Peter Windisch, I feel very grateful to have had the opportunity from him to be part of the clinical team he leads.

I would like to thank my wonderful parents for their great advice and support during these years. At last, I would like to thank my loving wife for always boosting up my motivation whenever I was down. Her support and encouragement were crucial in me finishing the thesis.

DOI:10.14753/SE.2022.2638

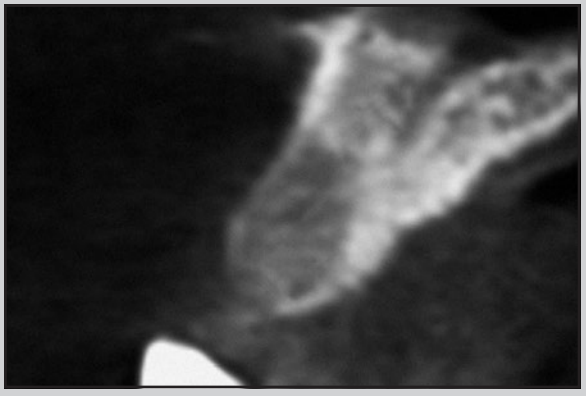

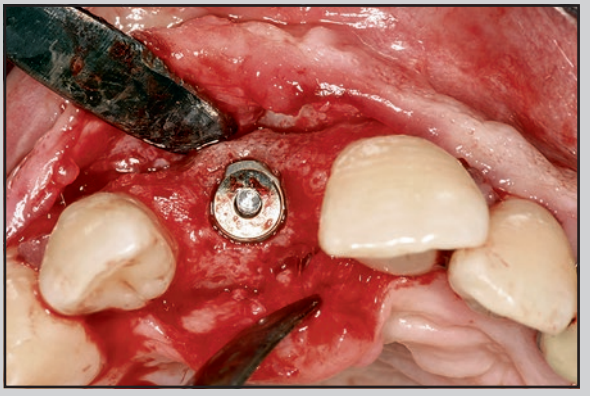

Demonstration of Radiographic Bone Fill in Postextraction Sockets Using a Novel Implant-Site Development Technique: A Retrospective Comparative Case Series

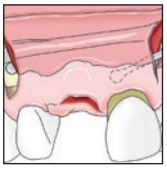

Bálint Molnár, DMD, PhD[1]
Tibor Deutsch, PhD[2]
Rita Marton, DMD[1]*/Kristóf Orbán, DMD*[1]
Anna Martin, DMD[1]*/Peter Windisch, DMD, PhD*[1]

The objective of this study was to compare the novel extraction-site development (XSD) technique with spontaneous healing. Advanced alveolar defects (extraction defect sounding, classes 3 and 4) at 33 single-rooted teeth were treated by XSD (test), and 21 extraction sites of single-rooted teeth were left for spontaneous healing (control). In pre- and postoperative cone beam computed tomography (CBCT) data sets, orovestibular and vertical socket dimensions were assessed, as were socket areas. XSD resulted in complication-free healing with significantly higher radiographic bone fill compared to spontaneous healing. Application of the XSD approach may reduce the need for augmentative procedures during implant placement.
Int J Periodontics Restorative Dent 2019;39:845–852. doi: 10.11607/prd.4106

[1]Department of Periodontology, Semmelweis University, Budapest, Hungary.
[2]Department of Imaging and Medical Instrumentation, Semmelweis University, Budapest, Hungary.

Correspondence to: Prof Dr Peter Windisch, Department of Periodontology, Semmelweis University, Budapest, Hungary; Faculty of Dentistry, Semmelweis University, 1088 Budapest Szentkirályi u. 47., Budapest, Hungary.
Fax: +36-1-267-4907. Email: peter.windisch@gmail.com

Submitted September 10, 2018; accepted March 31, 2019.

Bone resorption after tooth extraction is more pronounced on the buccal plate, especially in cases of inflammatory processes or surgical trauma.[1] To achieve optimal white and pink esthetics, harmonious periimplant hard and soft tissue contours are required. Measured immediately after tooth removal, the extraction defect sounding (EDS) classification provides a guideline on treatment selection based on direct measurements of alveolar dehiscences by way of a periodontal probe. According to EDS, immediate implant placement is a viable treatment option in cases of EDS classes 1 and 2 if the buccal alveolar plate is intact. In the vast majority of cases, however, clinicians are forced to treat compromised postextraction sockets.[2] In cases of EDS classes 2 and 3, early implant placement with additional augmentation is recommended if the remaining native bone allows it.[3–7] In cases of EDS classes 3 and 4, ridge augmentation with staged implant placement is a frequently chosen treatment modality. Nevertheless, as an alternative, alveolar ridge preservation (ARP) has been proposed to limit postextraction changes without extensive ridge reconstructions.[8] Several treatment options have been suggested for ARP. Grafting procedures might increase hard tissue quantity, but tissue quality showed wide variations following

the placement of xenogeneic or allogenic grafts.[8–12] Application of barrier membranes alone resulted in favorable hard tissue conditions due to the natural postextraction healing process. Connective tissue grafting during ARP alone or in combination therapy was reported to improve soft tissue conditions.[13–16] According to a systematic review, ARP procedures may be evaluated by direct clinical measurements, feasibility for implant placement, radiographic assessment, and histologic analysis.[17] Three-dimensional (3D) radiographic analysis was carried out only in three randomized clinical trials.[18–20] The aim of the present radiographic study was to comparatively evaluate a novel ARP technique, the extraction site development (XSD) technique, utilizing long-term resorbable membranes and connective tissue grafting to treat EDS classes 3 and 4 defects.

Materials and Methods

Patient Demographics and Study Design

XSD was radiographically evaluated in a comparative retrospective case series study at the Department of Periodontology at Semmelweis University in Budapest, Hungary, from 2007 to 2014. In the test group, the pre- and postoperative cone beam computed tomography (CBCT) data sets of 29 healthy patients (18 females and 11 males, aged 29 to 71 years) presenting 33 single-rooted teeth (27 incisors, 2 canines, 4 premolars; 29 teeth in the maxilla, 4 in the mandible) with EDS class 3 or 4 were included and treated by XSD. In the control group, archived pre- and postoperative CBCT data sets (from 2009 to 2013) of 14 patients (8 females and 6 males, aged from 29 to 71 years, mean age 52 years) presenting 21 extracted single-rooted teeth (16 incisors, 2 canines, 3 premolars; 11 teeth in the maxilla, 10 in the mandible) were included from the digital library of the Department of Oro-Maxillofacial Surgery and Stomatology, Semmelweis University in Budapest, Hungary. Between pre- and postoperative CBCT scans, neither ARP nor any other treatments were performed in the control group. Exclusion criteria in the test group were any relevant systematic disease, poor oral hygiene, and smoking more than 10 cigarettes a day. The study was conducted in full accordance with ethical principles, including the World Medical Association Declaration of Helsinki (version 2004, updated in 2008) and approved by the Semmelweis University Regional and Institutional Committee of Science and Research Ethics (Approval Number: 20/2007; 77/2011). Surgical interventions were undertaken with the understanding and written consent of each subject.

Surgical Procedure: The XSD Approach

EDS classes 3 and 4 extraction sockets were treated by a novel tunneled guided bone regeneration (GBR) approach (XSD) as a modification of the vestibular incision subperiosteal tunnel access approach (Fig 1).[21] Following tooth removal, extraction sockets were debrided. Buccal tunnel preparation was performed with dedicated instruments (Tunneling Knives Set, Deppeler) with a full-thickness crevicular approach up to the level of the mucogingival junction and extending to mesial and distal neighboring papillae, where two remote full-thickness vertical incisions were placed. Bilaminar partial-thickness tunnel preparation was continued from the mucogingival junction, dissecting the mucosal layer from underlying muscles and periosteum. A long-term resorbable membrane (Soft Cortical Lamina, Tecnoss) was fixed in the subperiosteal tunnel by two titanium pins (Frios Membrane Tacks, Dentsply Implants) on the healthy intact buccal bone of mesially and distally adjacent teeth to cover the buccal dehiscence. Subsequently, a subepithelial connective tissue graft was harvested by the single incision technique and inserted into the supraperiosteal tunnel, fixed with nonresorbable 5/0 horizontal mattress sutures (Dafilon, B. Braun).[22] The socket was filled with a resorbable collagen sponge (Lyostypt, B. Braun) to ensure stabilization of an enlarged blood clot. Remote vertical incisions were sutured, followed by crestal approximation of gingival margins with crossed sutures.

Postoperative Care

Patients were prescribed systemic antibiotics (Augmentin Duo, GlaxoSmithKline; 1,000 mg twice a day for 7

days) and a nonsteroidal anti-inflammatory drug (Cataflam, Novartis). Patients used a 0.2% chlorhexidine-gluconate–containing mouth rinse solution (Curasept 220, Curaden Swiss) twice a day during the first 14 days postsurgery. Sutures were removed 14 days after surgery.

Reentry Procedure and Implant Placement

Six to 9 months after XSD (7.5 months on average), patients selected for implant therapy underwent reentry surgery with 3D radiographic planning. After elevation of a full-thickness flap, titanium pins were removed, and newly formed vital hard tissue was observed in each XSD-treated case. Minor remnants of the lamina membrane were occasionally present. If necessary, implant placement with simultaneous ridge augmentation or staged ridge augmentation was carried out by GBR.

Radiographic Evaluation

Evaluation was performed using I-CAT Vision (Imaging Sciences International) and ImageJ (National Institutes of Health) software programs. CBCT scans taken prior to tooth extraction and 6 to 9 months later were selected for further analysis. 3D alignment was performed at pre- and postoperative data sets simultaneously on two separate computer screens at equal magnification levels. Orthoradial cross-sections were created on midbuccal, mesiobuccal, and distobuccal aspects of extraction sites. A 1-mm^2 grid was laid over the cross-sectional images. Parallel with a reference base, 15 orovestibular sections were registered. Orovestibular (OV) and vertical (VER)

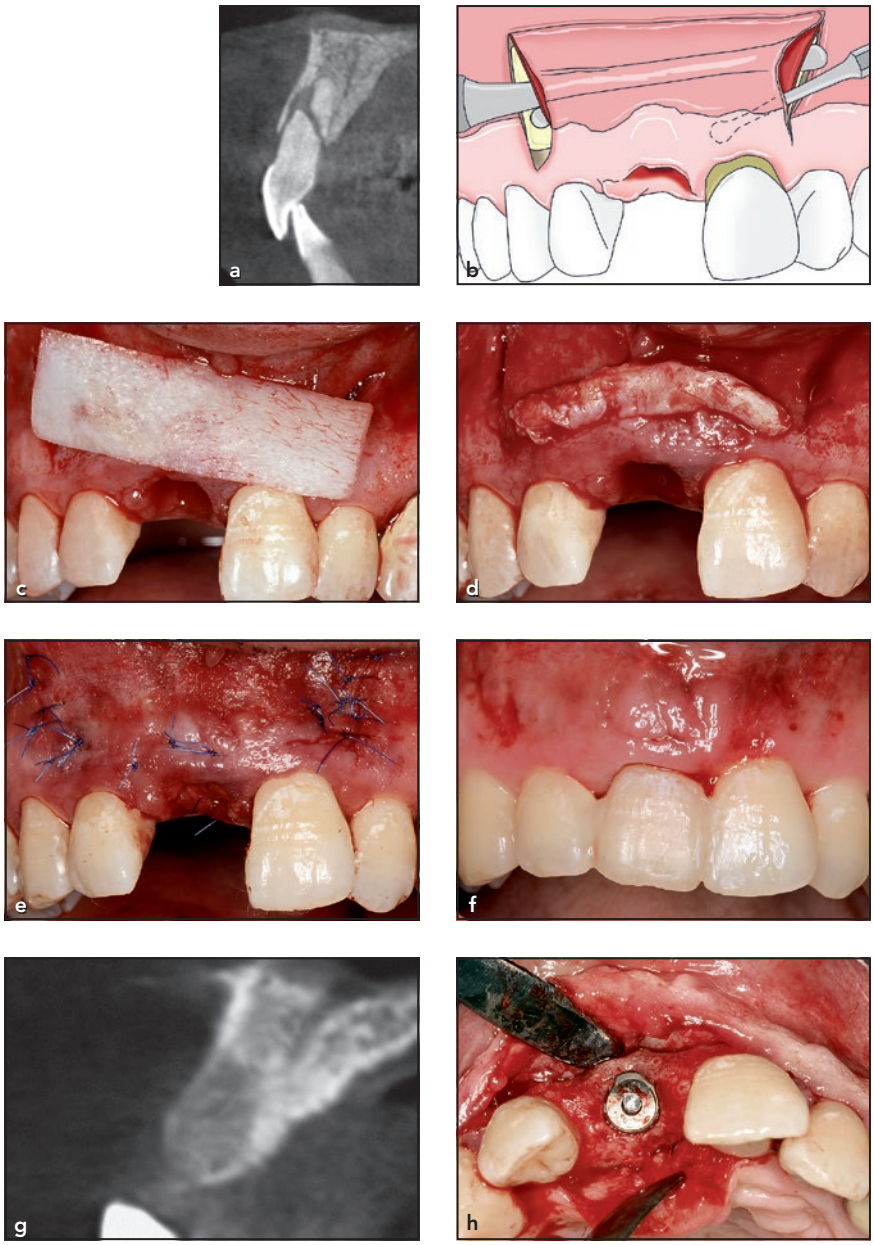

Fig 1 *Representative case of the XSD approach.* (a) *Baseline CBCT scan. Treating the maxillary right central incisor is irrational due to fracture of the root. During tooth removal, the buccal bony plate fractured and was removed.* (b) *Schematic drawing of XSD, utilizing bilaminar tunnel flap for membrane and connective tissue graft insertion.* (c) *Cortical layer of xenograft with a long-term resorbable membrane function (Soft Cortical Lamina, Tecnoss).* (d) *Subperiosteal connective tissue graft harvested from the palate to improve the keratinized tissue contour.* (e) *Wound closure.* (f) *Early wound healing at 2.* (g) *The 6-month CBCT presents radiographic bone fill with reconstructed buccal bone.* (h) *Implant placement in maintained alveolar ridge with buccal bone support.*

DOI:10.14753/SE.2022.2638

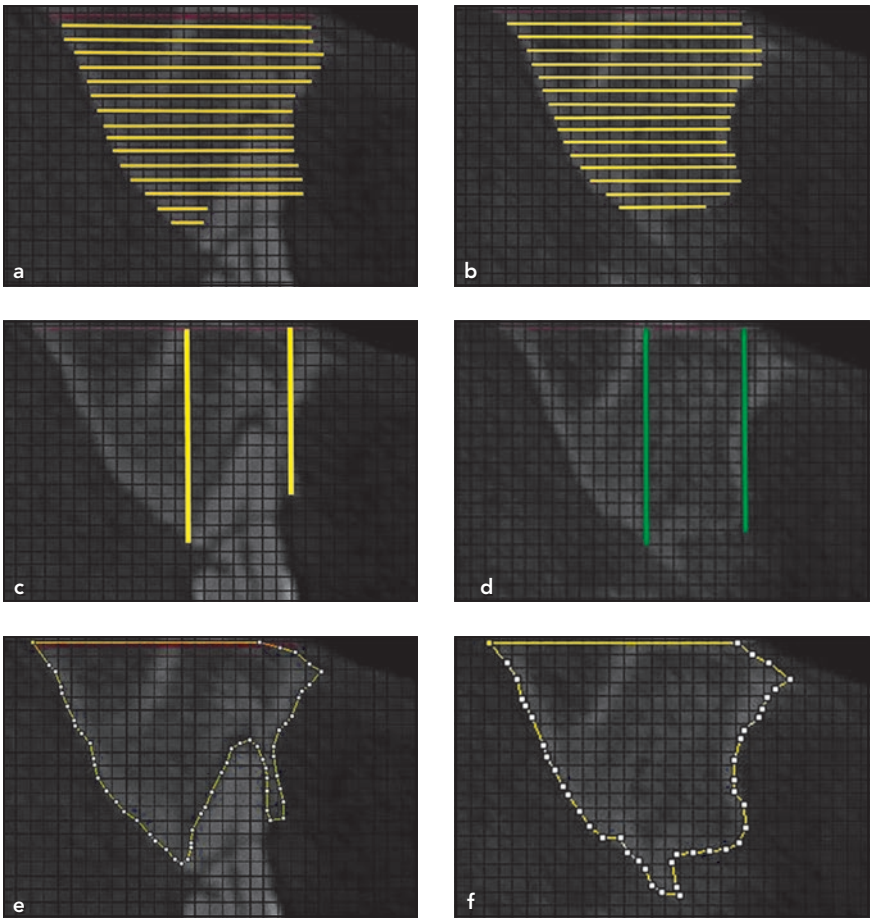

Fig 2 *Radiographic evaluation protocol.* (a) *Baseline socket dimension (OV).* (b) *Postoperative OV.* (c) *Baseline vertical socket dimension (VER).* (d) *Postoperative VER.* (e) *Baseline socket area (SA).* (f) *Postoperative SA.*

socket dimensions were assessed. Minimal OV feasible for implant placement (OVimpl) was defined as 6 mm, according to Fiorellini at al[18] and Nevins et al.[19] Planimetric measurements were carried out using the 1-mm^2 grid, excluding tooth area in preoperative images. Socket areas (SAs) were assessed (Fig 2).

Statistical Analyses

Statistical analysis was conducted using IBM SPSS (version 22) and Microsoft Excel 2013. Quantitative data, including CBCT measurements, were presented in the form of mean ± standard deviation for descriptive purposes. Differences between baseline and reentry data in both groups were analyzed by paired *t* test. Differences in the dependent variables between test and control groups were analyzed by independent samples *t* test. The odds ratio (OR) was used as effect statistics (ie, to assess the intervention's ability to create conditions that make the extraction sites feasible for implantation without prior augmentation). Significance of the OR was evaluated using Fisher exact test. The level of statistical significance was set at $\alpha = .05$.

Results

Initial Defect Distribution

Baseline defect dimensions in both groups are summarized in Tables 1 to 3. As postextraction bone remodeling did not affect the apical two-thirds of the socket (sections 1 to 10), only data registered at the most coronal proportion (sections 11 to 15) are shown. Test sites represented severely compromised EDS classes 3 and 4 defects with missing buccal bone. Most cross-sections presented significantly less baseline OV than control sites. The same tendency was observed in baseline mean mesiobuccal (13.8 ± 4.7 mm vs 19.1 ± 5.5 mm), midbuccal (11.6 ± 4.4 mm vs 17.5 ± 5.6 mm), distobuccal (15.1 ± 5.2 mm vs 18.3 ± 5.3 mm), mesiopalatal (15.3 ± 4.4 mm vs 19.0 ± 6.0 mm), and midpalatal (15.0 ± 4.0 mm vs 18.5 ± 5.5 mm) VER data for test and control groups, respectively (Table 1). There was no statistically significant difference distopalatally between the two groups (Table 2). Significantly less baseline mean SA was observed midbuccally (122.8 ± 50.5 mm^2 vs 163.8 ± 52.7 mm^2) in test compared to control (Table 3).

Hard Tissue Changes

Given the inhomogeneity of initial socket characteristics in the two groups, the impact of XSD

Table 1 Baseline Orovestibular Socket Dimensions (OV) and Postoperative OV Changes (ΔOV)

	Mean baseline OV (mm)			Mean ΔOV (mm)		
Section	Test	Control	*P*	Test	Control	*P*
Mesial						
11	5.8 ± 2.8	6.5 ± 2.3	NS	0.19 ± 1.78	0.90 ± 1.55	NS
12	4.5 ± 3.4	6.2 ± 2.6	.041*	–0.23 ± 1.76	1.46 ± 2.27	.003*
13	3.8 ± 3.1	5.4 ± 3.1	NS	–0.24 ± 1.85	1.33 ± 1.57	.002*
14	2.4 ± 2.5	4.8 ± 2.9	.002*	–0.39 ± 1.83	1.52 ± 2.30	.001*
15	1.4 ± 1.9	3.3 ± 3.2	.01*	–0.42 ± 1.51	1.40 ± 3.04	.017*
Midbuccal						
11	4.8 ± 3.4	7.5 ± 2.8	.004*	–0.73 ± 2.09	2.55 ± 2.52	< .001*
12	3.9 ± 3.4	7.0 ± 3.3	.002*	–0.86 ± 2.47	2.73 ± 2.90	< .001*
13	3.2 ± 3.5	6.3 ± 3.2	.002*	–0.73 ± 2.04	2.63 ± 3.09	< .001*
14	2.6 ± 3.4	5.8 ± 3.6	.003*	–0.16 ± 1.97	2.73 ± 3.12	< .001*
15	1.4 ± 2.3	4.7 ± 3.5	< .001*	–0.48 ± 1.60	2.71 ± 3.46	.001*
Distal						
11	6.2 ± 3.0	6.9 ± 3.0	NS	–0.05 ± 1.30	1.41 ± 2.02	.006*
12	5.5 ± 3.2	5.4 ± 2.8	NS	0.05 ± 1.76	1.42 ± 1.79	.002*
13	4.2 ± 3.2	5.9 ± 2.7	NS	0.01 ± 2.13	1.40 ± 2.49	.033*
14	3.8 ± 3.0	5.5 ± 2.6	.033*	0.57 ± 1.98	2.35 ± 3.24	.015*
15	2.4 ± 2.6	3.8 ± 2.7	NS	0.62 ± 1.70	1.62 ± 3.38	NS

NS = not significant.
Changes measured in the coronal third of the alveoli (sections 11 to 15).
Positive differences denote bone loss, and negative differences represent bone gain.
All numeric *P* values shown here are statistically significant.

Table 2 Baseline Vertical Socket Dimensions (VER) and Postoperative VER Changes (ΔVER)

	Mean baseline VER (mm)			Mean ΔVER (mm)		
Section	Test	Control	*P*	Test	Control	*P*
Mesial						
Buccal	13.8 ± 4.7	19.1 ± 5.5	< .001*	–0.77 ± 2.45	1.31 ± 1.39	< .001*
Palatal	15.3 ± 4.4	19.0 ± 6.0	.011*	–0.01 ± 1.45	1.26 ± 2.21	.027*
Midbuccal						
Buccal	11.6 ± 4.4	17.5 ± 5.6	.011*	–2.23 ± 3.35	2.26 ± 2.41	< .001*
Palatal	15.0 ± 4.0	18.5 ± 5.5	.010*	0.25 ± 2.15	1.64 ± 1.57	.013*
Distal						
Buccal	15.1 ± 5.2	18.3 ± 5.3	.035*	0.36 ± 2.73	0.54 ± 2.17	NS
Palatal	16.0 ± 4.9	18.3 ± 5.2	NS	0.97 ± 4.3	1.42 ± 2.24	NS

NS = not significant.
Positive differences denote bone loss, and negative differences represent bone gain.
All numeric *P* values shown here are statistically significant.

Table 3 Baseline Socket Area Dimensions (SA) and Postoperative SA Changes (ΔSA)

	Mean baseline SA (mm)			Mean ΔSA (mm)		
Section	Test	Control	*P*	Test	Control	*P*
Mesial	124.3 ± 64.3	158.7 ± 56.4	NS	–5.65 ± 23.34	20.05 ± 13.72	< .001*
Midbuccal	122.8 ± 50.5	163.8 ± 52.7	.006*	–11.34 ± 23.74	26.34 ± 20.13	< .001*
Distal	141.6 ± 49.6	159.8 ± 61.5	NS	0.62 ± 21.50	21.76 ± 24.19	< .001*

NS = not significant.
Positive differences denote bone loss, and negative differences represent bone gain.
All numeric *P* values shown here are statistically significant.

DOI:10.14753/SE.2022.2638

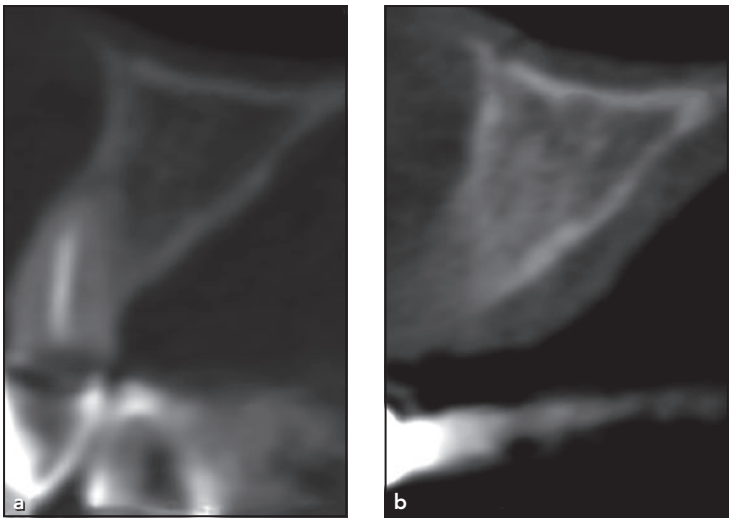

Fig 3 *Radiographic changes of a representative case in the control group. CBCT scans taken at* (a) *baseline and* (b) *6 months.*

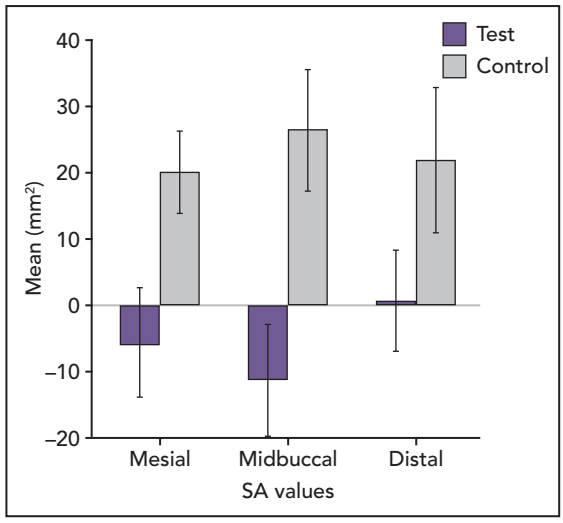

Fig 4 *Changes of SA values. Error bars represent 95% confidence interval.*

was evaluated using the differences in pre- and postoperative linear and planimetric cross-section measurements. Mean changes (ΔOV, ΔVER, and ΔSA) at mesial and distal OV cross-sections are also summarized in Tables 1 to 3. ΔOV, ΔVER, and ΔSA readings are highly correlated. Each control site showed radiographic bone loss (mean ΔOV, ΔVER, and ΔSA all > 0), which is most pronounced at OV midbuccal sections (Fig 3). Most test sites showed not only less bone loss compared to control but also radiographic bone gain, which was detected at several OV cross-sections. Statistically significant differences were found in average midbuccal changes (ΔOV15 to ΔOV11) between test and control groups. Figure 4 illustrates the impact of the novel method in terms of changes in SA values. The success of alveolar preservation is most directly measured by the ratio of sites, which were feasible for postoperative implant placement (OVimpl; minimum 6-mm OV). OVimpl was registered in 15 out of 33 sites compared to 6 out of 21 sites in test and control groups, respectively. These data at reentry correspond to an odds ratio of 2.055 (95% confidence interval: 0.6 to 7.1), which implies a substantial, albeit not statistically significant difference, in effect size.

Clinical Results

Postoperative healing was uneventful in all 33 surgical sites in the test group following XSD. No complications, such as allergic reactions, abscesses, or infections, were observed during the healing period. At reentry, formation of vital hard tissues was confirmed visually and by implant osteotomy. In the test group, 33 teeth were removed and treated with XSD. A total of 25 dental implants were placed into the treated sockets. Compared to baseline measurement, all XSD-treated sites showed hard tissue gain 6 months after surgery. Fourteen sites received implants without needing any hard tissue augmentation, which was in accordance with the 15 sites showing a radiographically predefined OVimpl of 6 mm. Five sites received implants, requiring minor simultaneous GBR. Six sites (patients with a high lip line) were treated with staged vertical GBR before implant placement to allow for optimal and predictable esthetic outcomes. Four sites received fixed partial dentures with pontics, and 4 sites had not received further treatment. All inserted implants received final prosthetics and survived during the study period. Final outcomes were well accepted by the patients, and optimal functional and esthetic results were achieved.

Discussion

The present retrospective comparative case series provided radiographic and clinical evidence on the efficacy of the newly introduced XSD approach in achieving bone fill as compared to spontaneous healing. The surgical concept is based on supporting the natural healing process by fulfilling three critical prerequisites: *(1)* reconstruction of the missing buccal bony wall by fixation of a long-term resorbable membrane; *(2)* stabilization and enlargement of the alveolar blood clot by inserting a fully resorbable collagen sponge into a secluded space; and *(3)* improving soft tissue conditions by connective tissue grafting. The authors were able to show average midbuccal horizontal bone fill (ΔOV15) of –0.48 ± 1.60 mm vs average midbuccal bone loss (ΔOV15) of 2.71 ± 3.46 mm at the most coronal aspect of the extraction aveoli in test vs control sites, respectively, which is a unique phenomenon previously not reported in the literature. Current consensus suggests that using bone graft to fill sockets can help to preserve the physical dimensions of the alveolar ridge.[23] However, various authors reported impaired quality of preserved ridges due to connective tissue encapsulation of grafting materials.[24,25] Confirming the results of Lekovic et al, who utilized only GBR membranes,[26,27] the present authors found favorable hard tissue conditions following XSD. Test sites presented vital, mineralized hard tissue conditions at reentry. Application of a connective tissue graft provided sufficient tissue thickness to avoid membrane exposure and to create an enlarged space over the early healing period. In the present study, a standardized comparative radiographic analysis of hard tissue changes was conducted. Previous studies used the same methodology by comparing pre- and postoperative horizontal and vertical alveolar ridge dimensions.[18,19] In both studies, adequate horizontal bone dimension for implant placement was defined as a 6-mm-wide reconstructed alveolar ridge. A more recent randomized clinical trial using the same measurement approach also reported on planimetric measurements,[20] using the 6-mm OV width as a basic criterion to allow for implant placement. At baseline, only 9 out of 33 cases in the test group showed more than 6 mm OV, and these sites were workable for implant placement at reentry. Furthermore, 6 out of the remaining 24 cases with baseline OV less than 6 mm showed additional horizontal bone gain and thus became candidates for implant placement at reentry. This unique phenomenon was neither observed in the control group nor in any other study reporting on ARP. In contrast, in the control group, several sockets with adequate bone structure initially lost substantial bony mass and would require augmentation before or at the time of the implant placement. All initially nonimplantable sockets suffered further bone loss, as anticipated after tooth extraction.

Conclusions

The XSD approach decreased the need for augmentative procedures by improving baseline tissue conditions at extraction sites. As a result, both reduced bone loss and additional bone formation were observed at several treated sites. By applying the XSD approach, the need for augmentative procedures may be reduced by improving baseline quality and quantity of hard and soft tissues at extraction sites. Furthermore, in some cases, XSD may enable implant placement without further augmentation in the second surgical session.

Acknowledgments

The authors would like to thank co-workers of the Department of Periodontology and the Department of Oro-Maxillofacial Surgery and Stomatology at the Semmelweis University Budapest, who contributed to data collection for the study. The authors declare no conflicts of interest.

References

1. Schropp L, Wenzel A, Kostopoulos L, Karring T. Bone healing and soft tissue contour changes following single-tooth extraction: A clinical and radiographic 12-month prospective study. Int J Periodontics Restorative Dent 2003;23: 313–323.
2. Caplanis N, Lozada JL, Kan JY. Extraction defect assessment, classification, and management. J Calif Dent Assoc 2005; 33:853–863.

3. Buser D, Bornstein MM, Weber HP, Grütter L, Schmid B, Belser UC. Early implant placement with simultaneous guided bone regeneration following single-tooth extraction in the esthetic zone: A cross-sectional, retrospective study in 45 subjects with a 2- to 4-year follow-up. J Periodontol 2008;79: 1773–1781.
4. Buser D, Wittneben J, Bornstein MM, Grütter L, Chappuis V, Belser UC. Stability of contour augmentation and esthetic outcomes of implant-supported single crowns in the esthetic zone: 3-year results of a prospective study with early implant placement postextraction. J Periodontol 2011;82:342–349.
5. Buser D, Chappuis V, Bornstein MM, Wittneben JG, Frei M, Belser UC. Long-term stability of contour augmentation with early implant placement following single tooth extraction in the esthetic zone: A prospective, cross-sectional study in 41 patients with a 5- to 9-year follow-up. J Periodontol 2013;84: 1517–1527.
6. Sanz I, Garcia-Gargallo M, Herrera D, Martin C, Figuero E, Sanz M. Surgical protocols for early implant placement in post-extraction sockets: A systematic review. Clin Oral Implants Res 2012; 23(suppl 5):s67–s79.
7. Schropp L, Wenzel A, Stavropoulos A. Early, delayed, or late single implant placement: 10-year results from a randomized controlled clinical trial. Clin Oral Implants Res 2014;25:1359–1365.
8. Darby I, Chen ST, Buser D. Ridge preservation techniques for implant therapy. Int J Oral Maxillofac Implants 2009;24 (suppl):s260–s271.
9. Becker W, Becker BE, Caffesse R. A comparison of demineralized freeze-dried bone and autologous bone to induce bone formation in human extraction sockets. J Periodontol 1994;65: 1128–1133.
10. Becker W, Urist M, Becker BE, et al. Clinical and histologic observations of sites implanted with intraoral autologous bone grafts or allografts. 15 human case reports. J Periodontol 1996;67: 1025–1033.
11. Darby I, Chen S, De Poi R. Ridge preservation: What is it and when should it be considered. Aust Dent J 2008;53:11–21.
12. Froum S, Cho SC, Rosenberg E, Rohrer M, Tarnow D. Histological comparison of healing extraction sockets implanted with bioactive glass or demineralized freeze-dried bone allograft: A pilot study. J Periodontol 2002;73:94–102.
13. Cohen ES. Ridge enhancement and socket preservation utilizing the subepithelial connective tissue graft: A case report. Pract Periodontics Aesthet Dent 1995;7:53–58.
14. Hanser T, Khoury F. Extraction site management in the esthetic zone using autogenous hard and soft tissue grafts: A 5-year consecutive clinical study. Int J Periodontics Restorative Dent 2014; 34:305–312.
15. Meloni SM, Tallarico M, Lolli FM, Deledda A, Pisano M, Jovanovic SA. Postextraction socket preservation using epithelial connective tissue graft vs porcine collagen matrix. 1-year results of a randomised controlled trial. Eur J Oral Implantol 2015;8:39–48.
16. Stimmelmayr M, Allen EP, Reichert TE, Iglhaut G. Use of a combination epithelized-subepithelial connective tissue graft for closure and soft tissue augmentation of an extraction site following ridge preservation or implant placement: Description of a technique. Int J Periodontics Restorative Dent 2010;30: 375–381.
17. Horváth A, Mardas N, Mezzomo LA, Needleman IG, Donos N. Alveolar ridge preservation. A systematic review. Clin Oral Investig 2013;17:341–363.
18. Fiorellini JP, Howell TH, Cochran D, et al. Randomized study evaluating recombinant human bone morphogenetic protein-2 for extraction socket augmentation. J Periodontol 2005;76:605–613.
19. Nevins M, Camelo M, De Paoli S, et al. A study of the fate of the buccal wall of extraction sockets of teeth with prominent roots. Int J Periodontics Restorative Dent 2006;26:19–29.
20. Araújo MG, da Silva JC, de Mendonça AF, Lindhe J. Ridge alterations following grafting of fresh extraction sockets in man. A randomized clinical trial. Clin Oral Implants Res 2015;26:407–412.
21. Zadeh HH. Minimally invasive treatment of maxillary anterior gingival recession defects by vestibular incision subperiosteal tunnel access and platelet-derived growth factor BB. Int J Periodontics Restorative Dent 2011;31:653–660.
22. Hürzeler MB, Weng D. A single-incision technique to harvest subepithelial connective tissue grafts from the palate. Int J Periodontics Restorative Dent 1999; 19:279–287.
23. Araújo MG, Lindhe J. Ridge preservation with the use of bio-oss collagen: A 6-month study in the dog. Clin Oral Implants Res 2009;20:433–440.
24. Lindhe J, Cecchinato D, Donati M, Tomasi C, Liljenberg B. Ridge preservation with the use of deproteinized bovine bone mineral. Clin Oral Implants Res 2014;25:786–790.
25. Barone A, Aldini NN, Fini M, Giardino R, Calvo Guirado JL, Covani U. Xenograft versus extraction alone for ridge preservation after tooth removal: A clinical and histomorphometric study. J Periodontol 2008;79:1370–1377.
26. Lekovic V, Kenney EB, Weinlaender M, et al. A bone regenerative approach to alveolar ridge maintenance following tooth extraction. Report of 10 cases. J Periodontol 1997;68:563–570.
27. Lekovic V, Kenney EB, Weinlaender M, et al. Preservation of alveolar bone in extraction sockets using bioabsorbable membranes. J Periodontol 1998;69: 1044–1049.

Clinical Oral Investigations (2021) 25:2969–2980
https://doi.org/10.1007/s00784-020-03617-6

DOI:10.14753/SE.2022.2638

ORIGINAL ARTICLE

Vertical-guided bone regeneration with a titanium-reinforced d-PTFE membrane utilizing a novel split-thickness flap design: a prospective case series

Peter Windisch[1] · Kristof Orban[1] · Giovanni E. Salvi[2] · Anton Sculean[2] · Balint Molnar[1]

Received: 1 June 2020 / Accepted: 1 October 2020 / Published online: 10 October 2020

Abstract

Objectives To evaluate the feasibility of a newly proposed minimally invasive split-thickness flap design without vertical-releasing incisions for vertical bone regeneration performed in either a simultaneous or staged approach and to analyze the prevalence of adverse events during postoperative healing.

Materials and methods Following preparation of a split-thickness flap and bilaminar elevation of the mucosa and underlying periosteum, the alveolar bone was exposed over the defects, vertical GBR was performed by means of a titanium-reinforced high-density polytetrafluoroethylene membrane combined with particulated autogenous bone (AP) and bovine-derived xenograft (BDX) in 1:1 ratio. At 9 months after reconstructive surgery, vertical and horizontal hard tissue gain was evaluated based on clinical and radiographic examination.

Results Twenty-four vertical alveolar ridge defects in 19 patients were treated with vertical GBR. In case of 6 surgical sites, implant placement was performed at the time of the GBR (simultaneous group); in the remaining 18 surgical, sites implant placement was performed 9 months after the ridge augmentation (staged group). After uneventful healing in 23 cases, hard tissue fill was detected in each site. Direct clinical measurements confirmed vertical and horizontal hard tissue gain averaging 3.2 ± 1.9 mm and 6.5 ± 0.5 mm respectively, in the simultaneous group and 4.5 ± 2.2 mm and 8.7 ± 2.3 mm respectively, in the staged group. Additional radiographic evaluation based on CBCT data sets in the staged group revealed mean vertical and horizontal hard tissue fill of 4.2 ± 2.0 mm and 8.5 ± 2.4 mm. Radiographic volume gain was 1.1 ± 0.4 cm^3.

Conclusion Vertical GBR consisting of a split-thickness flap and using titanium-reinforced non-resorbable membrane in conjunction with a 1:1 mixture of AP+BDX may lead to a predictable vertical and horizontal hard tissue reconstruction.

Clinical relevance The used split-thickness flap design may represent a valuable approach to increase the success rate of vertical GBR, resulting in predicable hard tissue regeneration, and favorable wound healing with low rate of membrane exposure.

Keywords Guided bone regeneration · Vertical augmentation · Split-thickness flap · Implant placement · Non-resorbable membrane · Autogenous bone · Xenograft

Introduction

During the past decades, dental implant therapy has become a frequently chosen solution to replace missing teeth. In order to achieve long-term success and esthetic results, optimal amounts of vertical and horizontal hard tissue dimension as well as an adequate soft tissue environment are required. The three-dimensional resorption of the alveolar ridge is one of the most unwanted biological processes following tooth extraction; resorption is more progressive in patients with periodontal disease due to unfavorable hard and soft tissue conditions [1–3]. As a result, edentulous sites often present compromised dimensions, and therefore, ridge augmentation may be required before or at the time of implant placement.

Electronic supplementary material The online version of this article (https://doi.org/10.1007/s00784-020-03617-6) contains supplementary material, which is available to authorized users.

✉ Anton Sculean
anton.sculean@zmk.unibe.ch

[1] Faculty of Dentistry, Department of Periodontology, Semmelweis University, Budapest, Hungary

[2] Department of Periodontology, School of Dental Medicine, University of Bern, Freiburgstrasse 7, 3010 Bern, Switzerland

Several reconstructive surgical methods are suggested in literature to rebuild the deficient alveolar ridge. Transplantation of autogenous bone blocks (AB) is a well-documented surgical approach to reconstruct three-dimensional alveolar defects. This technique requires a relatively moderate healing time of 4–6 months, but the resorption rate of AB as well as the quality and survival of transplanted tissues shows high individual variations [4–6]. The most frequently reported surgical technique to rebuild missing alveolar bone is guided bone regeneration (GBR), which has been shown to deliver predictable long-term results in terms of crestal bone stability, implying however a longer healing period (i.e., 6–9 months) [7–9]. By using a barrier membrane, a secluded space should be created to prevent epithelial migration into the wound and while the particulated auto- or xenografts may stabilize the blood clot and facilitate bone formation [10]. The GBR technique is feasible for both horizontal and vertical reconstruction of edentulous sites utilizing resorbable or non-resorbable membranes [6, 11–13].

Vertical ridge augmentation yields less predictable treatment outcomes compared with horizontal ridge augmentation due to the fact that it requires advanced flap management and uncompromised soft tissue coverage of the wound to protect the grafts and to support supracrestal blood clot stabilization [14]. It has been demonstrated that the blood and cell supply during the healing process following ridge reconstructions mainly originates from the periosteum [15]. The elevation of the periosteum in order to support both revascularization and tissue integration of supracrestally positioned grafting materials is not only surgically extremely challenging but also implies a longer healing time for the regeneration process. Numerous studies have demonstrated the advantages of reinforced non-resorbable membranes to achieve successful vertical hard tissue reconstruction by maintaining and protecting the space for the blood clot and the filler material and by excluding soft tissue penetration [16].

Non-resorbable expanded polytetrafluoroethylene (e-PTFE) membranes are accepted as the gold standard for vertical GBR due to their favorable mechanical and barrier properties. Since the main rationale for GBR membrane rigidity is to ensure space maintenance, the most commonly used e-PTFE membranes are reinforced by titanium. In this way, the risk for graft compression during the healing period can be reduced over the biologically determined 9 months of healing required for graft maturation and corticalization.

Early wound dehiscence and membrane exposure are the main reasons for decreased treatment predictability following the application of non-resorbable membranes during GBR procedures. Bacterial colonization of exposed membrane surfaces inevitably leads to tissue inflammation and graft disintegration requiring premature membrane removal before the completion of the healing period, which leads to reduced hard tissue formation [17].

If properly executed, the conventional full-thickness flap design with vertical and horizontal releasing incisions results in tension-free wound closure and subsequent primary intention wound healing; however, insufficient healing and membrane exposure is a well-documented complication of this approach [18]. Apart from decreasing flap tension, the placement of incisions, which disrupt the continuity of the periosteal layer, may negatively affect periosteal blood supply. As an alternative to the classical full-thickness flap design for vertical GBR, a split-thickness flap approach was suggested by several authors, which might similarly result in a tension-free wound closure but at the same time avoiding the previously mentioned adverse events related to full-thickness flaps [19, 20]. More recently, in order to additionally improve the healing and to improve the predictability of vertical augmentation procedures, our group proposed a novel minimally invasive split-thickness flap design without vertical-releasing incisions [13].

Particulated autogenous bone grafts (AP) have highly active biological capacity and are preferred based on their osteoinductive properties; nevertheless, they are prone to early resorption when used alone for GBR [16]. Therefore, in order to prolong graft stability and to minimize the amount of harvested autogenous bone, recent studies have suggested to combine AP with bovine-derived xenograft (BDX). The efficacy of a mixed 1:1 ratio of AP + BDX has been reported by several authors [21–24]. BDX is the most commonly used and researched xenogeneic material for GBR with proven osteoconductive effect and volumetric stability [25].

According to the literature, when applying non-resorbable membranes in combination with AP + BDX for vertical GBR, approximately 9 months of healing is needed for proper graft maturation and tissue integration, allowing for implant placement and long-term crestal bone maintenance. In cases of minor vertical alveolar defects with mild to moderate hard tissue loss, primary stability of a dental implant in standard length and width can be achieved. In such cases, a GBR approach can be used simultaneously to implant placement [26]. If the abovementioned prerequisites for implant placement are not given, the staged approach is indicated, implying ridge reconstruction 9 months prior to implant placement [22].

However, at present, the data on the outcomes of vertical bone augmentation by means of GBR are still scarce and controversy exists on the predictability of these approaches. However, at present, it is unknown to what extent our recently described minimally invasive split-thickness flap design without vertical-releasing incisions [13] may lead to predictable clinical outcomes in terms of postoperative complications and treatment outcomes. Therefore, the aims of the present prospective case series study were (**a**) to evaluate the feasibility of the proposed minimally invasive split-thickness flap design without vertical-releasing incisions for vertical bone regeneration performed in either a simultaneous or staged approach and (**b**) to record and analyze the prevalence of adverse events during postoperative healing.

Materials and methods

The present case series was performed in patients with advanced chronic periodontitis (grade III, stage B) [27] presenting localized three-dimensional alveolar ridge defects requiring surgical bone augmentation to allow implant placement. Patients underwent comprehensive periodontal treatment prior to surgery, no residual pockets deeper than 3 mm were present, full-mouth plaque score were less than 20%, and full-mouth bleeding scores were less than 15%. Teeth were extracted at least 6 months prior to surgery. The reasons for tooth loss were either severe attachment and bone loss (i.e., attachment and bone loss reaching the apex of the teeth and/or class III furcation involvements) or complicated perio-endodontic lesions.

All patients were selected and treated at the Department of Periodontology, Semmelweis University, Budapest, Hungary, between January 2012 and June 2015.

The study protocol was approved by the Semmelweis University Regional and Institutional Committee of Science and Research Ethics (Approval Number 77/2011). Surgical interventions were undertaken with the understanding and written informed consent of each subject. The patients were treated in full accordance with ethical principles, including the World Medical Association Declaration of Helsinki (version 2008).

Preoperative care

Preoperatively, supra- and subgingival scaling was performed, patients received individual oral hygiene instructions and maintained a high level of oral hygiene throughout the whole treatment period (full-mouth plaque score and full-mouth bleeding score did not exceed 25%). Presurgical patients used chlorhexidine digluconate 0.2% mouthrinse (Curasept ADS 220, Curaden AG, Kriens, Switzerland) for 2 min.

Surgical technique

The surgical approach was described in detail elsewhere [13]. Briefly, in both groups' local anesthesia (4% articaine-hidrocloride with 0.0001% epinephrine - Ultracain DS Forte, Sanofi-Aventis, Paris, France), a midcrestal incision was placed on the keratinized mucosa with no. 15 blades (Aesculap, Braun AG, Tuttlingen, Germany). The midcrestal incision was continued intracrevicularly at the two adjacent teeth mesially and distally both buccally and orally with no. 15C blades. In case of posterior edentulism, the midcrestal incision line length was two-thirds of the entire surgical area, and one-third length was continued mesially to the neighboring two teeth. No vertical-releasing incisions were performed. A full-thickness buccal flap was reflected with elevators up to the MJ, followed by split-thickness mucosal flap preparation over the mucogingival line (MJ). Subsequently, the underlying periosteal layer was elevated from the bone surface. In the simultaneous group, 3.3-mm or 4.1-mm diameter bone level implants (Straumann AG, Basel, Switzerland) were placed in a prosthetically predefined position using surgical guides. No implants with 3.3-mm diameter were placed in molar positions. All implants were positioned supracrestally according to their preplanned prosthetic positions. A single-use disposable bone scraper (Safescraper, Osteogenics Biomedical, Lubbock, TX, USA) was used to harvest AP from the lateral surface of the adjacent alveolar ridge. Bone chips were mixed with BDX (Bio-Oss, Geistlich AG, Wolhusen, Switzerland) in a 1:1 ratio. The 1:1 mixture of AP + BDX was placed laterally and supracrestally to the alveolar ridge. A non-resorbable high-density PTFE (d-PTFE) membrane (Cytoplast, Osteogenics Biomedical, Lubbock, USA) was fixed with titanium pins (Frios Membrane Tacks, Dentsply, York, USA). Double-layer suturing was performed using 4-0 horizontal mattress sutures (Supramid, Braun AG, Tuttlingen, Germany) in order to cover the membrane with the periosteal layer, while 5-0 horizontal mattress and non-interrupted sutures (Supramid, Braun AG, Tuttlingen, Germany) were utilized to close the mucosal layer and to reach a tension-free wound closure. Sutures were removed after 14 days.

In the staged group, at 9 months, a split-thickness flap was elevated in the same way as described above. The titanium pins and the d-PTFE membrane were removed, and 3.3-mm or 4.1-mm diameter bone level implants (Straumann AG, Basel, Switzerland) were placed in a prosthetically predefined position using a surgical template (Fig. 1a–p). Also, in this group, no implants with 3.3-mm diameter were placed in molar positions. The flap was closed with horizontal mattress sutures and single interrupted sutures. Soft tissue augmentation was performed at the time of implant placement if the vertical dimension of the soft tissue thickness was less than 2 mm over the inserted implants. Two months later, in cases where less than 3-mm width of keratinized mucosa was present, palatal epithelialized free gingival grafts were harvested and placed. After another 2 months, implant uncovery was performed.

In the simultaneous group, membranes and titanium pins were removed at 9 months after the first surgery, and the implants were only uncovered if an adequate peri-implant soft tissue width (i.e., at least 3 mm) surrounding the implants was present (Fig. 2 a–n). Soft tissue augmentation was performed at the time of membrane removal if the peri-implant soft tissue thickness (vertical dimension) was less than 2 mm. The above described reconstruction of keratinized tissues was performed 2 months before the second-stage surgery only in cases without an adequate width and thickness or absence of keratinized tissue.

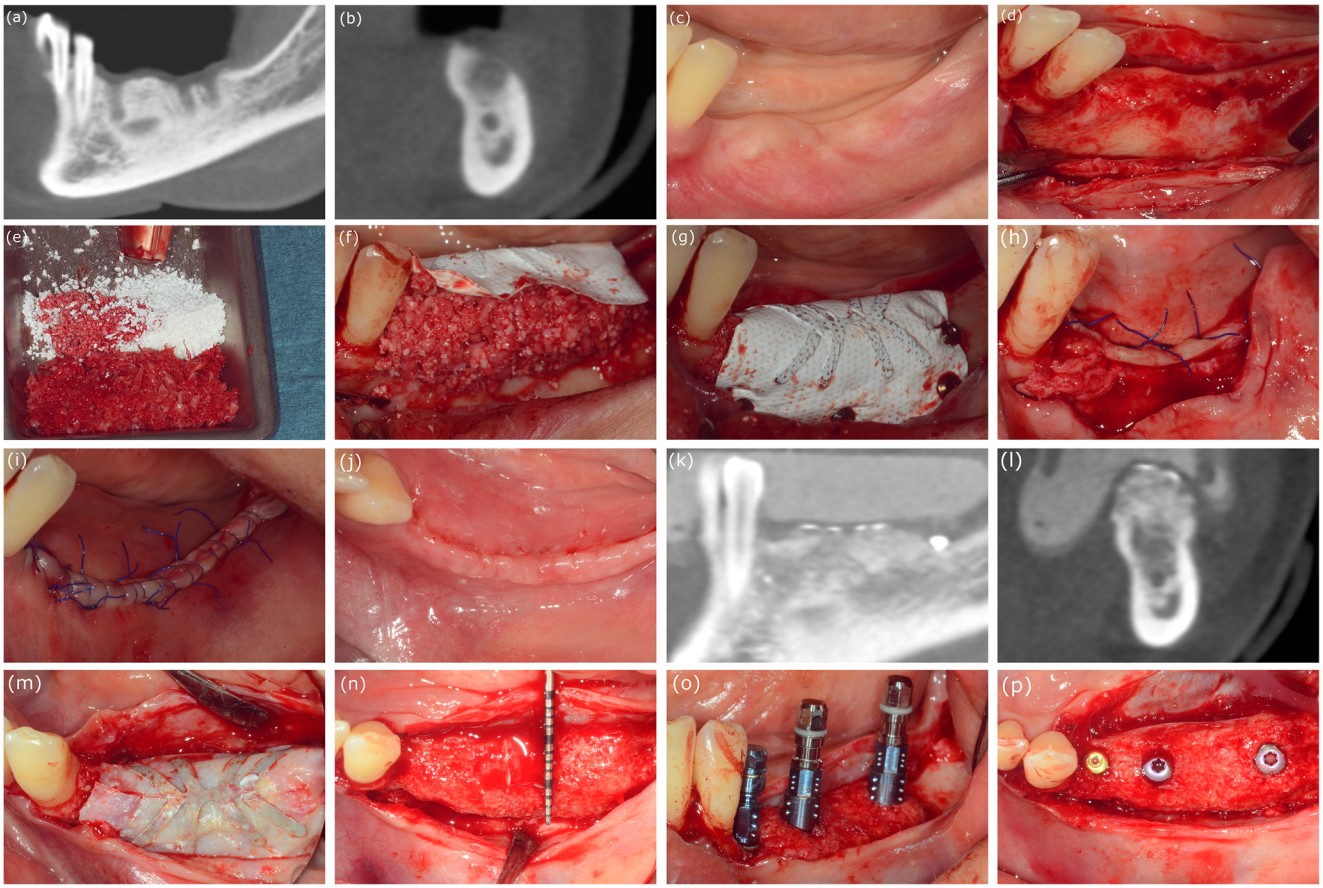

Fig. 1 Case presentation of patient no. 11, (case no. 13 - left mandible) from the staged group. **a** Baseline CBCT scan, parasagittal section: 2 months after tooth extraction, horizontovertical alveolar defect. **b** Baseline CBCT scan, frontal section: 2 months after tooth extraction, horizontovertical alveolar defect. **c** Clinical view of edentulous mandible. **d** Split-thickness flap preparation. **e** Bovine-derived xenograft (Geistlich Bio-Oss) and particulate autogenous bone graft. **f** Adaptation of non-resorbable membrane (Osteogenics Cytoplast) over the composite graft. **g** Membrane fixation using titanium pins. **h** Double-layer suturing: tension-free periosteal layer closure with horizontal mattress sutures. **i** Mucosal layer closure with horizontal mattress and non-interrupted sutures. **j** Wound healing 2 weeks after surgery. **k** Postoperative CBCT scan: 9 months after GBR parasagittal section: vertical bone gain. **l** Postoperative CBCT scan: 9 months after GBR, frontal section: vertical and horizontal bone gain. **m** Membrane removal at 9 months reentry. **n** Optimal amount of hard tissue for implant placement. **o** Guided implant placement (Straumann bone level). **p** Prosthetically driven implant positioning

Postoperative care

Postoperatively, antibiotic therapy (Penicillin with Clavulanic acid 2 × 1000 mg/day; Augmentin Duo, GlaxoSmithKline, Brentford, UK) and non-steroidal anti-inflammatory drugs (Diclofenac-Sodium 4 × 50 mg/day; Cataflam, Novartis International AG, Basel, Switzerland) were prescribed for 1 week in order to avoid infections and to decrease swelling and pain. In case of penicillin allergy, Clindamycin (Dalacin C, Pfizer, New York, USA) 4 × 300 mg per day was prescribed. Patients were instructed to gently brush teeth at surgical sites with a soft manual toothbrush. For chemical plaque control, 0.2% chlorhexidine digluconate mouthwash (Curasept ADS 220, Curaden AG, Kriens, Switzerland) was prescribed twice a day. Mucosal sutures were removed 7 days, periosteal sutures 14 days after surgery. Following suture removal, patients were scheduled for recall visits weekly in the first month, followed by visits every 3 months postoperatively. Patients received fixed partial dentures 2 weeks after implant uncovering. After delivery of the final prosthetic reconstructions, patients were enrolled in a periodontal maintenance program.

Clinical evaluation

Measurements were taken by a single investigator, KO, following examiner calibration. In the simultaneous group, direct measurements were performed by UNC-15 probes (HU-Friedy, Chicago, IL, USA) during the first surgery. The distance between crestal bone and the most coronal part of the supracrestally positioned implants (Clinical Vertical Dimension - c-VD) was recorded as a negative value (lack of hard tissue). Extent c-VD was recorded at 4 aspects of each implant (vestibular, oral, mesial, distal); mean values were

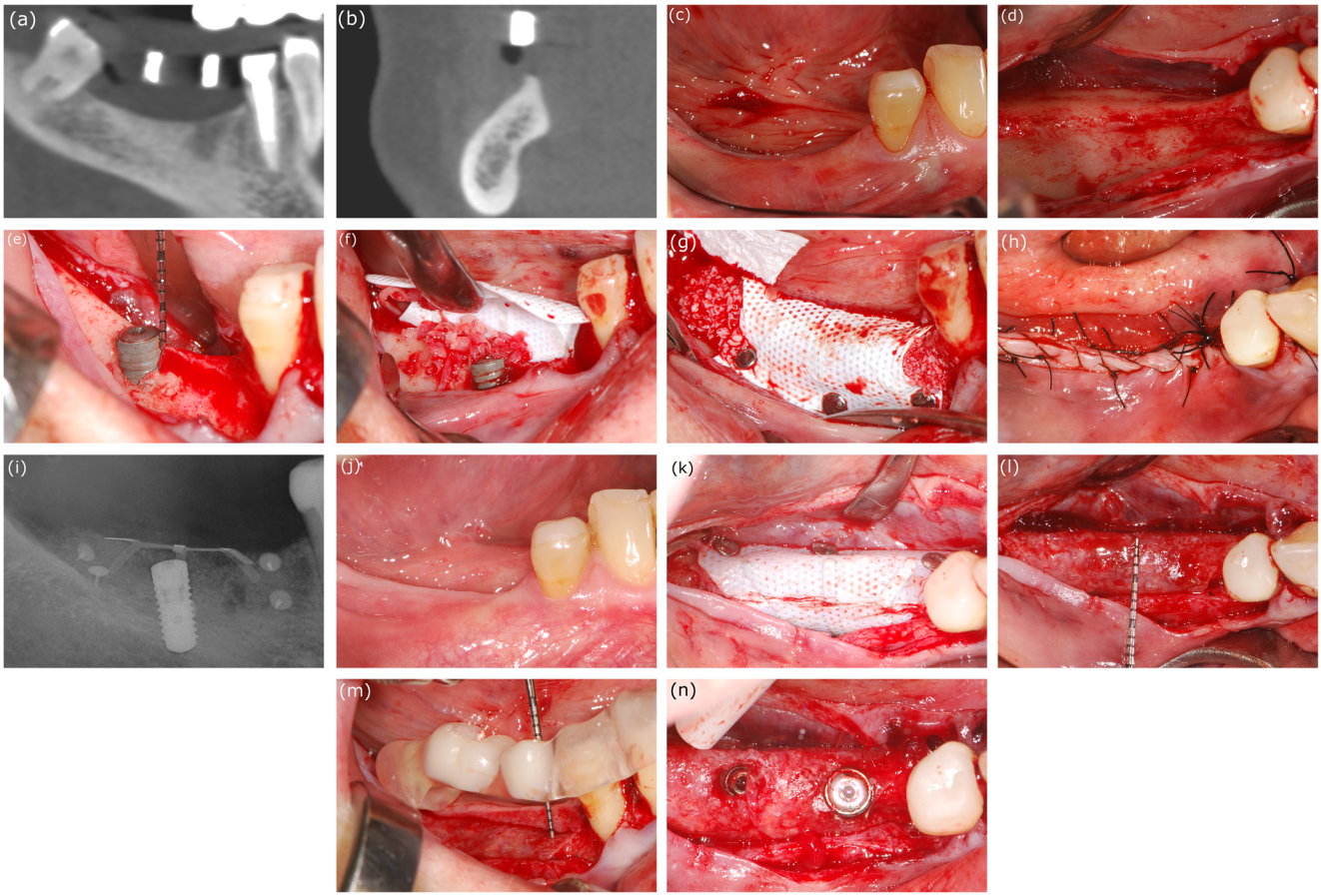

Fig. 2 Case presentation of patient no. 4 (case no. 5 - right mandible) from the simultaneous group. **a** Baseline CBCT scan, parasagittal section: horizontovertical alveolar defect. **b** Baseline CBCT scan, frontal section: horizontovertical alveolar defect. **c** Clinical view of edentulous mandible. **d** Split-thickness flap preparation. **e** Guided implant placement, supracrestally positioned implant (Straumann bone level). **f** Adaptation of non-resorbable membrane (Osteogenics Cytoplast) over the composite graft. **g** Membrane fixation using titanium pins. **h** Double-layer suturing. **i** Postoperative intraoral X-ray. **j** Healed alveolar ridge 9 months after simultaneous GBR. **k** Membrane removal at 9 months reentry. **l**, **m**, **n** Optimal amount of hard tissue; previously placed distal implant is covered with hard tissue, additional implant placed mesially

calculated. The orovestibular dimension of the ridge at the level of the most coronal part of the implant (Clinical Horizontal Dimension - c-HD) was by definition zero. During implant recovery, c-VD and c-HD were recorded again following membrane removal; vertical and horizontal hard tissue gain was calculated (Clinical Vertical Dimension Gain - c-VDG, Clinical Horizontal Dimension Gain - c-HDG). In the staged group, both direct and radiographic evaluations were performed. c-VD and c-HD were measured directly using by UNC-15 probes and individually fabricated surgical stent during augmentation and implant placement in the planned implant position. The distance between the surgical stent and crestal bone level was recorded at the time of GBR and at implant placement. Differences were registered as c-VDG. The orovestibular dimension of the alveolar ridge at the postopoperative crestal bone level was by definition zero; thus, c-HDG calculation was based on postop orovestibular dimension at the crestal bone level.

Radiographic evaluation

Measurements were taken by a single investigator, KO, following examiner calibration. Intraoral radiographs, orthopantomograms, and Cone Beam Tomography (CBCT) scans (i-CAT, KaVo, Biberach, Germany) were taken (120 kVp; 5 mA; 7.4 s; 0.200-mm voxel sizes; 360° rotation) to assess the three-dimensional morphology of edentulous alveolar ridges at baseline prior to surgery. Further intraoral radiographs were taken at implant loading and during recall visits on a yearly basis. Measurements were performed in the planned implant positions at every surgical site. In the staged group, a second CBCT scan was taken 9 months after GBR procedure for three-dimensional implant position planning; thus, radiographic evaluation was performed based on CBCT data (Radiographic Vertical Dimension - r-VD, Radiographic Horizontal Dimension - r-HD). For alignment of pre- and postoperative datasets, adjacent teeth were used as an anatomical reference. Radiographic Vertical Dimension Gain (r-VDG) and Radiographic Horizontal Dimension Gain

(r-HDG) were calculated. If more than 1 implant was placed in the surgical area, hard tissue gain was measured in every planned implant position, and the highest value was recorded. Radiographic linear measurements were performed by the i-CAT Vision software (Imaging Sciences International, Hatfield, PA, USA). Additional 3D volumetric measurement was performed in the staged group to evaluate the hard tissue gain (Radiographic Volume - r-VOL). Patients with GBR procedure and with sinus floor elevation were excluded from 3D measurement based on augmented area separation inaccuracy. Radiographic volume measurements were performed by the Osirix software (Pixmeo Sarl, Geneva, Switzerland).

Statistical analysis

Comparison of hard tissue changes between the two groups was not the aim of this study. "Horizontal and vertical dimension changes were recorded using the above described measurement method and therefore, only descriptive statistics were performed."

Mean values and standard deviations (SDs) were calculated.

Results

Systemically healthy, partially edentulous patients were treated at the Department of Periodontology, Semmelweis University, Budapest, Hungary: 24 surgical sites of 19 non-smoking subjects were selected. Treatments were performed at 8 maxillary and 16 mandibular sites. The average age was 50.3 ± 12.9 years, 2 patients were male, and 17 patients were female (Table 1.)

In the present study, 45 Straumann bone level implants were placed in 24 vertically augmented surgical sites. In the simultaneous group, implant placement was performed with simultaneous GBR (9 implants in 5 patients and 6 surgical sites) if at least 6-mm vertical bone height was detected coronally from the adjacent anatomical landmarks (floor of maxillary sinus or nasal cavity, mandibular nerve). In the staged group, implants were placed at 9 months after GBR (36 implants in 15 patients and 18 surgical sites) in cases where the residual vertical bone height was less than 6 mm. One patient was represented in both groups. Patient no. 4 in the simultaneous group is equivalent to patient no. 12 in the staged group. This patient received a dental implant in position no. 46 with simultaneous GBR, and after the healing period, the patient received another dental implant into the newly formed hard tissue in position no. 45 (Fig. 2). A total of 4 patients (i.e., 2 patients from the simultaneous and 2 patients from the staged group) displayed a single tooth gap, while the remaining patients had larger edentulous sites and received more than one implant.

All GBR procedures were successful; the healing period was uneventful in all 18 patients and 23 sites. Swelling and pain was moderate in all cases; additional medication, such as the prescription of systemic steroids, was not needed. Early membrane exposure was detected in 1 surgical site. In this particular case, the d-PTFE membrane was removed and replaced by a resorbable collagen membrane (Bio-Gide, Geistlich AG, Wolhusen, Switzerland) at 6 weeks after surgery. At the time of the reentry in the staged group, every augmented site was suitable for implant placement after membrane removal. The site with early membrane removal received additional connective tissue grafting to compensate for the loss of soft tissues.

In the simultaneous group, 5 patients with 6 surgical sites were treated, a total of 9 implants were placed simultaneously with the GBR procedure (Table 2). Mean c-VDG was 3.2 ± 1.9 mm, and mean c-HDG was 6.5 ± 0.5 mm. GBR procedure's success rate in the simultaneous group was 92.6%,

Table 1 Patient's demographics and treatment allocation

Characteristic	No. of subjects	No. of surgical sites	No. of implants	No. of patients with volume assessment
Gender				
Male	2	2	2	0
Female	17	22	43	13
Mean age (y)	50.25 ± 12.90			
Surgical area				
Maxilla	7*	8	13	2
Mandible	13*	16	32	11
Treatment allocation				
Simultaneous group	5	6	9	0
Staged group	15	18	36	13

*One patient was presented in both groups

Table 2 Simultaneous group

Patient no. (site no.)	Age (y)	Sex	Arch	Mean c-VDG (mm)	Mean c-HDG (mm)
1 (1)	38	F	Maxilla	2	6.6
2 (2)	35	M	Maxilla	6.9	6.3
3 (3)	36	F	Mandible	1.75	7
4 (4)	63	F	Mandible	2.75	7
4 (5)	63	F	Mandible	2.75	6
5 (6)	42	F	Mandible	3	6
Mean				3.19	6.48
STDEV				1.88	0.46

c-VDG clinical vertical dimension gain, *c-HDG* clinical horizontal dimension change

where a 100% success rate refers to implant surfaces fully covered with new hard tissue. The most coronal part of the implants was covered with newly formed hard tissue around 7 implants, representing 100% successful augmentation. Around 1 implant, implant coverage was incomplete, a mean postoperative c-VD of 2 mm (patient 1, implant in position 16) was recorded. In this case, the success rate (hard tissue gain in percentage) of the augmentation was 50%.

In the staged group, 15 patients with 18 surgical sites were treated, a total of 36 implants were placed 9 months after GBR (Table 3). Mean c-VDG was 4.5 ± 2.2 mm, and mean c-HDG was 8.7 ± 2.3 mm.

Additional linear radiographic measurements in the staged group based on alignment of baseline and 9 months CBCT scans showed lower hard tissue gain compared with direct clinical measurements. Mean r-VDG was 4.2 ± 2.0 mm, while mean r-HDG was 8.5 ± 2.4 mm.

Thirteen augmented sites of 11 patients from the staged group were suitable for 3D volumetric measurement to compare the amount of the hard tissue before and 9 months after the surgery. The main r-VOL was 1.1 ± 0.4 cm^3.

In cases which required soft tissue augmentation, the reason for the soft tissue deficiency either occured due to the baseline defect or occurred due to extensive flap mobilization

Table 3 Staged group

Patient no, (site no.)	Age (y)	Sex	Arch	c-VDG (mm)	c-HDG (mm)	r-VOL (ccm)
1 (1)	69	F	Mandible	1	4	0.82
2 (2)	62	F	Maxilla	6	11	-
3 (3)	67	F	Maxilla	2	8	0.96
4 (4)	57	F	Maxilla	3	15	-
4 (5)			Maxilla	3	10	-
5 (6)	57	F	Mandible	5	8	0.89
5 (7)			Mandible	9	8	1.48
6 (8)	22	F	Maxilla	4	8	1.00
7 (9)	46	F	Mandible	6	8	0.87
8 (10)	56	F	Mandible	4	7	1.01
9 (11)	42	F	Mandible	6	10	0.60
10 (12)	43	M	Maxilla	8	7	-
11 (13)	49	F	Mandible	4	8	1.88
11 (14)			Mandible	6	9	1.81
12 (15)	64	F	Mandible	1	7	-
13 (16)	59	F	Mandible	4	10	1.49
14 (17)	38	F	Mandible	5	8	0.60
15 (18)	60	F	Mandible	4	11	0.96
Mean				4.50	8.72	1.11
STDEV				2.15	2.30	0.42

c-VDG clinical vertical dimension change, *c-HDG* clinical horizontal dimension change, *r-VOL* radiographic volume

and the fact that non-resorbable membranes impair periosteal blood supply of the supracrestal soft tissues. Following our protocol, the minimally required keratinized tissue thickness of 2 mm and width of 3 mm was successfully obtained in all cases.

Discussion

The present case series has evaluated the feasibility of a newly proposed minimally invasive split-thickness flap design without vertical-releasing incisions for vertical bone regeneration performed in either a simultaneous or staged approach and also analyzed the prevalence of adverse events during postoperative healing. According to the best of our knowledge, this is the first report demonstrating predictable outcomes following vertical GBR using a split-thickness flap design.

The present material comprised a total of 24 surgical sites treated by means of vertical GBR, while hard tissue changes were assessed by clinical and 3D radiographic evaluation. Although short implants and horizontal ridge augmentation using non-resorbable membranes were considered alternative treatment options, vertical ridge augmentation was carried out to achieve an optimal implant to crown ratio, thereby minimizing open interproximal spaces, enhancing cleansability, and esthetics. Edentulous ridges were reconstructed in order to be leveled off with the adjacent periodontium of neighboring teeth, thus avoiding or minimizing negative bone remodeling.

A complicated compromised alveolar defect morphology often requires three-dimensional reconstructive surgery before or at the time of implant placement resulting in proper crestal bone levels with long-term stability around dental implants. The GBR procedure has high efficacy and predictability and is suitable for both horizontal and vertical ridge reconstructions [28]. However, the literature related to vertical GBR is very scarce, consisting of either prospective or retrospective case series.

The number of cases included in the present case series exceeds those reported in previous studies [16]. In the present study, 6 sites were treated by simultaneous GBR, while 18 sites received a staged approach. The majority of the patients were females, presumably with better compliance, with more health consciousness, and willing to undergo complex therapy. All cases were treated using the same split-thickness flap design, and all implants demonstrated successful osseointegration. Favorable peri-implant hard tissue surroundings were created around 36 out of 36 of the implants treated with the staged and around 7 out of 9 implants treated with the simultaneous approach.

Periosteal fenestration and vertical-releasing incisions are commonly used for vertical GBR to elevate a tensionless flap [11, 18, 29, 30]. Nevertheless, this flap design often results in complications such as swelling, bleeding, and patient discomfort, as well as flap perforation and graft exfoliation in 2.5–10% of the cases, depending on the augmentation technique [19]. One of the main causes behind these complications is probably the placement of deep periosteal incisions, which interrupts periosteal blood vessel circulation. Increased tissue swelling due to postoperative blood stasis generates tension at the crestal incision line which, in turn, may compromise wound healing and may lead to premature membrane exposure [20, 31].

The advantage of the present, prospectively evaluated surgical technique is the possibility of the bilaminar wound closure and the increased extensibility of the buccal mucosa, which will lead to a tension-free flap adaptation thus minimizing postoperative complications related to wound dehiscences. Uninterrupted blood supply induces optimal flap revascularization, which predictably results in uneventful early wound healing and moderate postoperative swelling and bleeding as well as membrane exposure. In the present study, only 1 out of 24 surgical sites (4.2%) demonstrated early membrane exposure, which is lower compared with that in literature [21, 25, 28, 32–35]. The only patient demonstrating early membrane exposure displayed one single tooth gap, where flap mobilization and tension-free wound closure are technically more challenging, compared with cases involving larger edentulous sites.

AP can be harvested either extraorally or intraorally and possesses substantial osteoinductive activity; however, it is prone to resorption. Particulate xenogeneic bone substitutes exhibit long-term volume stability and excellent osseoconductive capacity. In the present study, the application of a 1:1 mixture of AP and BDX was chosen, similarly to that described by Urban and co-workers [36]. This appears to represent a golden mean allowing for an optimal balance between graft remodeling and tissue stability. At reentry, clinically sufficient quality and quantity of newly formed hard tissues were observed in all cases. This is comparable with the results reported by several other authors applying 1:1 mixture of AP + BDX [24].

The titanium-reinforced non-resorbable e-PTFE membrane as a mechanical barrier is capable of preventing soft tissue migration and protecting the blood clot to achieve vertical hard tissue gain. The outer surface of the e-PTFE membrane has an open microstructure portion, while the inner surface is completely cell occlusive [37]. Former studies have demonstrated that the porous size determines regenerative capacity and clinical handling. Larger porous size could enhance biological effects; nevertheless, bone-membrane surface contact is considered to be too high, and therefore, membrane removal is difficult [38]. Bacterial colonization in case of membrane exposure could lead to bacterial infection after 4 weeks, which results in decreased hard tissue formation. In the present study, we have successfully used a new type of PTFE membrane for

vertical GBR. The d-PTFE membrane has smaller pores; nevertheless, recent studies proved that the regenerative capacity is similar to e-PTFE membranes. d-PTFE is suggested for socket preservation, and staged and simultaneous vertical augmentation [22, 39]. In case of membrane exposure, the d-PTFE membrane temporarily inhibits biomaterial-centered bacterial adhesion and infection. Previous studies demonstrated successful socket preservation with d-PTFE membrane when left intentionally exposed [40, 41]. In our study, unexpected membrane exposure occurred only in one case of the simultaneous group. Six weeks later, the membrane was removed, and soft tissue ingrowth was observed underneath. A healing abutment was placed; the implant showed no considerable crestal bone loss at the time of loading.

The amount of newly formed hard tissues is critical to create a stable environment around implants for long-term success. The efficacy of augmentation procedures is directly related to the extent of the newly created peri-implant bony surroundings. Therefore, accurate standardized evaluation of vertical and horizontal hard tissue dimensions before and after augmentation procedures is necessary to judge treatment efficacy. With the recent development in 3D imaging and computer technology, pre- and postoperative linear dimensions and volumetric changes may be measured and visualized precisely. Still, the vast majority of data reported in literature is based on direct clinical measurements only. These assessments rely on the application of several types of probes or surgical calipers. Moreover, measurement inaccuracy due to limited visualization and positioning of the registration devices cannot be avoided intraoperatively. According to most of the relevant publications, vertical and horizontal gains following augmentation procedures are routinely registered at the utmost extent of reconstructed sites; however, this does not always represent actual implant positions. Due to the abovementioned inevitable difficulties, direct clinical measurements cannot be standardized over a large number of interventions. Therefore, we aimed at applying a standardized radiographic 3D evaluation approach, registering utmost linear and volumetric changes at actual implant positions in the present study. Cases treated by simultaneous GBR represented the only exception, since a second CBCT scan could not be accepted ethically according to the ALARA principles [42].

According to previous studies, 3.6–5.5-mm vertical hard tissue gain can be obtained after staged 3D GBR procedures utilizing different grafting materials. In 2003, Artzi and co-workers could reach 5.2-mm vertical hard tissue gain on average with titanium meshes and BDX [25]. In 2004, Roccuzzo and co-workers used AB covered by titanium meshes, and reported an average vertical gain of 4.8 mm [43]. In 2005, Proussaefs and Lozada's vertical hard tissue gain was 4.8 mm 6 months after GBR, utilizing AP and AP + BDX without any barrier membranes [44]. Roccuzzo and co-workers used AB with and without titanium meshes. They observed a mean of 4.8-mm vertical hard tissue gain in the titanium mesh group, and a mean 3.6-mm new hard tissue with blocks alone [44]. In our study, 4.5 ± 2.2 mm was the average vertical hard tissue gain in the staged group, which compares well with the previous achievements despite utilizing AP + BDX only without bone blocks, covered by d-PTFE membranes. Urban and co-workers found 5.5-mm vertical hard tissue gain following the application of AP + BDX and d-PTFE membranes, nevertheless, with a conventional full-thickness flap design with vertical and periosteal releasing incisions [22].

According to the literature, 2.1–5-mm vertical hard tissue gain can be obtained after simultaneous 3D GBR procedures utilizing various grafting materials. In 1997, Corrente and co-workers utilized calcium carbonate and fibronectin sealing system around dental implants and observed a mean gain of 2.1 mm [45]. Simion and co-workers used e-PTFE membranes with AP or demineralized freeze-dried bone allograft (DFDBA) particles around implants. The AP group showed an average of 5 mm; the DFDBA group showed an average of 3.1-mm vertical hard tissue gain [12]. In 2007, Merli and co-workers applied e-PTFE membranes or resorbable collagen barriers with osteosynthesis plates for vertical augmentation at implant placement. The grafting material was AP. In the e-PTFE group, the mean vertical hard tissue gain was 2.5 mm, while in the resorbable barrier group, the amount of newly formed hard tissue measured 2.2 mm [34]. In our present study, we observed a mean 3.2 ± 1.9 mm vertical hard tissue gain by combining AP + BDX with d-PTFE membranes in the simultaneous group. Among previous reports, only Simion and co-workers showed higher vertical hard tissue fill (5 mm), nevertheless by utilizing AP only in combination with e-PTFE membranes.

The horizontal dimension of vertically augmented sites is crucial for long-term crestal bone stability. Based on the available data from the literature, a 1.5–2-mm facial bone width around dental implants is needed, which practically requires 7–8-mm crestal bone width in the horizontal dimension in cases of a standard, approximately 4-mm diameter implant [46–48]. Data reporting on the horizontal hard tissue gain following vertical GBR is scarce and are available only for horizontal GBR procedures, which cannot be compared with the results of the present study. Buser and co-workers measured the width of the alveolar ridge before and after horizontal GBR and reported an average horizontal hard tissue gain of 3.5 mm [49]. In 2008, Hämmerle and co-workers reported comparable outcomes, achieving 3.6-mm horizontal hard tissue gain [50]. Wallace and co-workers detected 4.6-mm horizontal hard tissue gain 6 months after horizontal augmentation with cancellous freeze-dried allograft bone blocks, as confirmed by CBCT radiographic evaluation [51]. Da Costa and co-workers applied allogenic bone blocks alone or impregnated with autogenous bone marrow during horizontal

GBR. Their results have shown a mean horizontal gain of 2.2 mm and 4.6 mm, respectively [52]. In our study, the horizontal hard tissue gain 9 months after vertical GBR averaged 8.7 ± 2.3 mm after staged GBR procedures, and 6.5 ± 0.5 mm after simultaneous GBR procedures, respectively. From a clinical point of view, these results may ensure predictable crestal bone stability which is one of the important criteria for short- and long-term clinical success.

Conclusions

Within their limits, the present results have shown that staged and simultaneous vertical reconstruction of deficient alveolar ridges by means of GBR with titanium-reinforced d-PTFE membranes combined with a bilaminar split-thickness flap design delivered predictable hard tissue formation as determined clinically and radiographically. The used surgical approach resulted in favorable wound healing, low patient morbidity, and low rate of membrane exposure.

Authors' contributions Windisch, P: principal investigator; conceived the idea; contributed to conception and design; performed bone augmentation procedure; contributed to data interpretation; drafted the manuscript; gave final approval; and agreed to be accountable for all aspects of work ensuring integrity and accuracy.

Orban, K: contributed to conception and design, drafted the manuscript; coordinated the research; contributed to data acquisition, analysis and interpretation; gave final approval; and agreed to be accountable for all aspects of work ensuring integrity and accuracy.

Sculean, A: contributed to data interpretation; critically revised the manuscript; gave final approval; and agreed to be accountable for all aspects of work ensuring integrity and accuracy.

Salvi, G, E: contributed to data interpretation; critically revised the manuscript; gave final approval; and agreed to be accountable for all aspects of work ensuring integrity and accuracy.

Molnar, B: conceived the idea; contributed to conception and design; drafted the manuscript; coordinated the research; performed bone augmentation procedure; contributed to data acquisition and interpretation; critically revised the manuscript; gave final approval; and agreed to be accountable for all aspects of work ensuring integrity and accuracy, supervised the research.

Funding Open access funding provided by University of Bern. The work was supported by the Department of Periodontology, Semmelweis University, Budapest, Hungary.

Compliance with ethical standards

Conflict of interest The authors declare that they have no conflict of interest.

Ethical approval All procedures performed in studies involving human participants were in accordance with the ethical standards of the institutional and/or national research committee and with the 1964 Helsinki declaration and its later amendments or comparable ethical standards.

Informed consent Informed consent was obtained from all individual participants included in the study.

References

1. Araújo MG, Silva CO, Misawa M, Sukekava F (2015) Alveolar socket healing: what can we learn? Periodontol 2000 68(1):122–134
2. Trombelli L, Farina R, Marzola A, Bozzi L, Liljenberg B, Lindhe J (2008) Modeling and remodeling of human extraction sockets. J Clin Periodontol 35(7):630–639
3. Ahn JJ, Shin HI (2008) Bone tissue formation in extraction sockets from sites with advanced periodontal disease: a histomorphometric study in humans. Int J Oral Maxillofac Implants 23(6):1133–1138
4. Khoury F, Hanser T (2015) Mandibular bone block harvesting from the retromolar region: a 10-year prospective clinical study. Int J Oral Maxillofac Implants 30(3):688–697
5. Chiapasco M, Casentini P, Zaniboni M (2009) Bone augmentation procedures in implant dentistry. Int J Oral Maxillofac Implants 24(Suppl):237–259
6. Von Arx T, Buser D (2006) Horizontal ridge augmentation using autogenous block grafts and the guided bone regeneration technique with collagen membranes: a clinical study with 42 patients. Clin Oral Implants Res 17(4):359–366
7. Gottlow J, Nyman S, Karring T, Lindhe J (1984) New attachment formation as the result of controlled tissue regeneration. J Clin Periodontol 11(8):494–503
8. Nyman S (1991) Bone regeneration using the principle of guided tissue regeneration. J Clin Periodontol 18(6):494–498
9. Dahlin C, Linde A, Gottlow J, Nyman S (1988) Healing of bone defects by guided tissue regeneration. Plast Reconstr Surg 81(5): 672–676
10. Polimeni G, Koo K, Qahash M, Xiropaidis AX, Albandar JM, Wikesjö UME (2004) Prognostic factors for alveolar regeneration: bone formation at teeth and titanium implants. J Clin Periodontol 31(11):927–932
11. Buser D, Dula K, Belser UC, Hirt H-P, Berthold H (1995) Localized ridge augmentation using guided bone regeneration. II. Surgical procedure in the mandible. Int J Periodontics Restorative Dent 15(1):10–29
12. Simion M, Jovanovic SA, Trisi P, Scarano A, Piattelli A (1998) Vertical ridge augmentation around dental implants using a membrane technique and autogenous bone or allografts in humans. Int J Periodontics Restorative Dent 18(1):8–23
13. Windisch P, Martin A, Shahbazi A, Molnar B (2017) Reconstruction of horizontovertical alveolar defects. Presentation of a novel split-thickness flap design for guided bone regeneration: a case report with 5-year follow-up. Quintessence Int 48(7):535–547
14. Rocchietta I, Fontana F, Simion M (2008) Clinical outcomes of vertical bone augmentation to enable dental implant placement: a systematic review. J Clin Periodontol 35(Suppl 8):203–215

15. Drake R, Vogl AW, Mitchell AWM (2009) Gray's Anatomy for Students E-Book. 123Library. 2 ed: Churchill Livingstone
16. Jensen SS, Terheyden H (2009) Bone augmentation procedures in localized defects in the alveolar ridge: clinical results with different bone grafts and bone-substitute materials. Int J Oral Maxillofac Implants Suppl 24:218–236
17. Simion M, Baldoni M, Rassi P, Zaffe D (1994) A comparative study of the effectiveness of e-PTFE membranes with and without early exposure during the healing period. Int J Periodontics Restorative Dent 14(2):166–180
18. Tinti C, Parma-Benfenati S, Polizzi G (1996) Vertical ridge augmentation: what is the limit? Int J Periodontics Restorative Dent 16(3):220–229
19. Ogata Y, Griffin TJ, Ko AC, Hur Y (2013) Comparison of double-flap incision to periosteal releasing incision for flap advancement: a prospective clinical trial. Int J Oral Maxillofac Implants 28(2):597–604
20. Yong H, Tsukiyama T, Tae-Ho Y, Griffin T (2010) Double flap incision design for guided bone regeneration: a novel technique and clinical considerations. J Periodontol 81(6):945–952
21. Simion M, Fontana F, Rasperini G, Maiorana C (2007) Vertical ridge augmentation by expanded-polytetrafluoroethylene membrane and a combination of intraoral autogenous bone graft and deproteinized anorganic bovine bone (Bio Oss). Clin Oral Implants Res 18(5):620–629
22. Urban IA, Lozada JL, Jovanovic SA, Nagursky H, Nagy K (2014) Vertical ridge augmentation with titanium-reinforced, dense-PTFE membranes and a combination of particulated autogenous bone and anorganic bovine bone-derived mineral: a prospective case series in 19 patients. Int J Oral Maxillofac Implants 29(1):185–193
23. Meloni SM, Jovanovic SA, Urban I, Canullo L, Pisano M, Tallarico M (2017) Horizontal ridge augmentation using GBR with a native collagen membrane and 1:1 ratio of particulated xenograft and autologous bone: a 1-year prospective clinical study. Clin Implant Dent Relat Res 19(1):38–45
24. Merli M, Migani M, Bernardelli F, Esposito M (2006) Vertical bone augmentation with dental implant placement: efficacy and complications associated with 2 different techniques. A retrospective cohort study. Int J Oral Maxillofac Implants 21(4):600–606
25. Artzi Z, Dayan D, Alpern Y, Nemcovsky CE (2003) Vertical ridge augmentation using xenogenic material supported by a configured titanium mesh: clinico histopathologic and histochemical study. Int J Oral Maxillofac Implants 18(3):440–446
26. Simion M, Jovanovic SA, Trisi P, Scarano A, Piattelli A (1998) Vertical ridge augmentation around dental implants using a membrane technique and autogenous bone or allografts in humans. Int J Periodontics Restorative Dent 18:8–23
27. Papapanou PN, Sanz M, Buduneli N, Dietrich T, Feres M, Fine DH, Flemmig TF, Garcia R, Giannobile WV, Graziani F, Greenwell H, Herrera D, Kao RT, Kebschull M, Kinane DF, Kirkwood KL, Kocher T, Kornman KS, Kumar PS, Loos BG, Machtei E, Meng H, Mombelli A, Needleman I, Offenbacher S, Seymour GJ, Teles R, Tonetti MS (2018) Periodontitis: consensus report of workgroup 2 of the 2017 World Workshop on the Classification of Periodontal and Peri-Implant Diseases and Conditions. J Clin Periodontol 45(Suppl 20):S162–S170
28. Elnayef B, Monje A, Gargallo-Albiol J, Galindo-Moreno P, Hom-Lay W, Hernandez-Alfaro F (2017) Vertical ridge augmentation in the atrophic mandible: a systematic review and meta-analysis. Int J Oral Maxillofac Implants 32:291–312
29. Buser D, Dula K, Belser U, Hirt H-P, Berthold H (1993) Localized ridge augmentation using guided bone regeneration. I. Surgical procedure in the maxilla. Int J Periodontics Restorative Dent 13(1):28–45
30. Romanos GE (2010) Periosteal releasing incision for successful coverage of augmented sites. A technical note. J Oral Implantol 36(1):25–30
31. Maridati PC, Cremonesi S, Fontana F, Cicci M, Maiorana C (2016) Management of d-PTFE membrane exposure for having final clinical success. J Oral Implantol 42(3):289–291
32. Chiapasco M, Casentini P, Zaniboni M (2014) Implants in reconstructed bone: a comparative study on the outcome of Straumann® tissue level and bone level implants placed in vertically deficient alveolar ridges treated by means of autogenous onlay bone grafts. Clin Implant Dent Relat Res 16(1):32–50
33. Llambés F, Silvestre F-J, Caffesse R (2007) Vertical guided bone regeneration with bioabsorbable barriers. J Periodontol 78:2036–2042
34. Merli M, Migani M, Esposito M (2007) Vertical ridge augmentation with autogenous bone grafts: resorbable barriers supported by ostheosynthesis plates versus titanium-reinforced barriers. A preliminary report of a blinded, randomized controlled clinical trial. Int J Oral Maxillofac Implants 22(3):373–382
35. Todisco M (2010) Early loading of implants in vertically augmented bone with non-resorbable membranes and deproteinised anorganic bovine bone. An uncontrolled prospective cohort study. Eur J Oral Implantol 3:47–58
36. Urban IA, Jovanovic SA, Lozada JL (2009) Vertical ridge augmentation using guided bone regeneration (GBR) in three clinical scenarios prior to implant placement: a retrospective study of 35 patients 12 to 72 months after loading. Int J Oral Maxillofac Implants 24(3):502–510
37. Ronda M, Rebaudi A, Torelli L, Stacchi C (2014) Expanded vs. dense polytetrafluoroethylene membranes in vertical ridge augmentation around dental implants: a prospective randomized controlled clinical trial. Clin Oral Implants Res 25(7):859–866
38. Simion M, Dahlin C, Blair K, Schenk RK (1999) Effect of different microstructures of e-PTFE membranes on bone regeneration and soft tissue response: a histologic study in canine mandible. Clin Oral Implants Res 10(2):73–84
39. Bartee BK (2001) Extraction site reconstruction for alveolar ridge preservation. Part 2: membrane-assisted surgical technique. J Oral Implantol 27(4):194–197
40. Barboza EP, Stutz B, Ferreira VF, Carvalho W (2010) Guided bone regeneration using nonexpanded polytetrafluoroethylene membranes in preparation for dental implant placements–a report of 420 cases. Implant Dent 19(1):2–7
41. Barber HD, Lignelli J, Smith BM, Bartee BK (2007) Using a dense PTFE membrane without primary closure to achieve bone and tissue regeneration. J Oral Maxillofac Surg 65(4):748–752
42. Implications of Commission recommendations that doses be kept as low as readily achievable. 1st ed. ed. Oxford :: Published for the International Commission on Radiological Protection by Pergamon Press; 1973
43. Roccuzzo M, Ramieri G, Spada MC, Bianchi SD, Berrone S (2004) Vertical alveolar ridge augmentation by means of a titanium mesh and autogenous bone grafts. Clin Oral Implants Res 15(1):73–81
44. Proussaefs P, Lozada J (2005) The use of intraorally harvested autogenous block grafts for vertical alveolar ridge augmentation: a human study. Int J Periodontics Restorative Dent 25(4):350–363
45. Corrente G, Abundo R, Cardaropoli G, Martuscelli G, Trisi P (1997) Supracrestal bone regeneration around dental implants using a calcium carbonate and a fibrin-fibronectin sealing system: clinical and histologic evidence. Int J Periodontics Restorative Dent 17(2):170–181
46. Buser D, Chappuis V, Kuchler U, Bornstein MM, Wittneben JG, Buser R, Cavusoglu Y, Belser UC (2013) Long-term stability of early implant placement with contour augmentation. J Dent Res 92(12 Suppl):176S–182S

47. Grunder U, Gracis S, Capelli M (2005) Influence of the 3-D bone-to-implant relationship on esthetics. Int J Periodontics Restorative Dent 25(2):113–119
48. Jung RE, Benic GI, Scherrer D, Hämmerle CHF (2015) Cone beam computed tomography evaluation of regenerated buccal bone 5 years after simultaneous implant placement and guided bone regeneration procedures - a randomized, controlled clinical trial. Clin Oral Implants Res 26(1):28–34
49. Buser D, Ingimarsson S, Dula K, Lussi A, Hirt HP, Belser UC (2002) Long-term stability of osseointegrated implants in augmented bone: a 5-year prospective study in partially edentulous patients. Int J Periodontics Restorative Dent 22(2):109–117
50. Hämmerle CHF, Jung RE, Yaman D, Lang NP (2008) Ridge augmentation by applying bioresorbable membranes and deproteinized bovine bone mineral: a report of twelve consecutive cases. Clin Oral Implants Res 19(1):19–25
51. Wallace S, Gellin R (2010) Clinical evaluation of freeze-dried cancellous block allografts for ridge augmentation and implant placement in the maxilla. Implant Dent 19(4):272–279
52. Da Costa CE, Pelegrine AA, Fagundes DJ, Simoes Mde J, Taha MO (2011) Use of corticocancellous allogeneic bone blocks impregnated with bone marrow aspirate: a clinical, tomographic, and histomorphometric study. Gen Dent 59(5):e200–e205

Clinical Oral Investigations
https://doi.org/10.1007/s00784-021-04087-0

DOI:10.14753/SE.2022.2638

ORIGINAL ARTICLE

Accuracy of half-guided implant placement with machine-driven or manual insertion: a prospective, randomized clinical study

Kristof Orban[1] · Endre Varga Jr[2] · Peter Windisch[1] · Gabor Braunitzer[2] · Balint Molnar[1]

Received: 23 April 2021 / Accepted: 18 July 2021

Abstract

Objectives To compare the accuracy of implant placement performed with either a surgical motor or a torque wrench as part of a half-guided surgical protocol.

Materials and methods Implant insertion with half-guided surgical protocol was utilized by surgical motor (machine-driven group) or torque wrench (manual group) in the posterior maxilla. After the healing period, accuracy comparison between planned and actual implant positions was performed based on preoperative cone beam computed tomography and postoperative digital intraoral scans. Coronal, apical, and angular deviations, insertion time, and insertion torque were evaluated.

Results Forty patients were treated with 1 implant each; 20 implants were inserted with a surgical motor and 20 implants with a torque wrench. Global coronal and apical deviations were 1.20 ± 0.46 mm and 1.45 ± 0.79 mm in the machine-driven group, and 1.13 ± 0.38 mm and 1.18 ± 0.28 mm in the manual group (respectively). The mean angular deviation was $4.82 \pm 2.07°$ in the machine-driven group and $4.11 \pm 1.63°$ in the manual group. Mean insertion torque was 21.75 ± 9.75 Ncm in the machine-driven group, compared to 18.75 ± 7.05 Ncm in the manual group. Implant placement duration was 9.25 ± 1.86 s in the machine-driven group at a speed of 50 rpm, and 36.40 ± 8.15 s in the manual group.

Conclusion No significant difference was found between the two groups in terms of accuracy and mean insertion torque, while machine-driven implant placement was significantly less time-consuming.

Clinical relevance Optimal implant placement accuracy utilized by half-guided surgical protocol can be achieved with both machine-driven and torque wrench insertion.

Trial registration ID: NCT04854239

Keywords Dental implants · Guided surgery · Intraoral digital scan · Accuracy · Machine-driven implant insertion · Manual implant insertion

Introduction

Dental implant therapy is a widespread, safe, and predictable treatment option to replace missing teeth. Long-term success is determined, among other factors, by the amount of alveolar bone, the condition of the surrounding soft tissues, and the accuracy of implant placement, as well as the accuracy of the implant-borne restorations.

Conventional implant position planning is based on the shape and volume of native alveolar bone as determined in two-dimensional radiographs. Using cone beam computed tomography (CBCT) scans, the three-dimensional structure of the alveolar bone can be precisely mapped, which allows optimal implant positioning both prosthetically and by minimizing the risk of damage to neighboring anatomical structures such as the mandibular nerve or the sinuses

✉ Kristof Orban
kristof.orban.dr@gmail.com

Endre Varga Jr
endre.varga@dicomlab.com

Peter Windisch
peter.windisch@gmail.com

Gabor Braunitzer
gabor.braunitzer@dicomlab.com

Balint Molnar
molbal81@gmail.com

[1] Faculty of Dentistry, Department of Periodontology, Semmelweis University, Budapest, Hungary

[2] dicomLAB Dental, Ltd., Szeged, Hungary

Published online: 16 August 2021

[1]. In the case of single-tooth replacement, the axis and distance of neighboring teeth may help the clinician to insert the implant in a prosthetically favorable position. Larger edentulous sites make implant placement more difficult and a surgically driven approach without recognizable anatomical landmarks often results in prosthetically inappropriate implant position and angulation. In turn, this may lead to an esthetically and functionally suboptimal outcome [2–5].

Due to the increased patient demand for aesthetic implant-borne restorations that resemble the lost natural dentition as much as possible, implant positioning accuracy has gradually become a central issue in implant dentistry. To achieve optimal aesthetics and cleansability, a prosthetically driven surgical approach was reported to increase implant placement precision, which allows for easily retrievable screw-retained restorations, eliminating the risk of harmful submucosal cement residues [6]. The introduction of computer-aided design (CAD) for guided implant surgery meant the beginning of a new era in implant dentistry [7]. With the help of CAD software, it is possible for the clinician to first determine the ideal restoration design and then to plan the position of the implants in a way that enables the realization of the desired prosthetic outcome. A prerequisite for optimal virtual implant positioning and execution of guided surgery is the 3D reconstruction of peri-implant hard tissues either simultaneously or in a staged approach. Frequently, the condition of hard tissues is compromised at the planned implant position, thus hard and soft tissue augmentation procedures may be required before or at the time of implant placement.

Several methods have been described in the literature to increase the accuracy of implant positioning. Studies have confirmed the superiority of guided implant placement over freehand implant placement [8]. A diagnostic wax-up-based surgical template fabricated by the dental technician is a conventional but efficient and cost-effective solution. Nevertheless, this method only allows for more precise, although freehand implant positioning without vertical depth control, strongly depending on the individual stent design. Computer-assisted implant planning and template-guided implant placement represent a more advanced treatment modality. The alignment of a CBCT dataset and the digital image of a diagnostic wax-up in a CAD planning software allows the clinician to virtually plan the implant position in three dimensions. This approach makes it possible to plan directly with the digital model of the implant to be inserted and to determine its exact angulation and position within the bone, which increases the accuracy of planning to a considerable extent [9, 10]. Subsequently, the digital plan is converted into an individually fabricated stereolithographic surgical template.

Such templates are used according to different protocols defined by the degree of guidance. The pilot protocol uses the template only for the initial drill ("pilot drill"), which guides subsequent osteotomies and implant placement. The half- (or partially) guided protocol uses the template for all osteotomies; only implant placement is performed without the template. Finally, the fully guided protocol uses the template during the complete drilling sequence as well as for implant placement. A major advantage of the guided approach is that it greatly reduces the role of the surgical skills. Operator experience has no significant effect on the outcome—if the outcome is inaccurate, it is mostly because of the malpositioning of the surgical guide [11, 12].

In contrast, Joda et al. in 2018 in their consensus report summarized that static computer-aided implant surgery, in terms of postoperative pain, discomfort, and intraoperative complications, is not proven superior to conventional implant surgery [13]. Error during conventional or digital impression, implant malpositioning during digital planning, or surgical guide inaccuracy can influence final implant position. If the positioning of the surgical guide is accurate, the half-guided surgical protocol cannot completely eliminate implant placement inaccuracy, given that the final step, insertion, is unguided. There is no clear recommendation in the literature as to whether the clinician can achieve higher accuracy with a surgical motor or a torque wrench and, as a matter of fact, hardly any literature is available on this question. The only work that explicitly mentions the choice between the manual and machine-driven options leaves the decision to the clinician without discussing the possible effects on accuracy [14].

The primary aim of this study was to compare the accuracy of implant placement performed with either a surgical motor or a torque wrench as part of a half-guided surgical protocol. Secondary analyses were conducted regarding the duration of implant insertion and maximum insertion torque.

Materials and methods

Patient demographics and allocation

Forty patients (21 women and 19 men, mean age: 49 ± 10 years) were selected and treated at the Department of Periodontology, Semmelweis University, Budapest, Hungary, between January 2017 and January 2019. The study conformed to the tenets of the Declaration of Helsinki (as amended in 2013) in all respects. The study protocol was approved by the Regional and Institutional Committee of Science and Research Ethics at the Semmelweis University (Approval Number: SE TUKEB 7/2017). Surgical interventions were undertaken with the understanding and written consent of each subject.

The inclusion criteria were as follows: at least one edentulous maxillary premolar or molar site treated successfully by sinus floor elevation with a xenogenic bone substitute

DOI:10.14753/SE.2022.2638

(cerabone, botiss biomaterials, Zossen, Germany) confirmed by preoperative CBCT. Full-mouth plaque and bleeding scores (FMPS and FMBS) < 20%, as well as good patient compliance (including willingness to participate in the follow-up procedures). All patients had to understand the study procedure as confirmed by a signed informed consent.

The exclusion criteria were as follows: clinically relevant diseases (e.g., diabetes, rheumatism, cancer), untreated periodontitis, systemic steroid or bisphosphonate use, acute or chronic inflammatory processes. All clinical and radiographic parameters were ascertained by an experienced examiner to check the eligibility of each patient for the study.

Six months after sinus elevation, the patients were allocated to either of two groups before implant surgery with a computer-generated randomization scheme (https://www.randomizer.org). The groups were defined by the method of implant insertion. Patients in both groups received one implant each according to a half-guided protocol, but patients in the machine-driven group had their implant inserted by means of a surgical motor, while patients in the manual group had their implant inserted by means of a torque wrench.

Preoperative imaging and planning

Six months after sinus floor elevation, custom-made surgical guides were prepared for each patient according to the SMART Guide workflow (SMART Guide, dicomLAB Dental, Szeged, Hungary). The workflow was described in detail elsewhere [5]. Briefly, C-silicone impressions (Zetaplus, Zhermack, Badia Polesine, Italy) were taken of the patients' upper dentition with a plastic impression tray containing radiographic markers. For the digital planning, a CBCT scan (Planmeca Viso, Planmeca, Helsinki, Finland) was taken of each patient with the impression in situ, followed by another scan of the impression alone. In this imaging protocol, the impression of the patient's dentition serves as the model for the surgical template to be printed, and the patient's CBCT scan is used to generate a three-dimensional model in which the position of the implants can be planned. One 4.1-×10-mm Straumann RN Standard Plus implant (Straumann, Basel, Switzerland) was planned for each patient in the previously augmented sinus area. If necessary, further implants were planned, and length and shape of the implants were chosen based on individual patients' needs. One implant per patient placed into the augmented sinus area was selected for the study, and the rest of the implants (if any) were excluded to standardize bone quality and implant parameters at the study sites. Following the prosthetic implant planning procedure, dentally supported stereolithographic surgical templates were fabricated (Figs. 1 and 2).

Preoperative care

All patients underwent supra- and subgingival scaling 4 weeks before the implant surgery. The patients also received individualized oral hygiene instructions and maintained a high level of oral hygiene throughout the treatment period (FMPS, FMBS ≤ 25%). Immediately before the surgery, the patients were instructed to rinse with chlorhexidine digluconate 0.2% mouthrinse (Curasept ADS 220, Curaden AG, Kriens, Switzerland) for 2 min.

Implant placement

Implant surgeries were performed under local anesthesia (4% articaine-hydrochloride with 0.0001% epinephrine—Ultracain DS Forte, Sanofi-Aventis, Paris, France) by the same surgeon (BM). A slightly palatal incision was placed

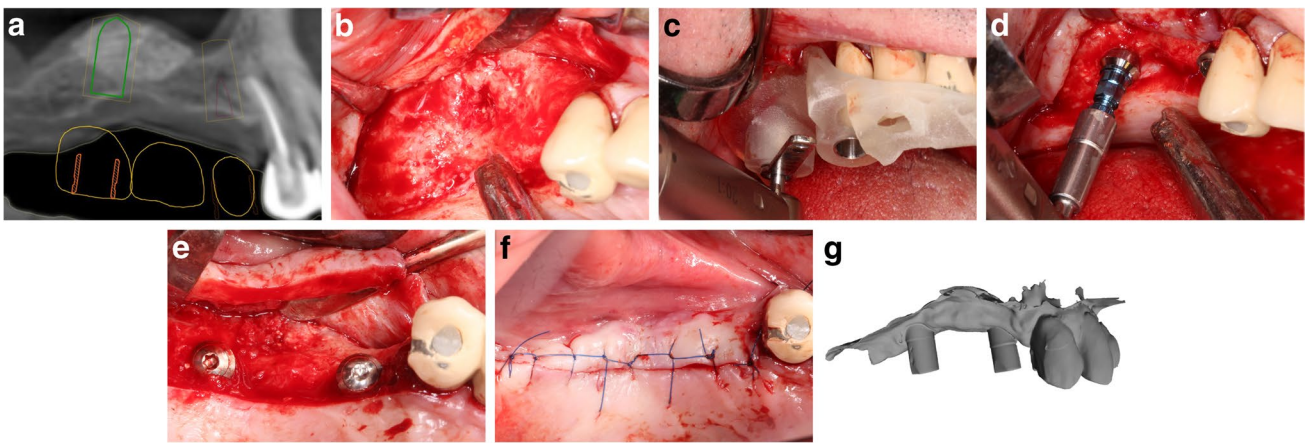

Fig. 1 Machine-driven group (patient no. 26) **a** Planned implant position. **b** Reentry 6 months after sinus elevation. **c** Half-guided implant surgery. **d** Motor-driven implant placement. **e** Inserted implant. **f** Wound closure. **g** Intraoral scan at implant uncovery

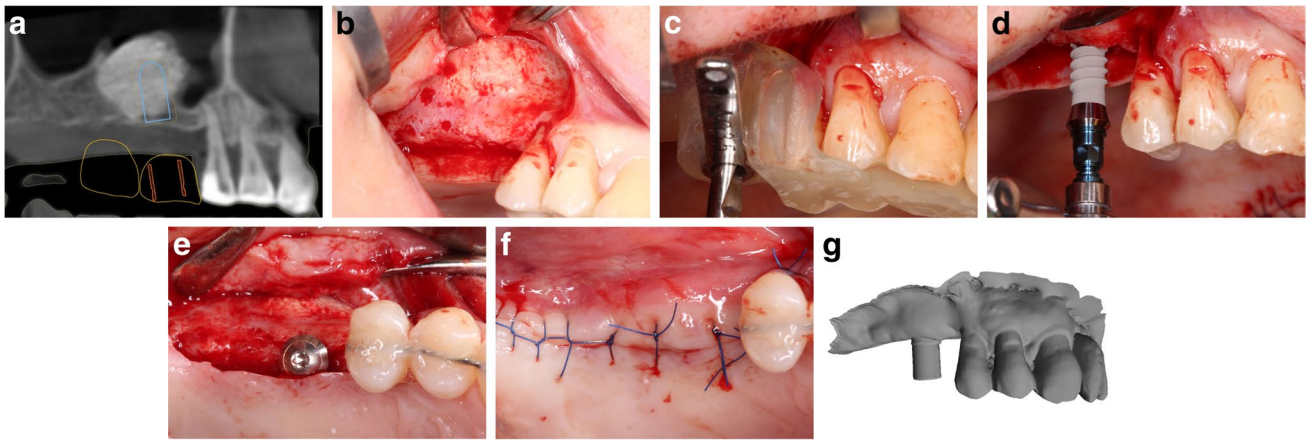

Fig. 2 Manual group (patient no. 2). **a** Planned implant position. **b** Reentry 6 months after sinus elevation. **c** Half-guided implant surgery. **d** Manual implant placement. **e** Inserted implants. **f** Wound closure. **g** Intraoral scan at implant uncovery

on the keratinized mucosa of edentulous sites with No. 15 blades (Aesculap, Braun AG, Tuttlingen, Germany), continued intracrevicularly at the adjacent teeth. If deemed necessary, a single remote vertical releasing incision was placed mesially. A full-thickness mucoperiosteal buccal flap was reflected with elevators. Flap elevation was not performed on the palatal side. Implant osteotomy was performed in the pre-planned position through the custom-made surgical guide, with a surgical motor (NSK Surgic Pro, Nakanishi, Kanuma Tochigi, Japan) using a universal implant drill kit designed for guided surgery (SMART Guide Universal Kit, dicomLAB Dental, Szeged, Hungary).

In the machine-driven group, implant insertion was performed with a 20:1 surgical contra-angle handpiece. The surgical motor was configured to 50 RPM and a maximum torque of 35 Ncm without water cooling. In the manual group, implant insertion was performed with a torque wrench. Duration of implant insertion was measured in seconds from the time when implant touched the bone surface until the final position was reached. Measurements were registered by a stopwatch. After implant insertion, a depth control device was placed into the implants through the sleeves to verify the vertical position compared to the guide.

Implant closure screws were placed for submucosal healing. After implant insertion, 5–0 horizontal mattress and single interrupted sutures (Supramid, Braun AG, Tuttlingen, Germany) were placed to close the mucoperiosteal flap and to reach a tension-free wound closure. Sutures were removed 7 days postoperatively (Figs. 1 and 2).

Implant reentry and intraoral scanning for the positional analyses

After 3 months of healing, implant reentry was performed in local anesthesia. PMMA implant scanbodies (CARES CI RD Mono Scanbody, Straumann, Basel, Switzerland) were connected to the implants, and a digital impression was taken with an intraoral scanner (Planmeca PlanScan; Planmeca, Helsinki, Finland) in the regions of interest (ROI) under partial isolation (Optragate, Ivoclar Vivadent, Schaan, Liechtenstein). At least 3 neighboring teeth were involved in each ROI. After recording the implant position, healing abutments were connected and 5–0 sutures (Supramid, Braun AG, Tuttlingen, Germany) were placed if necessary. Sutures were removed 7 days postoperatively (Figs. 1 and 2).

Postoperative care

After implant placement, systemic antibiotic therapy (penicillin with clavulanic acid 2 × 1000 mg/day; Augmentin Duo, GlaxoSmithKline, Brentford, UK), and non-steroidal anti-inflammatory drugs (diclofenac-sodium 4 × 50 mg/day; Cataflam, Novartis International AG, Basel, Switzerland) were prescribed for 7 days in order to avoid infections and to decrease swelling and pain. In case of penicillin allergy, 4 × 300 mg/day clindamycin (Dalacin C, Pfizer, New York, USA) was administered for 7 days. For chemical plaque control, 0.2% chlorhexidine digluconate mouthrinse (Curasept ADS 220, Curaden AG, Kriens, Switzerland) was prescribed 3 times a day. After the delivery of screw-retained fixed partial dentures, the patients were enrolled in a periodontal maintenance program.

Data analysis

The primary analyses were concerned with the positional accuracy of the inserted implants. Secondary analyses were conducted regarding the duration of implant insertion (s) and maximum insertion torque (Ncm).

DOI:10.14753/SE.2022.2638

Accuracy analysis was conducted in Amira 5.4.0 (Thermo Fisher Scientific, USA) with dedicated algorithms (dicomLAB Dental, Hungary). The present measurement protocol was previously published by our group [5]. Preoperative CBCT scans were aligned with postoperative intraoral scans in the coordinate system of the surgical plan. We applied this approach to minimize patients' radiation exposure. After registering the pre- and postoperative images, the planned implant positions were extracted from the guided surgery plan and transferred to a three-dimensional digital implant model that corresponded in all its dimensions to the implant that had been inserted. Then, a digital model of the scan abutment was aligned to the actual scan abutment of the postoperative image. In this procedure, the position of the inserted implant was defined by the position of the scan abutment, as the two were directly connected and their axes fell in the same line.

Having determined the position of the inserted implant, it became possible to compare the spatial relation of the planned and actual implant positions with the help of a custom algorithm written for this purpose.

The primary outcome variables were angular deviation (AD; the angle closed by the principal axis of the planned implant and the principal axis of the inserted implant in degrees), global coronal deviation (GCD; the distance between the coronal endpoints of the planned and the inserted implants in millimeters), and global apical deviation (GAD; the distance between the apical endpoints of the planned and the inserted implants in millimeters). GCD and GAD were each broken down to vectors in the three-dimensional space (*Cx*, *Cy*, *Cz*, and *Ax*, *Ay*, *Az*, respectively). As for the axes of the coordinate system, *x* marked the mesiodistal dimension, *y* the oro-vestibular dimension, and *z* the cranio-caudal dimension (Fig. 3).

Horizontal coronal deviation (HCD) and horizontal apical deviation (HAD) were calculated from the measured horizontal deviations as a vector sum of $Cx + Cy$ and $Ax + Ay$, respectively. Vertical deviation was measured apically and was equal to *Az*.

The statistical analyses were carried out in SPSS 23.0 (IBM, USA). The measured values were descriptively characterized as means and standard deviations. For the hypothesis tests (between-group comparisons), one-way ANOVA was used. Differences were considered significant at $p < 0.05$.

Results

The results are summarized in Table 1. Twenty patients were allocated to each study group and each patient received one implant; altogether, 40 implants were inserted in 40 patients. In both groups, distribution of edentulous sites was as follows: 3 single-tooth gaps (15%), 2 multiple-teeth gaps (10%), and 15 free-end tooth gaps (75%).

Mean GCD in the machine-driven group was 1.20 ± 0.46 mm, compared to 1.13 ± 0.38 mm in the manual group. Mean GAD in the machine-driven group was 1.45 ± 0.79 mm, compared to 1.18 ± 0.28 mm in the manual group. HCD averaged 1.06 ± 0.52 mm in the machine-driven group and 0.92 ± 0.40 mm in the manual group. HAD averaged 1.28 ± 0.83 mm in the machine-driven group and 0.99 ± 0.28 mm in the manual group. VD averaged 0.55 ± 0.28 mm in the machine-driven group compared to 0.62 ± 0.21 mm in the manual group. AD averaged $4.82 \pm 2.07°$ in the machine-driven group and $4.11 \pm 1.63°$ in the manual group. Mean insertion torque was 21.75 ± 9.75 Ncm in the machine-driven group, compared to 18.75 ± 7.05 Ncm in the manual group. The mean duration of implant insertion was 9.25 ± 1.86 s in the machine-driven group, compared to 36.40 ± 8.15 s in the manual group.

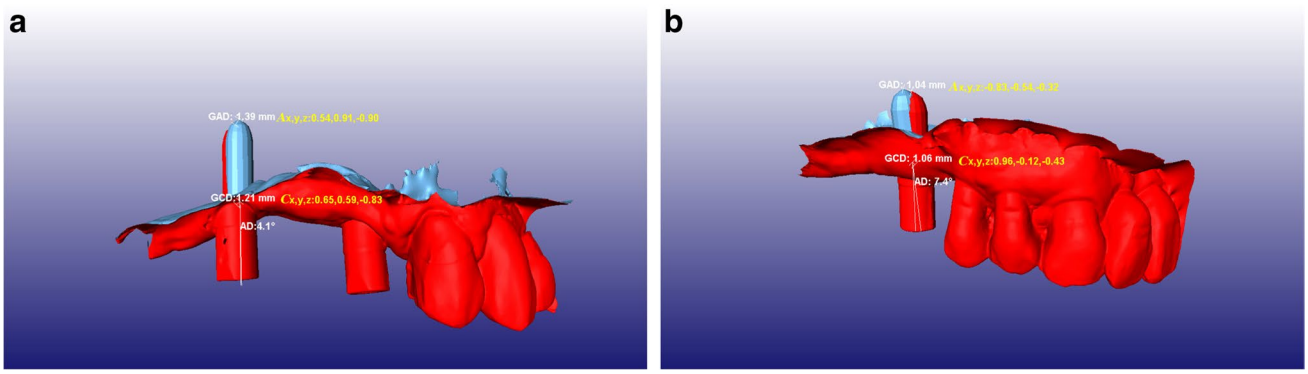

Fig. 3 Accuracy analysis. **a** Machine-driven group (patient no. 26). **b** Manual group (patient no. 2). The position of the inserted implant defined by the scan abutment (red), superimposed on the planned position (blue) extracted from the digital plan. GCD, global coronal deviation; *Cx*, *Cy*, *Cz*, vectoral components of GCD; GAD, global apical deviation; *Ax*, *Ay*, *Az*, vectoral components of GAD; AD, angular deviation

Table 1 Descriptive statistics of the studied parameters in the two study groups and significance levels from the hypothesis tests. *GCD*, global coronal deviation; *Cx*, *Cy*, *Cz*, vectoral components of GCD; *HCD*, horizontal coronal deviation; *GAD*, global apical deviation; *Ax*, *Ay*, *Az*, vectoral components of GAD; *HAD*, horizontal apical deviation; *AD*, angular deviation; *τ*, torque; *t*, time. **Az* = vertical deviation (VD)

	Machine-driven group ($N=20$)		Manual group ($N=20$)		Intergroup comparison
	Mean	SD	Mean	SD	Significance (p)
GCD (mm)	1.20	0.46	1.13	0.31	0.58
Cx (mm)	0.81	0.31	0.75	0.32	0.31
Cy (mm)	1.00	0.58	0.45	0.39	0.26
Cz (mm)	0.44	0.26	0.55	0.25	0.87
HCD (mm)	1.06	0.52	0.92	0.4	0.37
GAD (mm)	1.45	0.79	1.18	0.28	0.17
Ax (mm)	0.92	0.39	0.72	0.33	0.70
Ay (mm)	0.76	0.88	0.58	0.31	0.72
Az (mm)*	0.55	0.28	0.62	0.21	0.52
HAD (mm)	1.28	0.83	0.99	0.28	0.14
AD (°)	4.82	2.07	4.11	1.63	0.23
τ (Ncm)	21.75	9.75	18.75	7.05	0.27
t (s)	9.25	1.86	36.4	8.15	< 0.001

Statistical analysis did not reveal significant difference between the groups in any of the examined parameters, except for the duration of implant insertion ($F=201.84$, $df=1$, $p<0.001$), indicating the advantage of the machine-driven approach. F and df indicate the value of the F statistic and degrees of freedom, respectively.

Discussion

The present study is the first to investigate if the method of implant insertion (manual or machine-driven) makes a significant difference in the three-dimensional accuracy of implant placement in a half-guided surgical protocol. While equally capable for implant insertion, clinically, both insertion approaches have certain drawbacks. Optimal positioning of the ratchet during insertion usually requires the clinician to use both hands. As a result, reflecting the flap and visualization of the osteotomy site may be challenging. Furthermore, the vertical space required to attach the ratchet is higher compared to machine insertion. On the other hand, the weight of the contra-angled handpiece, the surgical motor, and the attached cables is higher, which might complicate appropriate positioning. Additionally, the procedure is operated with a foot pedal, which may detract attention from the clinician. Despite these characteristic differences, in the present study, we did not find any significant differences between the study groups in any of the accuracy variables.

Table 2 Descriptive statistics of the accuracy parameters used for comparison with the literature, for the entire patient population ($N=40$). *GCD*, global coronal deviation; *HCD*, horizontal coronal deviation; *GAD*, global apical deviation; *Az*, vertical deviation; *HAD*, horizontal apical deviation; *AD*, angular deviation

	Mean	SD
GCD (mm)	1.16	0.38
GAD (mm)	1.32	0.54
HCD(mm)	0.99	0.46
HAD (mm)	1.14	0.55
Az (mm)	0.59	0.24
AD (°)	4.46	1.85

Based on the lack of differences, it can be argued that the data are homogeneous in terms of accuracy. If so, the averaged accuracy results for the entire studied patient population (without grouping) should be comparable to published results on guided implant surgery in general. Thus, for the purposes of this discussion, we calculated accuracy for the entire population and used these values for comparison with the literature (Table 2). Emphasis was put on global (apical and coronal) deviation, horizontal deviation, vertical deviation, and angular deviation, these being the most frequently reported parameters.

Kühl et al. in 2013 presented a cadaver study; in 5 lower jaws altogether, 38 implants were placed with flapless guided surgery utilizing half-guided or fully guided protocol. Different dentitions were observed in the lower jaws; thus, both tooth-supported and mucosa-supported guides were used. They found a mean 1.56-mm global coronal deviation, a mean 1.84-mm global apical deviation, and a 4.2° angular deviation in case of half-guided implant placement. They found a non-significant difference in accuracy comparison between the fully guided and half-guided group, and results were comparable to our outcomes [15]. On the other hand, Jung et al. reported in their systematic review that implant position accuracy was better in studies with models and cadavers compared to clinical studies. They postulated that this can be explained by better visual control of the osteotomy axis, a more stable surgical stent position, and no saliva or blood in the models. According to their recommendations, accuracy of guided implant placement should be assessed in clinical situations [16]. Moreover, implant placement accuracy might depend on bone quality and anatomical region. A lower bone density or buccal/lingual undercuts can result in a lower implant accuracy with greater angular deviation after guided surgery [17]. In the present study, the choice of previously sinus-augmented areas in the posterior maxilla was made to avoid heterogeneity of bone morphology and quality of surgical sites.

Global implant position deviations are frequently reported in literature, but only limited data are available on the accuracy of half-guided protocols, only a few of these utilized

DOI:10.14753/SE.2022.2638

tooth-supported stents. Ersoy et al. in 2008 reported global coronal deviations of 1.1 ± 0.6 mm after fully guided implant placement using tooth-supported surgical guides. The mean angular deviation was 4.4 ± 1.6° [18]. Di Giacomo et al. in 2012 performed flapless half-guided implant surgeries in edentulous patients and they found a mean of 1.35 ± 0.65-mm global coronal deviation and 1.79 ± 1.01-mm global apical deviation [19]. Our results turned out to be somewhat more favorable, with 1.16 ± 0.38-mm global coronal deviation and 1.32 ± 0.54-mm global apical deviation. Derksen et al. in 2019 reported on even higher accuracy (0.75 ± 0.34-mm global coronal deviation, 1.06-mm ± 0.44-mm global apical deviation), nevertheless in a fully guided clinical setting [20].

The mean angular deviation was 6.53 ± 4.31° in the study of Di Giacomo et al. compared to 4.46 ± 1.85° in the present study [19]. Vercruyssen and co-workers, in 2014, used variously supported surgical guides for the treatment of full edentulism. In their half-guided group, where the surgical guide was mucosa-supported, they found a mean global coronal deviation of 1.23 ± 0.60 mm and a mean global apical deviation of 1.57 ± 0.71 mm [21]. These results are comparable to our findings, even if they indicate slightly less accurate implant placement. In contrast, the mean angular deviation was only 2.86 ± 1.6° in this study, which is lower than what we have found. In general, the results of the present study indicate slightly higher accuracy than those of Di Giacomo et al. and Vercruyssen et al., which is well in line with the observation that tooth-supported guides tend to be slightly more accurate than mucosa- or mucosa and pin–supported guides [22].

Valente and co-workers measured horizontal deviation after half-guided implant placement with various guide support. In their study, the average horizontal deviation between planned and actual implant positions at the coronal and apical ends of the implants were 1.4 ± 1.3 mm and 1.6 ± 1.2 mm, respectively, while the mean angular deviation was 7.9 ± 4.7° [9]. Cassetta et al. in 2012 performed flapless half-guided implant placement with a tooth-supported surgical guide. Fifteen implants were placed in 2 patients. The horizontal apical deviation was 1.28 ± 0.50 mm, and the angular deviation was 4.88 ± 3.38° [23]. These results are very similar to our findings, although in our study implant placement was performed with flap elevation. Our mean horizontal coronal and apical deviations were 0.99 ± 0.46 mm and 1.14 ± 0.55 mm, respectively, and our mean angular deviation was 4.46 ± 1.85°. That is, our study yielded more favorable outcomes in all horizontal parameters than what is reported in the literature.

In our study, we also evaluated the vertical deviation of the placed implant from its planned position. Vertical deviation was measured apically, as the optimal positioning of the implant apex is crucial to avoid interference with adjacent anatomical landmarks (e.g., nasal floor, sinus floor, mandibular nerve canal). Only a few articles reported data on vertical deviation. In the retrospective study by Cassetta et al., the authors inserted 15 implants with tooth support without depth control, and they found that the results were more favorable compared to mucosally supported stents. The mean vertical deviation in these cases was 1.51 ± 1.06 mm [23]. Van de Wiele et al., using mucosa-supported guides, found a mean vertical deviation of 0.75 ± 0.65 mm [12]. In a previously mentioned study, vertical coronal implant deviation was also presented. In this study, implant placement was half-guided but various guide supports were applied. They found a mean of 1.1 ± 1.0-mm apical deviation [9]. Bover-Ramos and colleagues (2018) examined the question of vertical deviation in a systematic review. The analysis was based on six selected clinical studies and found a mean vertical deviation of 0.74 ± 0.10 mm [24]. The mean 0.59 ± 0.24-mm apical vertical deviation we found indicates that we have managed to achieve slightly superior vertical accuracy compared to other studies.

Planned and actual implant positions can be superimposed and compared digitally to characterize outcome accuracy. Comparative studies mainly used postoperative CBCT scans for that purpose. However, in postoperative CBCT scans, implants may cause artifacts due to beam scattering, which is a potential source of measurement error. Furthermore, following the ALARA principles a second CBCT scan should be avoided if the sole purpose is to determine the accuracy of the outcome [25, 26]. The application of intraoral scanners to provide input for such comparisons offers a solution to this problem. The information that an intraoral scan contains on the spatial position of some superstructure (e.g., a scan abutment) attached directly to the implant in the bone makes it possible to reconstruct the spatial position of the implant in the bone, provided that the implant dimensions are known. Application of intraoral scans to detect actual implant location may represent an alternative approach at the same time lowering the total dosage required from the comparison.

By the applied method of comparison, it was possible to avoid additional CBCT scans, whereby we could minimize patient exposure to radiation. The accuracy of CBCT scans was previously reported to be within 0.5 and 0.7 mm but voxel size can influence the final characteristics of the image [27]. In 2017, Renne and co-workers found an average of 79.8 ± 5.17-µm precision and a mean of 48.4-µm trueness using Planmeca PlanScan for sextant scanning, which is one of the best in its category [28]. The presented CBCT followed by intraoral scanning method yielded comparable outcomes to the usual CBCT followed by CBCT alignment.

No significant difference was found between the two study groups in any insertion torque. The four times faster implant placement duration in the machine-driven group was

possibly observed due to 50-rpm insertion speed versus the manufacturer's recommended speed of 15 rpm. The benefit of using a contra-angled handpiece was the effortless acceleration of implant placement compared to the ratchet, which is limited by the operator's dexterity.

Conclusion

Within the limits of this study, it can be concluded that half-guided implant placement can result in a favorable implant positioning using a surgical motor, or a torque wrench. Between the two groups, there were no significant differences in terms of accuracy, while implant placement with a surgical motor at a speed of 50 rpm resulted in significantly lower duration. Investigation of implant placement accuracy can be performed based on a preoperative CBCT scan and a postoperative digital intraoral scan, minimizing irradiation dose by avoiding a second CBCT scan.

Funding Open access funding provided by Semmelweis University. The present study received material support from NSK Europe GmbH, Eschborn, Germany; Botiss Biomaterials GmbH, Zossen, Germany; Straumann AG, Basel, Switzerland; Dicomlab Kft., Szeged, Hungary; the Hungarian Human Resources Development Operational Program (EFOP-3.6.2–16-2017–00006); and the Excellence Program of the Ministry for Innovation and Technology in Hungary, within the framework of the Therapy thematic program of the Semmelweis University.

Declarations

Ethics approval The study conformed to the tenets of the Declaration of Helsinki (as amended in 2013) in all respects. The study protocol was approved by the Regional and Institutional Committee of Science and Research Ethics at the Semmelweis University (Approval Number: SE TUKEB 7/2017). Surgical interventions were undertaken with the understanding and written consent of each subject.

Informed consent Surgical interventions were undertaken with the understanding and written consent of each subject.

Conflict of interest Dr. Endre Varga Jr. and Dr. Gabor Braunitzer are employed in Dicomlab Kft. The other authors do not report any conflict of interest.

References

1. BouSerbal C, Jacobs R, Quirynen M, Steenberghe D (2002) Imaging technique selection for the preoperative planning of oral implants: a review of the literature. Clin Implant Dent Relat Res 4:156–172. https://doi.org/10.1111/j.1708-8208.2002.tb00167.x
2. Zechner W, Bernhart T, Zauza K, Celar A, Watzek G (2001) Multidimensional osteodistraction for correction of implant malposition in edentulous segments. Clin Oral Implants Res 12(5):531–538. https://doi.org/10.1034/j.1600-0501.2001.120515.x
3. Duff RE, Razzoog ME (2006) Management of a partially edentulous patient with malpositioned implants, using all-ceramic abutments and all-ceramic restorations: a clinical report. J Prosthet Dent 96(5):309–312. https://doi.org/10.1016/j.prosdent.2006.08.027
4. Kemper R, Galmiklos A, Aroca S (2013) Surgical and prosthetic correction of malposed maxillary implants: a case report. Int J Periodontics Restorative Dent 33(5):575–581. https://doi.org/10.11607/prd.1199
5. Varga E, Antal M, Major L, Kiscsatari R, Braunitzer G, Piffko J (2020) Guidance means accuracy: a randomized clinical trial on freehand versus guided dental implantation. Clin Oral Implants Res 31:417–430. https://doi.org/10.1111/clr.13578
6. Brugnami F, Caleffi C (2005) Prosthetically driven implant placement. How to achieve the appropriate implant site development. Keio J Med 54:172–178. https://doi.org/10.2302/kjm.54.172
7. Vercruyssen M, Jacobs R, Van Assche N, Van Steenberghe D (2008) The use of CT scan based planning for oral rehabilitation by means of implants and its transfer to the surgical field: a critical review on accuracy. J Oral Rehab 35:454–474. https://doi.org/10.1111/j.1365-2842.2007.01816.x
8. Hämmerle C, Cordaro L, Assche N et al (2015) Digital technologies to support planning, treatment, and fabrication processes and outcome assessments in implant dentistry. Summary and consensus statements. The 4th EAO consensus conference 2015. Clin Oral Implants Res 26:97–101. https://doi.org/10.1111/clr.12648
9. Valente F, Schiroli G, Sbrenna A (2009) Accuracy of computer-aided oral implant surgery: a clinical and radiographic study. Int J Oral Maxillofac Implants 24:234–242
10. Al-Harbi S, Sun A (2009) Implant placement accuracy when using stereolithographic template as a surgical guide: preliminary results. Implant Dent 18:46–56. https://doi.org/10.1097/ID.0b013e31818c6a50
11. Cassetta M, Di Mambro A, Giansanti M, Stefanelli L, Barbato E (2014) How does an error in positioning the template affect the accuracy of implants inserted using a single fixed mucosa-supported stereolithographic surgical guide? Int J Oral Maxillofac Surg 43:85–92. https://doi.org/10.1016/j.ijom.2013.06.012
12. Van de Wiele G, Teughels W, Vercruyssen M, Coucke W, Temmerman A, Quirynen M (2015) The accuracy of guided surgery via mucosa-supported stereolithographic surgical templates in the hands of surgeons with little experience. Clin Oral Implants Res 26:1489–1494. https://doi.org/10.1111/clr.12494
13. Joda T, Derksen W, Wittneben JG, Kuehl S (2018) Static computer-aided implant surgery (s-CAIS) analysing patient-reported outcome measures (PROMs), economics and surgical complications: a systematic review. Clin Oral Implants Res 29(Suppl 16):359–373. https://doi.org/10.1111/clr.13136
14. Buser D, von Arx T, ten Bruggenkate C, Weingart D (2000) Basic surgical principles with ITI implants. Clin Oral Implants Res 11:59–68. https://doi.org/10.1034/j.1600-0501.2000.011S1059.x
15. Kühl S, Zürcher S, Mahid T, Müller-Gerbl M, Filippi A, Cattin P (2013) Accuracy of full guided vs. half-guided implant surgery. Clin Oral Implants Res 24(7):763–9. https://doi.org/10.1111/j.1600-0501.2012.02484.x

DOI:10.14753/SE.2022.2638

16. Jung RE, Schneider D, Ganeles J, Wismeijer D, Zwahlen M, Hämmerle CH, Tahmaseb A (2009) Computer technology applications in surgical implant dentistry: a systematic review. Int J Oral Maxillofac Implants 24(Suppl):92–109
17. Ozan O, Orhan K, Turkyilmaz I (2011) Correlation between bone density and angular deviation of implants placed using CT-generated surgical guides. J Craniofac Surg 22(5):1755–1761. https://doi.org/10.1097/SCS.0b013e31822e6305
18. Ersoy A, Turkyilmaz I, Ozan O, McGlumphy E (2008) Reliability of implant placement with stereolithographic surgical guides generated from computed tomography: clinical data from 94 implants. J Periodontol 79:1339–1345. https://doi.org/10.1902/jop.2008.080059
19. Di Giacomo G, da Silva J, da Silva A, Paschoal G, Cury P, Szarf G (2012) Accuracy and complications of computer-designed selective laser sintering surgical guides for flapless dental implant placement and immediate definitive prosthesis installation. J Periodontol 83:410–419. https://doi.org/10.1902/jop.2011.110115
20 Derksen W, Wismeijer D, Flügge T, Hassan B, Tahmaseb A (2019) (2019) The accuracy of computer-guided implant surgery with tooth-supported, digitally designed drill guides based on CBCT and intraoral scanning. A prospective cohort study. Clin Oral Implants Res. 30(10):1005–1015. https://doi.org/10.1111/clr.13514
21. Vercruyssen M, Cox C, Coucke W, Naert I, Jacobs R, Quirynen M (2014) A randomized clinical trial comparing guided implant surgery (bone- or mucosa-supported) with mental navigation or the use of a pilot-drill template. J Clin Periodontol 41:717–723. https://doi.org/10.1111/jcpe.12231
22. Tahmaseb A, Wismeijer D, Coucke W, Derksen W (2014) Computer technology applications in surgical implant dentistry: a systematic review. Int J Oral Maxillofac Implants Suppl 29:25–42. https://doi.org/10.11607/jomi.2014suppl.g1.2
23. Cassetta M, Stefanelli L, Giansanti M, Calasso S (2012) Accuracy of implant placement with a stereolithographic surgical template. Int J Oral Maxillofac Implants 27:655–663
24. Bover-Ramos F, Vina-Almunia J, Cervera-Ballester J, Penarrocha-Diago M, Garcia-Mira B (2018) Accuracy of implant placement with computer-guided surgery: a systematic review and meta-analysis comparing cadaver, clinical, and in vitro studies. Int J Oral Maxillofac Implants 33:101–115. https://doi.org/10.11607/jomi.5556
25. Cohnen M, Kemper J, Möbes O, Pawelzik J, Mödder U (2002) Radiation dose in dental radiology. Eur Radiol 12:634–637. https://doi.org/10.1007/s003300100928
26. Loubele M, Bogaerts R, Van Dijck E, Pauwels R, Vanheusden S, Suetens P, Marchal G, Sanderink G, Jacobs R (2009) Comparison between effective radiation dose of CBCT and MSCT scanners for dentomaxillofacial applications. Eur J Radiol 71:461–468. https://doi.org/10.1016/j.ejrad.2008.06.002
27. Loubele M, Guerrero M, Jacobs R, Suetens P, van Steenberghe D (2007) A comparison of jaw dimensional and quality assessments of bone characteristics with cone-beam CT, spiral tomography, and multi-slice spiral CT. Int J Oral Maxillofac Implants 22:446–454
28. Renne W, Ludlow M, Fryml J, Schurch Z, Mennito A, Kessler R, Lauer A (2017) Evaluation of the accuracy of 7 digital scanners: an in vitro analysis based on 3-dimensional comparisons. J Prosthet Dent 118:36–42. https://doi.org/10.1016/j.prosdent.2016.09.024